Norges geologiske undersøkelse

7491 TRONDHEIM

RAPPORT

Rapport nr.: 2003.011	ISSN 0800-3416	Gradering: Åpen

Tittel:
Structural controls on graphite mineralisation, Senja, Troms

Forfatter:	Oppdragsgiver:
Iain Henderson & Mark Kendrick	Troms Fylkeskommune, NGU.

Fylke:	Kommune:
Troms	Berg
Kartblad (M=1:250.000)	Kartbladnr. og -navn (M=1:50.000)
Tromsø	1433 IV Mefjordbotn
Forekomstens navn og koordinater:	Sidetall: Pris:
Skaland Grafittgruve	Kartbilag: Vedlegg 1-6

Feltarbeid utført:	Rapportdato:	Prosjektnr.:	Ansvarlig:
August 2001/2002	01.03.03	290300	

Sammendrag:

Strukturanalyser av 6 grafittforekomster har blitt gjennomført på Senja, Troms. Detaljert 1:5000 kartlegging har blitt gjennomført på 4 av disse forekomster i tillegg til innsamlingen av prøver for grafittanalyser. Deler av Trælenforekomsten er kartlagt i målestokk1:400. Regionale undersøkelser har gitt ytterligere kunnskaper om strukturene i forekomstene og bidratt til å sette forekomstenes geometri inn i en regional sammenheng. Hovedmålet for denne studien har vært å karakterisere de komplekse strukturelle hendelser som både dannet og modifiserte grafittforekomstene. Studien viser at grafittmineraliseringen har nær sammenheng med utviklingen av F_2 folder, fordi grafitten er best utviklet i forbindelse med nord-sør strøkende F_2 foldeakser. F_2 foldene er deformerte av D_3 deformasjonsfase langs omtrent øst-vestgående foldeakser. Dette har dannet komplekse flerfase foldegeometrier. Geografisk sett, er grafitten mest utpreget der F_3 strukturer krysser F_2 strukturer som innholder grafitt. Utbredelsen av grafittblottinger henger nøye sammen med om både F_2 og F_3 skjærsoner er til stede. Lokalt (F_2) eller regionalt (F_3) kan 'skjære ut' grafittblottingene og dermed begrenser utbredelsen av grafittforekomstene. Dette studium viser derfor at kunnskap om kombinasjonene av D_2 og D_3 strukturer kan skape en bedre forståelse av grafittforekomstenes geometri. I noen av forekomstene (Trælen og Finnkona) har ytterligere en deformasjonsfase (D_4) blitt identifisert, en fase som har aldri vært dokumentert før. Dette antyder ennå mer kompleksitet i forståelsen av disse forekomstene. Det er åpenbart i mange av disse forekomstene at både F_2 og F_3 foldingene er svært usylindriske. Dette viser at det er problematisk å bruke småfold geometrier for å fastsette storskala forekomstgeometri. Derfor må man være ganske forsiktig med å utnytte denne metoden i en prospekteringssammenheng og særlig når man studerer enkelte forekomster med hensyn til eventuell drift.

18 grafittanalyser har blitt gjennomført fra 3 av forekomstene studert i detalj. Analysene viser verdier fra 0.1% til 37% total organisk karbon. Ingen systematiske variasjoner viser seg mellom forskjellige forekomster eller relatert til det strukturelle mønsteret. Imidlertid viser Vardfjellet forekomsten de høyeste grafittverdier i regionale foldelukninger. Mer detaljert prøveinnsamling trenger å bli gjennomført med hensyn til strukturkartleggingen som en basisramme for prøvetakingen. Regionale observasjoner bekrefter at skjærsonene som begrenser Senja skjærbelte er sideveisforkastninger. Disse skjærsoner viser en sinistral kinematikk. Men nye bevismateriale som er framlagt viser at disse skjærsoner har en kompleks reaktiviseringshistorie og kan bestå av mer enn en bevegelsesepisode. Skjærsoner som ligger innenfor Senja skjærbelte er kinematisk sett relatert til de store skjærsoner som begrenser Senja -skjærbelte. Disse skjærsoner har også har en duktil sideveis skjærbevegelse og er tolket som sekundære S-C type strukturer av de store skjærsoner som begrenser Senja skjærbelte. Det er disse sekundære strukturer som skjærer igjennom grafittforekomstene og danner dragfolder som leder til en mer komplisert grafittforekomstgeometri.

Preliminært ^{40}Ar-^{39}Ar geochronologi har blitt gjennomført på 7 prøver. Resultatene viser definitivt prekambrisk alder for skjærsonene som begrenser Senja-skjærbeltet. Dette stemmer dårlig med tidligere publisert materiale. Ytterliggere 20 prøver skal inn til geokronologisk analyse. Analysene kan forhåpentligvis bidra til å forstå den komplekse vekselvirkning mellom folding, skjæring og grafittmineraliseringen.

Emneord: grafitt	strukturgeologi	geometri
folding	skjærsone	industrimineraler
mineralressurser	kartlegging	geochronologi

CONTENTS

FIGURES

TABLES

ENCLOSURES

Enclosure 1: Detailed 1:400 structural mapping of the area north of Lyktegangen near the Trælen deposit.

Enclosure 2: Detailed 1:400 structural mapping of the Lyktegangen near the Trælen deposit.

Enclosure 3: Detailed 1:5000 structural mapping of the Krokelvdalen deposit.

Enclosure 4: Detailed 1:5000 structural mapping of the Bukkemoen deposit.

Enclosure 5: Detailed 1:5000 structural mapping of the Geitskaret deposit.

Enclosure 6: Detailed 1:6250 structural mapping of the Vardfjellet deposit.

ABSTRACT

Structural analysis of 6 graphite deposits has been carried out on the island of Senja, Troms. Detailed 1:5000 mapping has been undertaken on 4 of these deposits along with sample collection for graphite content analysis. Detailed 1:400 mapping has been carried out on parts of the Trælen deposit. Regional observations have also been undertaken to supplement the structural knowledge gained from the deposits and to put their geometries in a regional context. The main aim of this study was to characterise the complex structural episodes to have both created and modified the graphite deposits. This study reveals that the graphite is intimately associated with the development of F2 folds, as it is best developed geographically in association with north-south strikingF_2 fold hinges. However, the F_2 fold hinges are deformed by D_3 deformation on approximately E-W axes. This creates complex interference geometries. It is also noted that graphite is most geographically extensive where F_2 structures intersect graphite-bearing F_2 structures. The extent of graphite outcrop is also strongly affected by the presence of both F_2 and F_3 shear zone structures which locally (F_2) or regionally (F_3) 'shear-out' the graphite outcrops, thereby limiting the extent of the graphite deposits. Therefore, this study strongly suggests that a good knowledge of the combination of the D_2 and D_3 structures will allow for a better understanding of the geometry of the graphite deposits. In some deposits (Trælen and Finnkona) an additional (D_4) deformation episode has been identified, which has not been previously documented. This implies yet more complexity in the understanding of these deposits in particular. It is clear that in many of the deposits both the F_2 and F_3 folding is highly non-cylindrical, demonstrating that using small-fold geometries to determine the large scale deposit geometry is highly problematic. Therefore great care should be taken in further prospecting for graphite deposits in this area in general and in particular when an individual deposit is studied in more detail for potential mine working. Analyses on the graphite shows grades of up to 37% total organic carbon but no systematic variation between different deposits and no systematic relationship to structural development. However, it appears that the aerial extent of graphite is more extensive where D_3 structures has modified the deposits. Preliminary ^{40}Ar-^{39}Ar geochronology has been carried out on 7 samples showing a definitive Precambrian age for the bounding shear zones, contrary to previous workers. Further geochronological work (approximately 20 samples) will hopefully unravel the complex interplay between folding, shearing and mineralisation.

1. Sammendrag av forekomstevalueringen

Denne seksjonen er en kort sammenfatning av de enkelte grafittforekomster på Senja som har blitt kartlagt i detalj. Hensikten med sammenfatningen er å prioritere eventuelt videre arbeid gjennom å gi en oversikt over forekomstenes form og dannelse. Vurderingen av forekomstene er gitt i **Tabell 1**.

1.1 Bukkemoen

Bukkemoen er den best utviklete av de fire forekomster som omfattes av denne undersøkelsen. Grafitten påviser gehalt opp til 18%TOC og forekomsten har et stort areal som dekker et område på omtrent 1000m^2. Forekomsten er lett tilgjengelig fra veien. Den er imidlertid komplisert oppbygd fordi strukturer deler opp forekomsten i flere små biter ved en kombinasjon av folding og skjæring. Forekomsten er også foldet i to faser som har dannet usylindriske folder. Derfor er grafittgeometrien vanskelig å forutsi.

1.2 Vardfjellet

Vardfjellet har den klart største geografiske utbredelse av forekomstene studert her, og dekker et område på nesten 2 km lengde i nord og omtrent 500m lengde i sør. Grafittgehaltene er de høyeste av alle forekomstene (opp til 34%TOC) med rimelige høye verdier fra hele forekomsten. De høyeste verdier opptrer også i samband med foldelukninger. Videre dekker forekomsten et stort areal, den opprinnelige 1:50 000 kartleggingen viser en tykk grafittlinse: Forekomsten er imidlertid delt opp i minst 5 forskjellige tynne grafittlinser som ikke har noen tilknytning til hverandre. Dette betyr at det beregnede areal for forekomsten er mindre enn cirka 700m^2. På grunn av folding og skjæring er forekomsten også delt opp i to soner, en nordlig del og en sørlig del (Hesten). Den mest lovende del av forekomsten i den nordligste delen

opptrer i foldelukningen og er meget påvirket av axiplanar skjærsoner. Dette betyr at forekomsten vil være meget vanskelig å drive. Forekomsten har også svært usylindriske foldlukninger og er ganske utilgjengelig fra nærmeste vei som er minst 4 km unna.

1.3 Geitskaret

Denne forekomsten opptrer i et ganske utilgjengelig område med minst 3 km til nærmeste vei. Grafittgehaltene er rimelige høye (opp til 28%TOC) men de høyeste gehaltene ligger på nesten 700m over havet. Den geografiske utbredelse av forekomsten er også meget begrenset til mindre enn cirka 500m^2. Forekomsten er imidlertid mindre påvirket av struktur omdannelsen og er ikke påvirket av senere D_3 folding. Derfor har forekomsten lett forutsigbarhet med hensyn til strukturene.

1.4 Krokelvdalen

Av de fire forekomster studert i detalj, har Krokelvdalen den laveste prioritet for videre arbeide, selv om forekomsten ligger lett tilgjengelig ved veikanten mellom Straumsbotn og Skaland. Grafittprøver var ikke innsamlet på grunn av visuelt dårlig kvalitet av grafittlinsene og fordi linsene ikke var mer enn 1m brede. Forekomstens totale utbredelse er ikke mer enn 200m^2.

FOREKOMST	GRAFITT ANALYSER	AREAL	GEOMETRI	TRUNCATED	TILGENGELIG	TOTAL
BUKKEMOEN	*	*	-	*	*	****
VARDFJELLET	*	*	-	-	-	**
GEITSKARET	*	-	*	-	-	**
KROKELVDALEN	-	-	-	-	*	*

Tabell 1: Vurdering av de forskjellige grafittforekomster på Senja. Bukkemoen har mest interessant potensial ut fra strukturundersøkelsene.

2. Summary of deposit evaluation

This section provides a brief summary of the individual deposits which have been mapped in detail in an attempt to prioritise them for further study and to give a broad, qualitative overview of the nature of the graphite deposits on Senja. The deposits are summarised in **Table 1**.

2.1 Bukkemoen

Bukkemoen is the best developed of the four deposits studied in detail here. The graphite displays grades of up to 18% total organic carbon and the deposit is geographically extensive, covering an estimated area of approximately 1000m^2 and the deposit is easily accessible by road. The deposit is however, due to the complex nature of the structures, divided up into several geographically and structurally distinct zones by a combination of folding and shearing. The deposit is also folded in two deformation phases creating non-cylindrical folds, therefore the prediction of graphite plunge on the folds is problematic.

2.2 Vardfjellet

This is by far the most geographically extensive deposit, covering a distance of nearly 2km in the northern outcrop and approximately 500m in the southern outcrop. Graphite grades here where the highest encountered at maximum of 34% total organic carbon but with reasonably high values throughout the deposit. The highest grade samples also appear to concur with variations in the structural geology, the highest grades occurring in the F_2 fold closure. However, although this deposit is geographically extensive, (the previous mapping at 1:50 000 suggested a thick deposit of graphite), the deposit is map up of at least five different lenses of graphite, which have no connection to each other. This leaves the estimate of the aerial extent of the

deposit as less than approximately 700m^2. The deposit is also divided into two zones, the northern part and the southern part (Hesten) due to folding and shearing. The most promising part of the deposit in the north occurs in a fold closure and is extremely dissected by axial planar faults. This would make the deposit in this area very difficult to mine. This deposit also has extremely non-cylindrical folds. The deposit also lies at least 4km from the nearest road access across extremely boggy ground.

2.3 Geitskaret

This deposit occurs in a very inaccessible area, with at least 3km to the nearest road access. Graphite grades for this deposit are reasonably good (up to % total organic carbon). However, these high grades lie on a more or less inaccessible col at 700m above sea level. The geographical extent of the graphite in this deposit is also limited to less than approximately 500m^2. However, the structural complexity of this deposit is rather limited, as it appears to be relatively unaffected by D_3 folding and therefore has predicable fold structures.

2.4 Krokelvdalen

From the four deposit studied in detail, this was considered to be the lowest priority for further study, despite the fact that this is the most accessible deposit, lying in the vicinity of the main road between Straumsbotn and Skaland. Graphite samples were not collected from this deposit as the graphite lenses were so thin (less than 1m) and their aerial extent was limited to less than approximately 200m^2.

DEPOSIT	GRAPHITE ANALYSES	AREAL EXTENT	GEOMETRY	TRUNCATED	ACCESSIBILITY	TOTAL
BUKKEMOEN	*	*	-	*	*	****
VARDFJELLET	*	*	-	-	-	**
GEITSKARET	*	-	*	-	-	**
KROKELVDALEN	-	-	-	-	*	*

Table 1: Assessment of the different graphite deposits on Senja. Bukkemoen is the deposit with the most potential based on a combination of accessibility and structural constraints.

3. Introduction

This report presents a review of the present structural geology knowledge level in the genesis and modification of the graphite deposits on Senja, Troms. This work then goes on to present new structural observations which will contribute towards a greater understanding of the geometry and structural evolution of the deposits within a regional context. These interpretations are strengthened by the addition of ^{40}Ar-^{39}Ar age-dating of the different deformation phases, structures, and mineralisation. Specific questions which will be addressed in this report are:

- What is the sequence of structural events which are present in the deposits ?
- Do these events have a predictable geometry ?
- Where does the genesis of the graphite deposits fit into this deformation sequence ?
- What are the structural geometries which have modified the ore deposits ?
- Is there a relationship between graphite grade and structure ?
- Is there a consistent regional structural framework ?
- Where do the individual ore deposits fit into the regional geological interpretation ?
- How can these relationships then be used to help predict the presence of further graphite deposits ?
- What are the absolute ages of the various generations of faults, folds and mineralisation?

These questions will be returned to in the conclusions in **Section 9** and will hopefully provide satisfying answers.

4. Previous work

This section presents a literature review of the previous work that has been done on the graphite deposits on Senja. The overriding purpose of this section is to determine the areas of study in which more structural work needs to be done, thereby setting out the objectives for the work to be carried out in this study.

4.1 Regional Setting

The rocks formed on present day Senja formed the north-west margin of the Fennoscandian Shield and form the basement to the overlying Caledonian nappes. The zone from Lofoten in the south to Vanna in the north is referred to as the *Western Troms Basement Complex* (WTBC). This general zone consists of a complex mosaic of folded gneisses and intrusive rocks (**Figure 1**). However, the rocks under study in this report consist of those on Senja and the southern part of Kvaløya. These have been given a tripartite division by Zwaan (1995). To the north and south are early Proterozoic intrusive rocks consisting of gabbros, diorites and granites. These two zones bound the north and south margins of a zone of complexly folded paragneisses though to be of the oldest Early Proterozoic. This zone is termed by Zwaan (op.cit.) as the *Senja Shear Belt* (SSB). It is here that the graphite deposits are located. Both the northern and southern margins of the SSB are major zones of crustal detachment against the Early Proterozoic intrusives. The Svanfjellet forms the southern margin of the SSB and the Torsnes Shear Zone, on the southern tip of Kvaløya, forms the northern margin. Both shear zones are interpreted to have significant strike-slip displacement (Zwaan, op.cit.). The SSB itself displays a complex internal geometry, the latest Precambrian deformations probably be a reflection of the 'docking' of the three different crustal units together.

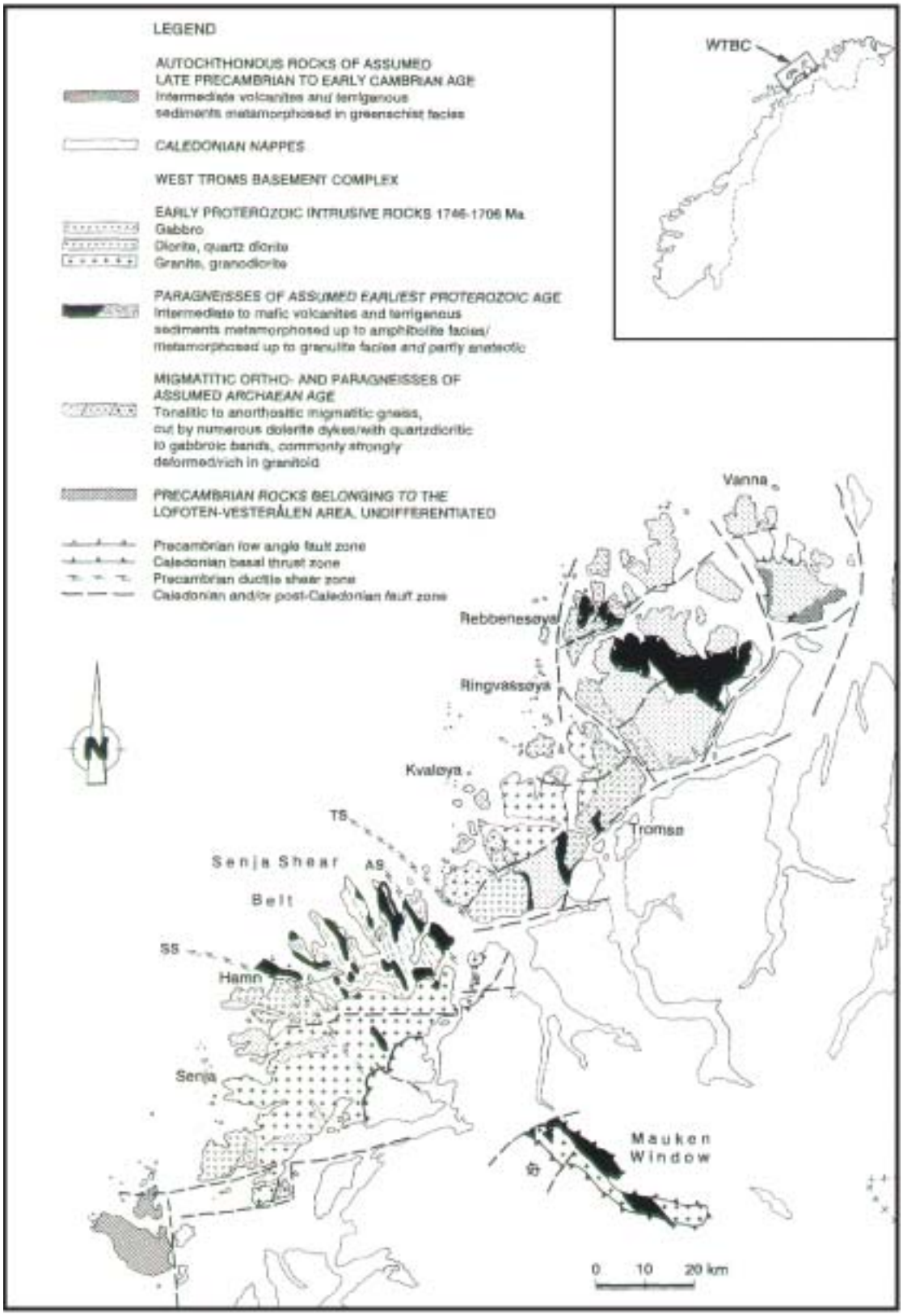

Figure 1: Summary map of the key tectonostratigraphic units in the Western Troms Basement Complex after Zwaan (1995).

Several phases of isoclinal folding, the most traceable on the regional scale having a NNW fold axis trend, is rotated approximately 25° clockwise from the bounding shear zones. An important aim of this study is to provide a framework of the large-scale structural development to provide a geometrical context for the study of the graphite deposits. These issues are discussed in further detail in **Section 4.3.2** and additional regional data is presented in **Section 6**.

4.2 Present understanding of the Graphite Deposits on Senja

This section provides an introduction to the individual graphite deposits, outside of the present mining areas (i.e. Skaland) on Senja and gives a brief description of each deposit, the work that has been done there and any outstanding structural problems which exist. The section following this (**Section 4.3**) looks at the location of the graphite deposits as a whole within the context of the regional structural knowledge. The location of the deposits is shown on **Figure 2**.

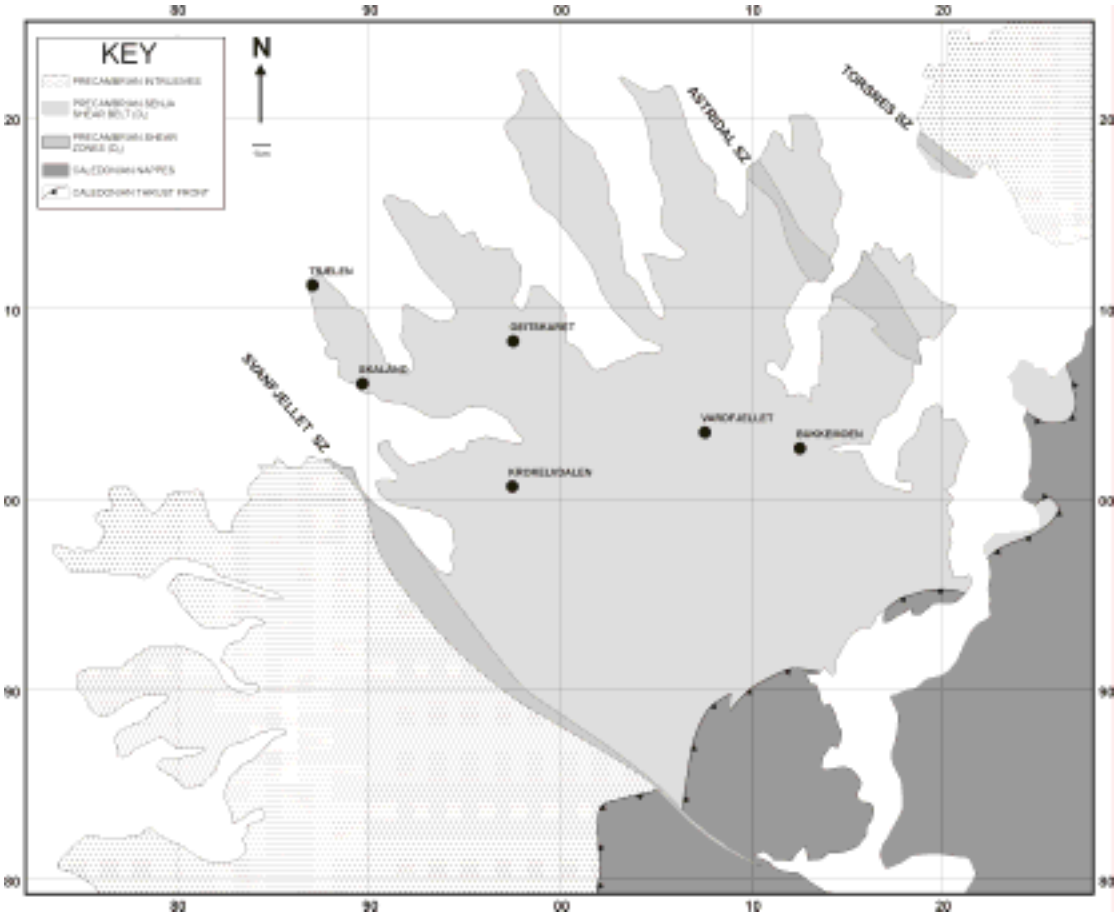

Figure 2: Location map of north-west Senja showing the location of the different graphite deposits. Trælen, Krokelvdalen, Bukkemoen, Geitskaret and Vardfjellet have been studied in detail.

4.2.1 Introduction

The most comprehensive study examining the regional-scale context of the Precambrian of Senja with respect to the graphite deposits is that of Heldal & Lund (1987). This study presented an understanding of the graphite deposits within the context of a regional-scale map of a large percentage of the Precambrian rocks of Senja. This demonstrated that the graphite was bounded to the layering presumably as a result of primary sedimentary layering. The graphite was then folded in S_1 isoclinal folds within the layering along NW-SE axial planes. Graphite was demonstrated to have a strong correlation with sulphide occurrences. This study also recognised at this early stage the rotation of S_1 foliation in the southern part of the area, near the

Svanfjellet shear zone, pre-empting the work of Zwaan (1995). Heldal & Lund (op.cit.) recognise a separate F_2 (presumably the F_1 of Pederson, 1997; see **Section 4.3.3**) on NNW-SSE axial planes. This deformation episode was responsible for the macroscopic present day appearance of outcrop pattern. F_3 is described as open-folds whose steep axial planes strike at high angles to F_2 foliation. These F_3 fold axes strike east-west and were thought responsible for *'trough and dome'* geometry of the gneissic rocks and were considered a controlling factor constraining the outcrop pattern of the amphibolite gneisses and therefore the graphite deposits (Heldal & Lund, op.cit.). These authors went on to demonstrate the relationship between the graphite location and the geometry of fold closures, showing that mineable graphite is preferentially located in these fold closures. Further structural examination of these graphite deposits must lay great weight on the detailed analysis of this hypothesis.

Heldal & Lund (op.cit.) also recognised the strike-parallel structures and refers to these as fractures and crush zones. It is possible that some of these correlate with structures observed by Olesen et al. (1993) and are Palaeozoic in age. However, Heldal and Lund (1987) identified mylonites associated with these structures. These clearly must be of Precambrian age, although their particular affinity to a deformation phase is, as yet, unknown,. These structures were observed to cut graphite mineralisation and may therefore be of D_3 age.

A key aspect of further structural study would be the identification of the geometrical pattern of the different types of structures on a regional scale and an assessment of their influence on the graphite mineralisation.

4.2.2 The Skaland Graphite Mine

The Skaland Graphite Mine has been extensively studied by previous authors (e.g. Opheim, 1962; Flood, 1990; Flood, 1986 & Dalsegg, 1986). Detailed mapping and interpretation of the Skaland field has been provided at a scale of 1:5000. It is therefore the opinion of this author that this represents a very accurate picture of the structural geology and that more detailed work in this area was not required.

4.2.3 Trælen

4.2.3.1 Introduction

Outside of the Skaland Mine area, Trælen is the single most important graphitic prospect area and many mapping (Heldal & Flood, 1985; Heldal & Lund, 1987) and exploration studies (Flood, 2000) have been undertaken in the area. Extensive geological and geophysical exploration has been carried out on the Trælen deposit to determine the continuity at depth of the many graphite lenses exposed on the surface (Flood, 2001) and to determine the location of further graphite lenses (Dalsegg, 1987). These studies in the 1980's gave rise to estimates of ore production of 10 000 tonnes per year for 12-13 years (Johannesen, 1989; Haug, 1991). Exploration studies have been taken up again in the last few years with the need to shift production away from the present mining site at Skaland (Flood, 1985). Access to the Trælen deposit was limited by the Skaland Graphite Mine to this author due to the sensitivity of the ongoing exploration program there. Therefore, the purpose of further structural study on Trælen by this author was to step back from the immediate necessity of finding more graphite lenses within the deposit and to define a process-oriented structural model within the context of the regional structural evolution. An important question

to try and answer is *"Are there structural conditions which have lead to the preferential enhancement of graphite mineralisation on Trælen ?"*.

4.2.3.2 Regional Setting

The Trælen deposit lies on the northern tip of the Skaland peninsula and consists, like so many of the Senja graphite deposits, of a lense of amphibolitic gneisses synformally down-folded into the surrounding granitic gneisses. This deposit has been mapped in detail by Heldal & Flood (1985). The amphibolitic gneisses form an enclosed, circular outcrop pattern within the surrounding granitic gneisses. In many of the graphite deposits, particularly those towards the north-east of the area, there is a tendency for the graphite to occur in sub-linear lenses parallel to NNW-SSE oriented, isoclinally-folded foliation. However, in the Trælen area, the structural complexity is much greater. In the southern part of the Trælen peninsula, the presence of graphite partially elucidates the 3D structural geometry. In this area the foliation lies in a WSW trend. However, in the northern part of the area the trend is WNW or NNW. On some of the ridges that mark the centre of the amphibolitic outcrop, open fold closures plunging eastward with an east-west trend are observed. The NNW limb of this fold probably represents the original F_2 layering whereas the WSW limb represents the attitude of the F_2 foliation after F_3 folding. These structures are clearly correlated with the F_n structures observed in the air photo interpretation of Barkey (1970). The fold geometry is consistent with drag-folding during the creation of the D_3 fault structures described by Zwaan (1995) and Pedersen (1997). However, the attitude of these fold structures (as mapped by Heldal & Flood, 1985) in the Trælen area relative to the orientation of the fault structures would suggest that the folds have been produced due to a dextral movement on the F_3 fault structures (see **Figure 3**). However, the work of Pederson (op.cit.) and Zwaan (op.cit.) demonstrate only a sinistral movement. This

critical observation strongly suggests that more detailed structural work is required on both the analysis of the fold structure and in the kinematic observations on the F_3 fault structures. Other aspects of the D_3 faulting which need to be considered as well as the fault geometry are the fault timing and deformation processes.

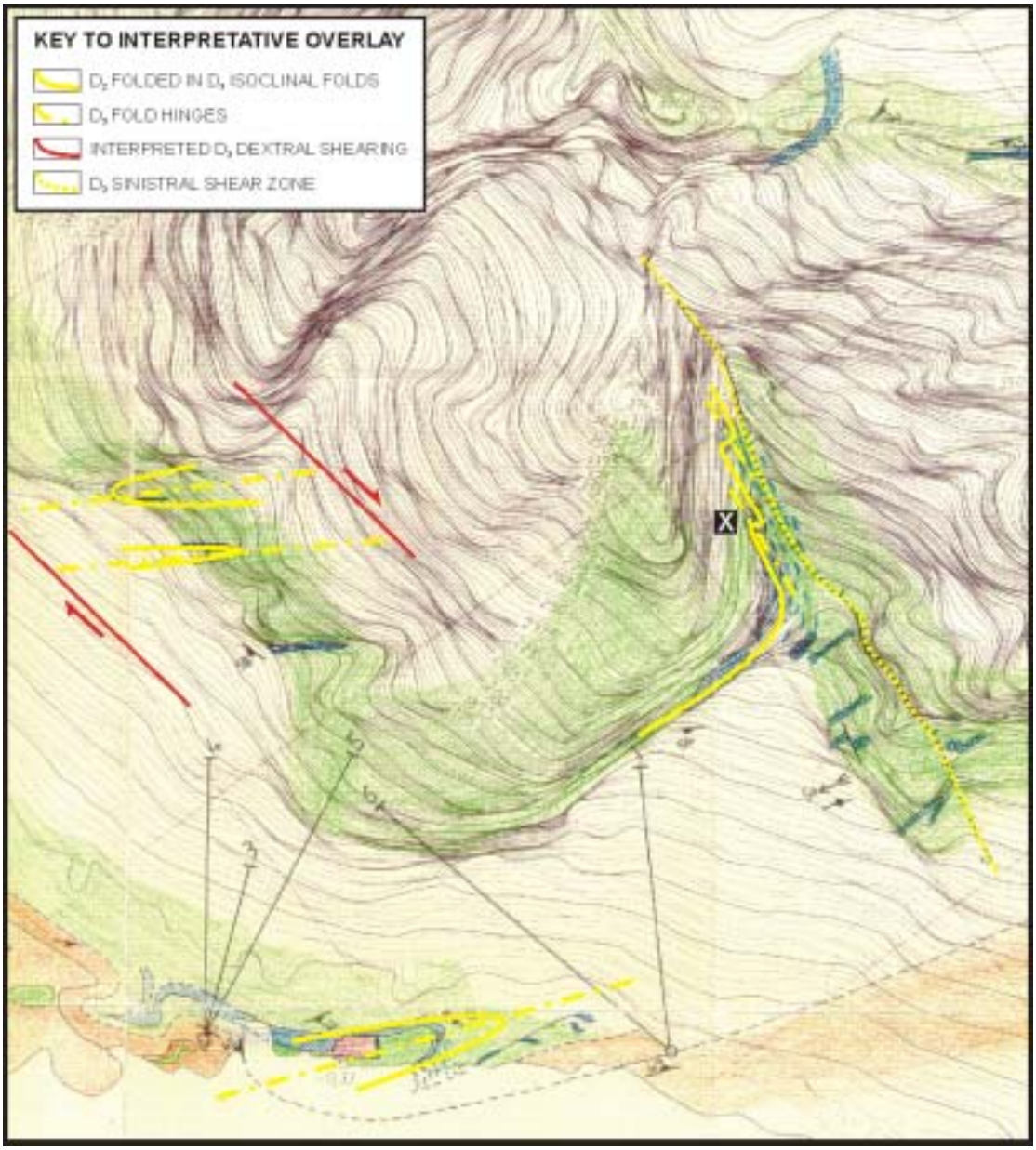

Figure 3: Extract from the map of Heldal & Flood (1987) showing the original mapping with a structural-kinematic interpretation by this author.

Zwaan (pers.comm., 2000) states that the north-south oriented fault structures are not Precambrian in age but are brittle Mesozoic structures. This agrees partially with the

work of Olesen et al. (1993). However, these authors suggested that there were pre-existing mylonitic structures in a north-south trend along which the brittle structures were a reactivation phenomena. This agrees well with the outcrop pattern of the deformation pattern of the graphite layers on Trælen. For example, the main graphite lense (12750, 1281400) is deflected into the north-south fault in such a fashion that suggests its deformation was ductile (*Point X* on **Figure 3**). Moreover, the kinematic of this fault deformation (from the drag-fold shape of the graphite lense) is sinistral. This agrees with the kinematic interpretation of Zwaan (1995) and Pederson (1997). However, this kinematic contradicts the F_3 fold geometry. Two explanations exist for this discrepancy:

- The D_3 faulting and the F_3 folding actually do not belong to the same deformation episode. (This may be suggested from the study of the Lyktegangen presented in **Section 5.3.2.3**, where there is clearly a D_4 phase of deformation *separate* from the D_3 deformation phase).
- The D_3 faulting displays more than one episode of movement in both dextral and sinistral movements. (Evidence preferring this hypothesis is presented in **Section 6**).

It is not clear from the present level of knowledge which of these two hypotheses is most realistic. Clearly testing of these two models is desirable to gain a better understanding of the structures modifying the graphite and clearly, a better understanding of both the F_3 fold structures and the D_3 faults will place better constraints on the evolution and geometry of the graphite deposits.

4.2.4 Krokelvdalen

The presence of graphite deposits has been known in this location since the 1930's. However, the first modern structural studies were carried out by Lund & Opheim

(1985). These authors establish the outcrop pattern of the deposit and that the graphite is particularly associated with sulphide concentrations. They characterise the fold structures in three stages:

- **F_1:** N-S intrafolial isoclinal folds (which folds the original layering).
- **F_2:** Regional scale isoclinal folds oriented NNW-SSE. These structures are responsible for the deposit scale outcrop pattern.
- **F_3:** Open folds with E-W axis which fold the F_2 axial planes, thereby constraining the northward-southward extension of the deposits.

These authors notice that the northern and southern extension of the deposit is constrained by fault displacements as well as F_3 fold geometry. These structures are considered as having dip-slip kinematics with at least tens of metres displacement. The deformation processes associated with these structures and there timing is unknown but may the same suite of structures as those identified by Olesen et al. (1993). i.e. Mesozoic structures. Mylonites parallel to F_2 fold axes are not documented from this area.

Dalsegg (1985) examined the nature of geophysical anomalies in the Krokelvdalen area in the same year. This work demonstrated that several anomalies, potentially graphite, were found in the area. Unlike the geological work carried out by Lund & Opheim (1985), the geophysical examination is unable to determine the structural location of the graphite as being in fold closures and partially attributes the geometry of the anomalies to a faulted geometry. These anomalies were considered both strike and dip continuous. Inferences on the depth of the synform in which the anomalies occur are several hundred metres. (This inference should be compared with the evidence presented from this study in **Section 5.3.3**).

Comprehensive mapping was carried out by Heldal & Lund (1987) of Krokelvdalen. This mapping showed that the graphite is enclosed within a pod of amphibolitic and ultramafic gneisses within granitic gneisses. This oval shaped pod lies on a N-S strike and its northern and southern boundaries are apparently controlled by F_3 folding, such that a synformal F_3 fold lies at the centre of the amphibolitic gneiss outcrop. Upward folding on this structure north and south produces apparent closures in the N-S F_2 fold axis. In addition to this work, Johannesen (1989) observes that the graphite is concentrated towards the outer margin of the amphibolitic pod near the contact with more granitic gneisses. It was also observed that the amphibolitic gneiss was more 'tectonised'. This critical observation suggests a close association between graphite location, lithological contacts and potentially flexural slip as a mechanism for graphite remobilisation (see **Section 5.3.3**). Johannesen (op.cit.) also suggests that more graphite may be present at depth.

4.2.5 Finnkona

Graphite mineralisation has been known on the mountain of Finnkona since the 1930's. However, due to the nature of the extreme topography further examination has been limited. Heldal & Lund (1987) provide the first reconnaissance mapping of this area. The summit of the mountain consists of a 'cap' of amphibolitic gneisses down folded into granitic gneisses in a synformal structure. The synform is described as having a NNW-SSE axial plane (F_2). However, the oval-shaped outcrop pattern can be accounted for by later F_3 open-folding along steeply-dipping, E-W axial planes. This structure is inferred from the work of Heldal & Lund (op.cit.) but is not actually stated in the text. However, on a visit by this author to Senja in December 2000, it was observed from a distance that a north-dipping (10-15°) calcareous band in the west-face of Finnkona defines an isoclinal 'S-fold' which verges to the north. It is

therefore assumed that this structure is an F_3 fold with an axial plane that dips very shallowly to the north. These fold structures could therefore be very closely related to an earliest phase of dip-slip overthrust movement on the structures described by Pedersen, 1997 and Zwaan, 1995 (see **Section 4.3**). For example, the structure observed on Finnkona may be a direct result of dip-slip overthrust kinematics on the Svanfjellet shear zone. It is clear from this observation alone that both a more detailed investigation of the structures on Finnkona and a more detailed examination of the supposedly F_3 strike-slip fault structures such as the Svanfjellet Shear zone will shed more light on the modification of graphite deposit geometry and therefore contribute to a better understanding of a structurally-oriented graphite exploration model.

4.2.6 Bukkemoen / Lysvannet

Studies of this most easterly lying of potential graphite deposits on Senja have been the most limited of all the deposit studies and have been constrained to limited ground magnetic studies, with a small amount of outcrop mapping. Amphibolite gneisses and graphite were first mapped by Lund & Heldal (1987) and then by Lund (1988) who suggested that geophysical mapping of magnetic anomalies was necessary to constrain the graphitic geometry. Opheim (1988) carried out this geophysical work as well as adding to the knowledge with more geological mapping of outcrops. This study suggests that there is a potentially large-displacement north-south striking shear zone in the vicinity of the graphite deposits and that a linear graphite anomaly is suggested by geological and geophysical evidence to have a width of 15m, possibly widening at depth.

However, some reconnaissance observations by this author and G-A Johannesen in December 2000 demonstrated that a complex structural history with potentially

several phases of shearing and folding are present. In light of the extensive geophysical anomalies in this area, and the apparent complex nature of the structures, a complete structural study of the vicinity of these anomalies is required.

4.2.7 Geitskaret

Geitskaret is one of the most investigated graphite targets on Senja but lies lowest on the list of priorities in this study due to poor results from previous geological and geophysical studies (Elvevold & Haug, 1985; Dalsegg, 1985). These studies demonstrated that the mineralisation is divided up in to small lenses which are spread out over a large area.

Johannesen (1989), in a review of geological and geophysical investigations in the Geitskaret vicinity, concluded that in most of the graphite occurrences in the deposit, the graphite impregnation was weak and that further investigation was not recommended. However, Johannesen (op.cit.) also notes that some of the graphite lenses, which have a close correlation with amphibolite lenses and isoclinal folding, are cut by shear zones. It is as yet unclear the structural timing and processes associated with these shear zones and therefore where they lie within the structural chronology and evolution. Although Elvevold & Haug (1985) concluded that the prospectivity of the Geitskaret deposit was poor, many question marks remain over the structural complexity. For example, the rather linear outcrop pattern interpreted by Heldal & Lund (1987) is tentatively interpreted by Elvevold & Haug (op.cit.) to be an isoclinal fold antiformal structure. The consequence of this is that to the east the antiform should be followed by a synform and therefore possibly graphite deposits hidden at depth. Several parasitic folds were observed in this area but no further

interpretation was made on their implications for the larger scale structures. Elvevold & Haug (op.cit.) make no further interpretation due to a lack of data.

It is concluded here that further investigation of the Geitskaret outcrops is therefore desirable with respect to the unravelling of both the fold and shear zone structures affecting the graphite within a regional context in terms of building a regional graphite exploration model.

4.3 Regional Structural Geology

4.3.1 Introduction

This section presents an introduction to the regional tectonic relationships and a review of the present understanding of the regional structural geology in the immediate area surrounding Senja. This is in order to place the graphite deposits within a framework of understanding as a starting point for further structural examination.

4.3.2 Regional Setting

The island of Senja consists of a Precambrian basement window (WTBC) in the western part of the island. This is overlain in the eastern region by the Caledonian Thrust Front, which is foreland (east) dipping. The Precambrian Basement in which the graphite deposits are located consists of tight to isoclinally folded gneisses of a wide range of compositions from banded granitic gneisses to amphibolitic gneisses. Regional structural studies of Senja have been rare and the only comprehensive regional study to date has been that of Zwaan (1995). This study distinguishes between different 'terrains' within the Precambrian rocks of the WTBC. **Figure 1** shows that the Precambrian rocks of western Troms can be subdivided tectonically into three distinct tectonic regions, two of which outcrop on the island of Senja.

- The southern region is characterised by granitic rocks with minor gabbro intrusion.

- The central zone, in which the graphite deposits are located, consists of isoclinally folded gneisses which are folded on NNW-SSE trending (F_2), steep to vertical axial planes, giving rise to a NNW-SSE oriented lineament on satellite images (Olesen et al., 1993) and air photos (Barkey, 1970). This zone has been named the Senja Shear Belt (Zwaan & Bergh, 1994; Zwaan, 1995). The trend of the structures within the Senja Shear Belt (SSB) passes beneath the Caledonian Rocks and is present across the whole Baltic Shield and the rocks on Senja are tentatively correlated with the Kautokeino Greenstone Belt in Finnmark (Olesen & Sandstad 1993). Henkel (1991) has called this feature the Botnia-Senja Fault Zone (BSFZ).

- The northern zone is characterised by tonalitic to anorthositic gneisses and banded migmatites.

These three tectonic zones of different lithological and structural character are juxtaposed along crustal scale shear zones. A key aspect to these shear zones is that they describe a clockwise rotation of 10-20° from the orientation of the NNW-SSE axial planes and therefore the isoclinal fold limbs in the SSB. This point was discussed by Zwaan (1995), who suggested that there was a relationship between the formation of the NW-SE linear shear zones and the NNW-SSE trending structures in the SSB that they juxtapose. These relationships may be a key aspect to understanding the processes of formation and subsequent deformation of the graphite deposits on Senja.

4.3.3 Deformation phases

It is clear from the above account that there are *at least* two main phases of structural development within the Precambrian rocks of the SSB. These are:

- The initial isoclinal folding of the inter-layered gneisses and graphite along NNW-SSE axial planes. There may be more than one deformation phase implied here (F_1 and F_2)

- Juxtaposition of the different terrains within the Precambrian basement. along several NW-SE crustal scale shear zones (F_3 and later).

Pedersen (1997) in a recent study has undertaken the most comprehensive and systematic observations of the kinematics and structural evolution of the Precambrian rocks on the north-eastern margin of Senja. This study considers the Precambrian structural chronology to consist of 3 main deformation episodes. These are:

- **D_1:** Isoclinal WSW-verging folds which strike NNW-SSE.

- **D_2:** Asymmetric folds which deform S_1 folding. New shear zone structures are developed during this phase which are oriented 15° clockwise of the S_1 trend. These structures are strike-slip and have sinistral displacements. In detail, they often have conjugate geometries. These produce drag folds (F_2) in the S_1 foliation with NE-SW axial planes.

- **D_3:** This phase consists of brittle to brittle ductile strike parallel shear zones with evidence for varied kinematics (dominantly dextral. with some sinistral and dip-slip). These structures are often accompanied by brittle en-echelon fractures.

4.3.4 Senja graphite deposits in a regional context

The graphite deposits on Senja occur solely within the SSB and are associated with the isoclinal folding related to the S_1 deformation described by Pederson (1997). Subsequent left-lateral juxtaposition of the different terrains along the Svanfjellet, Astridal and Torsnes shear zones led to the formation of drag-folds in the S_1 foliation to produce S_2 open folds with NE-SW axial planes.

Several shear zones have been mapped within the SSB related to graphite deposits which may be related to the structures described by Pederson (op.cit.). Some evidence suggests that these may be S_2 structures which have since deformed and potentially remobilised the graphite. For example, from the detailed structural mapping of Flood (1985) in the Trælen deposit, the graphite 'vein' (12750, 1281400) outcrops on the southern side of a north striking structure. This structure has previously been interpreted as a brittle 'forkastning', probably relayed to Permian or Tertiary tectonics (Olesen et al., 1993). However, the manner in which the graphite is deformed into this structure suggests that it has been ductiley deformed suggesting that there is an earlier Precambrian structure here and the brittle Mesozoic deformation reactivates this structure. The sinistral sense of shear of the deformation on the graphite is also consistent with the S_2 deformation documented by Pederson (1997). The air-photo interpretation of Barkey (1970) of the Trælen area also suggested that the NNW-SSE axial planes had been refolded on NE-SW axial planes. This is consistent with the observations of Pederson and with the kinematics of the refolding of the faulted graphite vein described above.

4.3.5 Potentially controlling regional structures on mineralised geometries on Senja.

The above observations suggest that that the S_2 shear zones which juxtapose the different terrains in the Precambrian of Western Troms not only bound the SSB but are an internal structural characteristic of the SSB. There close spatial association with graphite and F_2 fold hinges at Trælen may imply that S_2 deformation was an important factor in remobilising the graphite. Therefore, a key aspect to understanding the location, genesis and geometry of the graphite deposits on Senja lies in an understanding of how the regional aspects of the geology are manifested on a sub-regional and deposit scale. Therefore building a knowledge of the individual deposits

and the deposits as a whole within a systematic structural chronology based on the regional knowledge is critical to further structural study.

4.4 Summary of structural characteristics which may be important to graphite presence in the Senja area

This section briefly summarises the regional and outcrop scale structural factors which, from the studied literature, appear to be important in the development of graphite in the Precambrian rocks of Senja and inferences made from other studies worldwide. These are:

- The development of parasitic folds or kink bands on the primary S_1 foliation.
- Re-folding of this S_1 foliation by S_2 (or later) open folds with SW-NE axes. This has the result of constraining the lateral extent of amphibolite gneiss outcrops.
- The development of S_2 shear zones in the SSB and their location relative to amphibolite gneisses and therefore graphite deposits.
- The development of F_3 folds and potentially D_3 shear zones, therefore modifying the geometry of the earlier formed structures. This would have the affect of modifying the initial fold geometry of the graphite deposits.
- It appears from the existing literature that the range and magnitude of the above structural features has been different in the different graphite deposits. This structural aspect will be addressed in this study.
- The presence of later structures which may affect the graphite deposits which have not been observed previously. This question will be addressed in this study.

5. Structural analysis of the graphite deposits on Senja

5.1 Introduction

This section provides new information on the critical structural geology field observations made on each deposit during this study and of several regional scale observations for which fieldwork was carried out in the summer of 2001and the summer of 2002. Each deposit will be presented in turn and at the end of this chapter a model will be presented for structural evolution of the graphite deposits.

5.2 Aims of new structural examination based on present knowledge

The literature review in **Section 4** demonstrated the present level of structural knowledge of the graphite deposits on Senja. This knowledge is considered as a 'starting-point' for the definition of the aims of the further structural work presented in this report. These aims are:

- To carry out further mapping in the Trælen deposit to further constrain the inferences about surface outcrop of the graphite lenses.
- To examine all of the other graphite deposits in the area and to carry out detailed mapping on a selection of these where it is thought that a greater understanding of the structural geology and structural chronology can be achieved.
- To carry out detailed structural and kinematic observations on the D_3 shears described by Zwaan (1995) and Pederson (1997) in order to determine their relevance for the F_3 folds observed in some of the deposits (Trælen, Finnkona) and inferred to affect the outcrop pattern of other deposits (Krokelvdalen).
- To construct a genetic structural model for graphite generation and modification in the Precambrian rocks of Senja.

- To use the structural model as a framework for ^{40}Ar-^{39}Ar dating (see **Section 7**).

5.3 Structural observations

5.3.1 The Skaland Graphite Mine

Due to the very extremely high vegetation in the Skaland area and very poor mist conditions during the fieldwork, the structural work carried out in this area was rather limited. Only those outcrops along a thin band at the top of the ridge north of the Skaland mine (where there was limited vegetation) were examined. These show that:

- The northern fold closure of the deposit is complicated by the presence of axial planar faults which displace lithologies and rust zones, across them.
- The F_2 small-folds, which are regionally steeply-plunging, are steeply plunging, all the way to the fold closure in this deposit (**Figure 4**). This suggest that the northern fold closure here is related to primary F_2 folding and not to later D_3 'up-folding' as demonstrated in other deposits (see below) where the F_2 small-folds are often very shallowly-plunging.

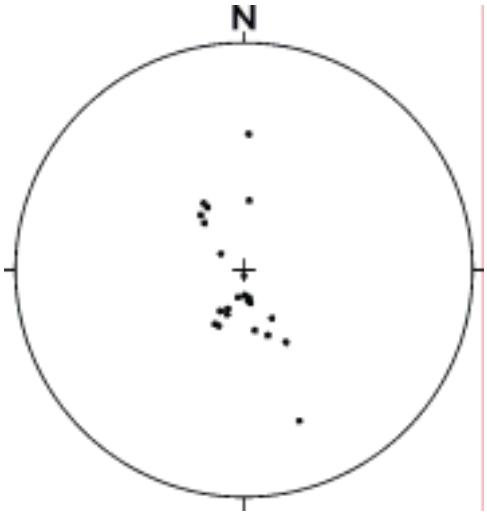

Figure 4: Stereonet of the F_2 small-fold relationships of the northern margin of the Skaland graphite deposit.

As the structural observations were so limited on this deposit and that the deposit has been studied and mapped in great detail, no graphite analyses were carried out for this deposit.

5.3.2 Trælen

5.3.2.1 Introduction

Access to the Trælen deposit was limited by the Skaland Graphite Mine to two rather short days. However, a great deal of structural data and observations were made around the coastal regions. Two areas were studied in great detail. These were the D_3 fold structure on the amphibolitic-acid gneiss contact north of Lyktegangen and secondly a detailed study of the Lyktegangen itself. These observations are summarised below.

5.3.2.2 North of Lyktegangen

On a regional scale, the D_2 fold geometries have a rather consistently striking geometry with steeply-dipping (east or west) axial planes striking NNW-SSE and steeply-plunging hinge lines (more than 80°). However, in the Trælen area, the D_2 fold geometries are greatly affected by the D_3 folding. The fold axes in the limbs of the D_3 fold are north-south striking and steeply plunging. However, around the hinges of the D_3 folds the D_2 small-folds are rotated to E-W striking and have a very variable plunge. D_2 anticline-syncline pairs have been systematically mapped around the D_3 fold hinges in one of these detailed sections (**Figure 5** and **Enclosure 1**). F_3 fault structures, which have not been previously mapped, are extensive and therefore may have a significant affect on the geometry of the orebody (**Figure 7**). These are strike slip structures of the same geometry and kinematics to the regional scale structures observed in the Krokelvdalen area.

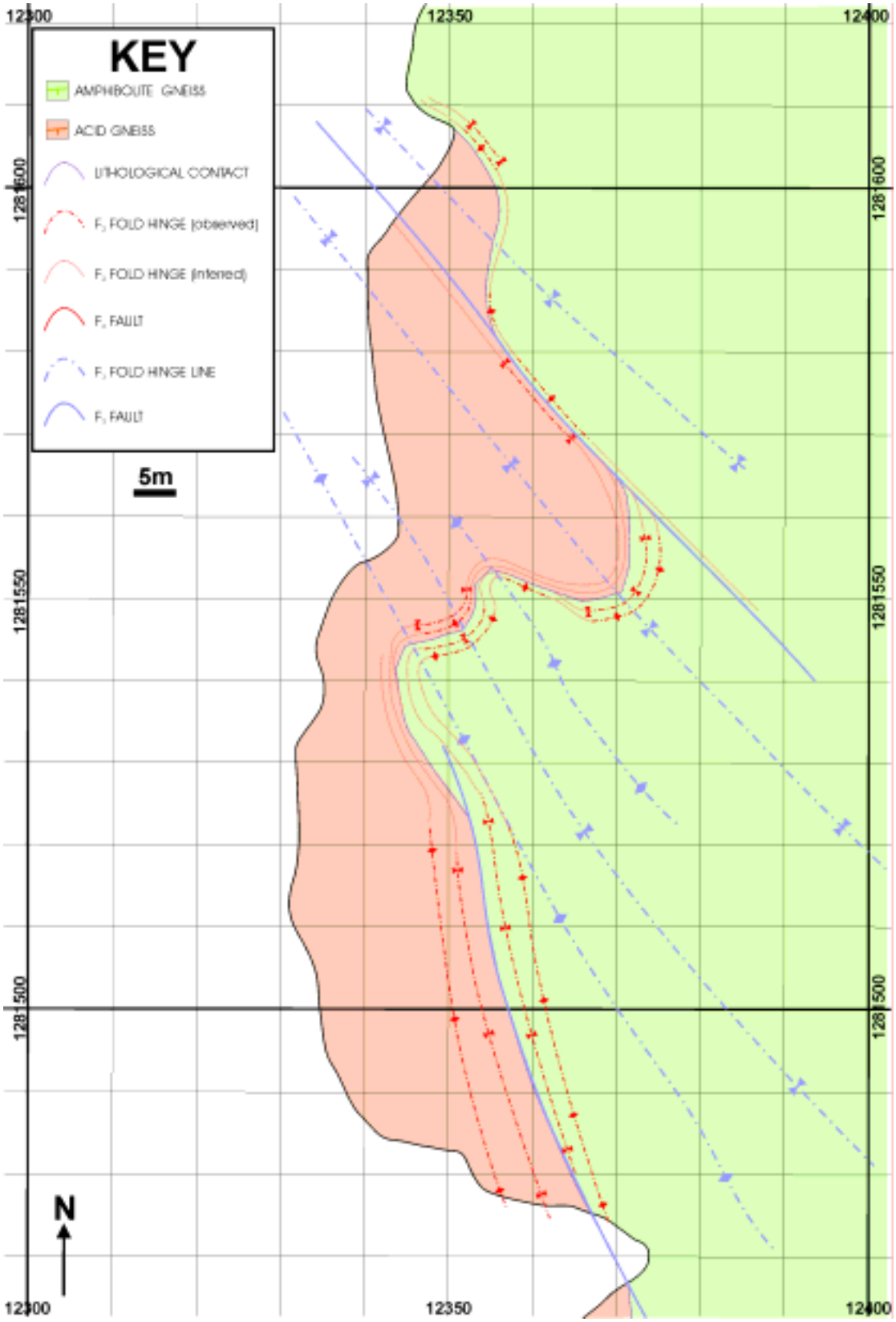

Figure 5: Detailed mapping from the west coast of the Trælen peninsula at the acid gneiss/amphibolitic gneiss contact. The full size mapping and cross-sections are *Enclosure 1* in the map pocket.

The existing 1:2500 mapping of the Lyktegangen carried out by Flood & Heldal (1987) was found to be a very accurate map. Additional features found by this author include parasitic folds, axial planar shear zones which displace lithological boundaries and the refolding of F_2 folds (**Figure 8**).

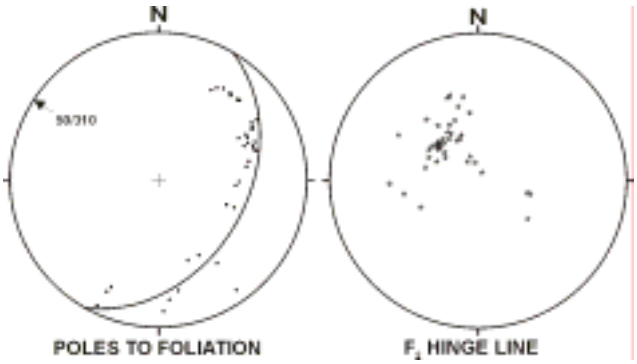

Figure 6: Stereonet data for the area north of the Lyktegangen on Trælen shown on Figure 5. The stereonet on the left shows that the poles to foliation lie on a great circle defining the shape of the D_3 fold, which plunges moderately to the WNW. The stereonet on the right shows the variation of the F2 fold hinges due to the affect of the D3 folding. The spread in azimuth and plunge of the F2 fold hinges is much greater than in an area less affected by D3 folding (For example compare this stereonet with those for Krokelvdalen in Figure 12.

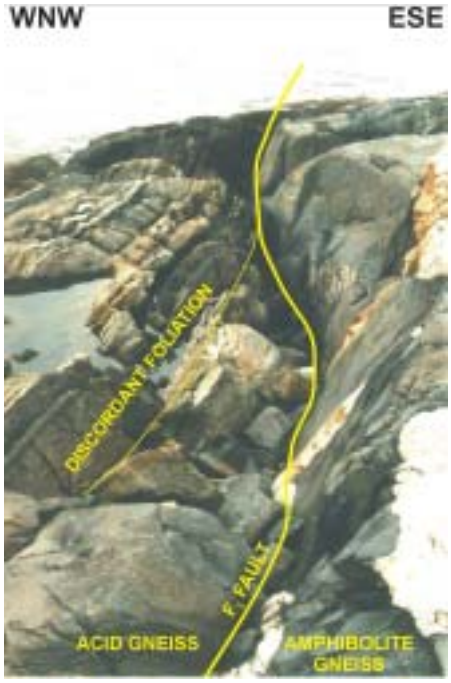

Figure 7 D_2 parallel ductile D_3 shear zone on the coastal section shown in Figure 5. The D_2 foliation on the left of the dashed line is discordant with that on the right hand side.

No graphite lenses were encountered on this detailed mapping and therefore no graphite analyses were carried out on this area.

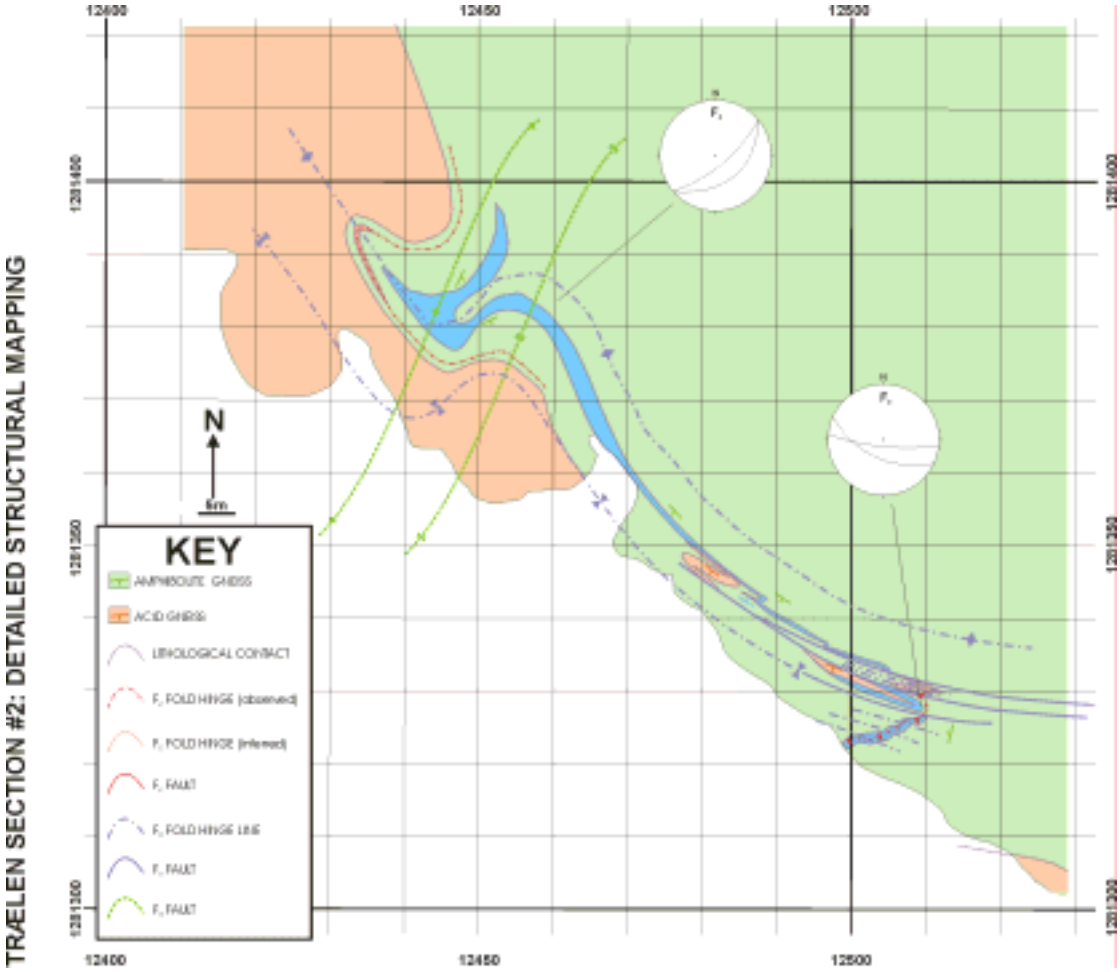

Figure 8: Detailed 1:400 mapping of the Lyktegangen on the Trælen peninsula. The full size mapping is *Enclosure 2* in the map pocket.

5.3.2.3 Lyktegangen

In addition to the detailed work on the section north of the Lyktegangen, the Lyktegangen itself was subject to detailed observations. **Figure 8** (and **Enclosure 2**) shows the 1:400 mapping for this section and demonstrates that the 1:2500 mapping carried out by Heldal & Flood (1985) is an accurate representation of the complex outcrop pattern. However, a few additional observations have been made from this study during the limited amount of time that it was possible to spend there. No demarcation of different fold or fault structure was provided from the Heldal & Flood

(op.cit.) mapping. This study reveals that the isoclinal folding seen in the graphite is not D_2 folding but is very tight D_3 folding. Therefore it appears that the D_3 deformation locally within the Trælen area has been relatively intense. This may be due to the proximity of the deposit to the offshore continuation of the Svanfjellet Shear Zone.

In Area 1 on **Figure 8** within the obvious south-eastern fold closure is the area where possibly the greatest additional information can be provided by this study to contribute to a greater understanding of the structural geology of Trælen. Several small parasitic F_3 folds can be seen to the south of the main F_3 fold. An obvious F_2 fold is seen her within the graphite layer where the F_2 fold is seen to close around the F_3 fold closure. (The same type of F_2 fold closure in an F_3 fold closure is also seen in Area 3 within acid gneiss). This F_3 fold plunges towards the NW in a similar fashion to those seen north of the Lyktegangen, expect that this fold is more isoclinal. This fold closure is cut by several D_3 shear zones in such a way that the graphite is not continuous. A fault bounded section contains only acid gneiss and no graphite. This suggests a displacement of a t least 40m on the axial planar faults. The second major addition to the Lyktegangen mapping is in Area 2, where the presence of a 'pegmatitic' intrusion' had been noted by Heldal & Flood (1987). Detailed mapping reveals that this is a pod of sheared-out coarse-grained acid gneiss 'floating' within the amphibolitic schist country rock. An F_2 fold closure is observed in the sheared terminations to one of the limbs of this structure. The F_2 structure is clearly re-folded into the isoclinal F_3 folds and then sheared by the F_3 axial planar folds. The NW fold 'closure' of the Lyktegangen has previously been mapped in detail and this study gas added nothing to the outcrop pattern observed. However, this author interprets the complex outcrop pattern to be the result of localised development of open, north-

south striking D_4 folds (**Figure 9**) around an initially complex D_3 parasitic fold geometry. This is the first time that these D_4 fold shave been documented in any of the graphite deposits on Senja. Evidence also exists for these structures on the Finnkona deposit but the nature of the outcrop meant that these were not measurable in the course of this study. No graphite analyses were carried out from this deposit due to the extreme time constraints in this area.

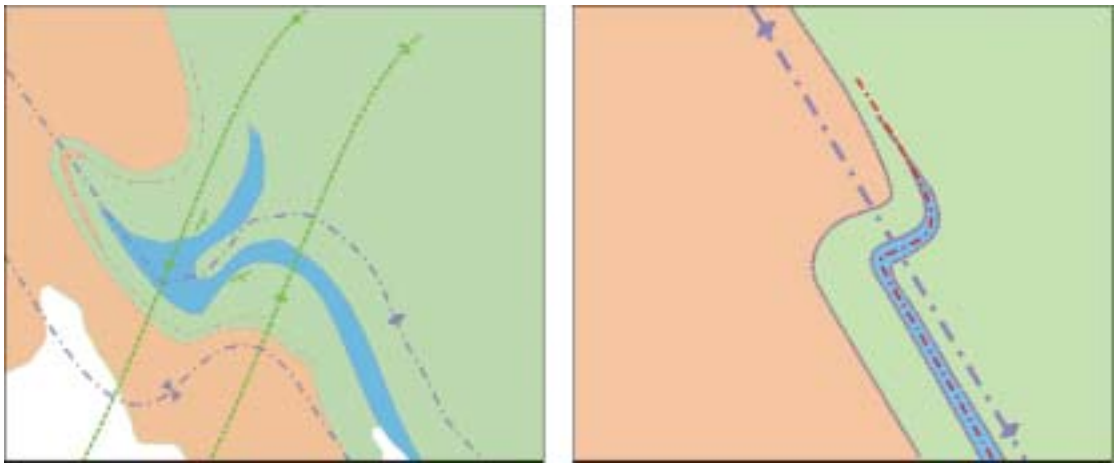

Figure 9; Schematic diagram of the geometric relationships of the Lyktegangen before (left) and after (right) D_4 deformation.

5.3.3 Krokelvdalen

This deposit transects the road between Skaland and Straumsbotn at 0597300, 7700400 and is shown as a simple synform on the Heldal & Lund map (1985). In this study, the deposit and its immediate surroundings have been mapped in detail at a scale of 1:5000 (see **Figure 10** and **Enclosure 3**). Detailed mapping along the core zone of the synform structure through the road-section demonstrates that this structure is not a simple synform but consists of a complex series of 'm-folds'. At least 5 fold-axes are observed in this section based on small-fold asymmetry reversal (see sketch in **Figure 11**). This complex structure may substantially increase the potential for graphite undetected underground in the anticlinal sections of this complex folding.

Graphite in many cases is shown dying out on the map of Heldal & Lund (1985) map but is the result of the minor axial plane fold closure (e.g. at *Point A* on **Figure 10**)

The large-scale syncline structure is also partially re-folded with a sense of vergence to the west. Small-fold (D_2) closures are generally steeply-plunging (north or south) but plunge less steeply towards the south of the deposit due to D_3 folding (compare the stereonets in **Figure 12** and the photo in **Figure 16**). This also happens along the road section due to the penetration of a D_3 fault through the strike of the road section (east-west). The mineral lineation in many places has a 20° strike slip component, but should normally be plunging steeply, like the D_2 fold hinges. This may demonstrate that the mineral lineation has been rotated due to F_3 faulting and folding.

The northern fold closure of the amphibolite is complex due to the presence of axial planar north-south faults (loc 139-141: see **Figure 10** and **Enclosure 3**; Cross-Section XY). A minimum of 5 north-south striking F_2 faults are seen around the fold closure. Local mylonitisation of the host amphibolite is observed at a ‘rust zone’ contact (*Point B* on **Figure 10**) suggesting deformation has been concentrated at competency contrast interfaces, suggesting that flexural slip has been an important process during folding.

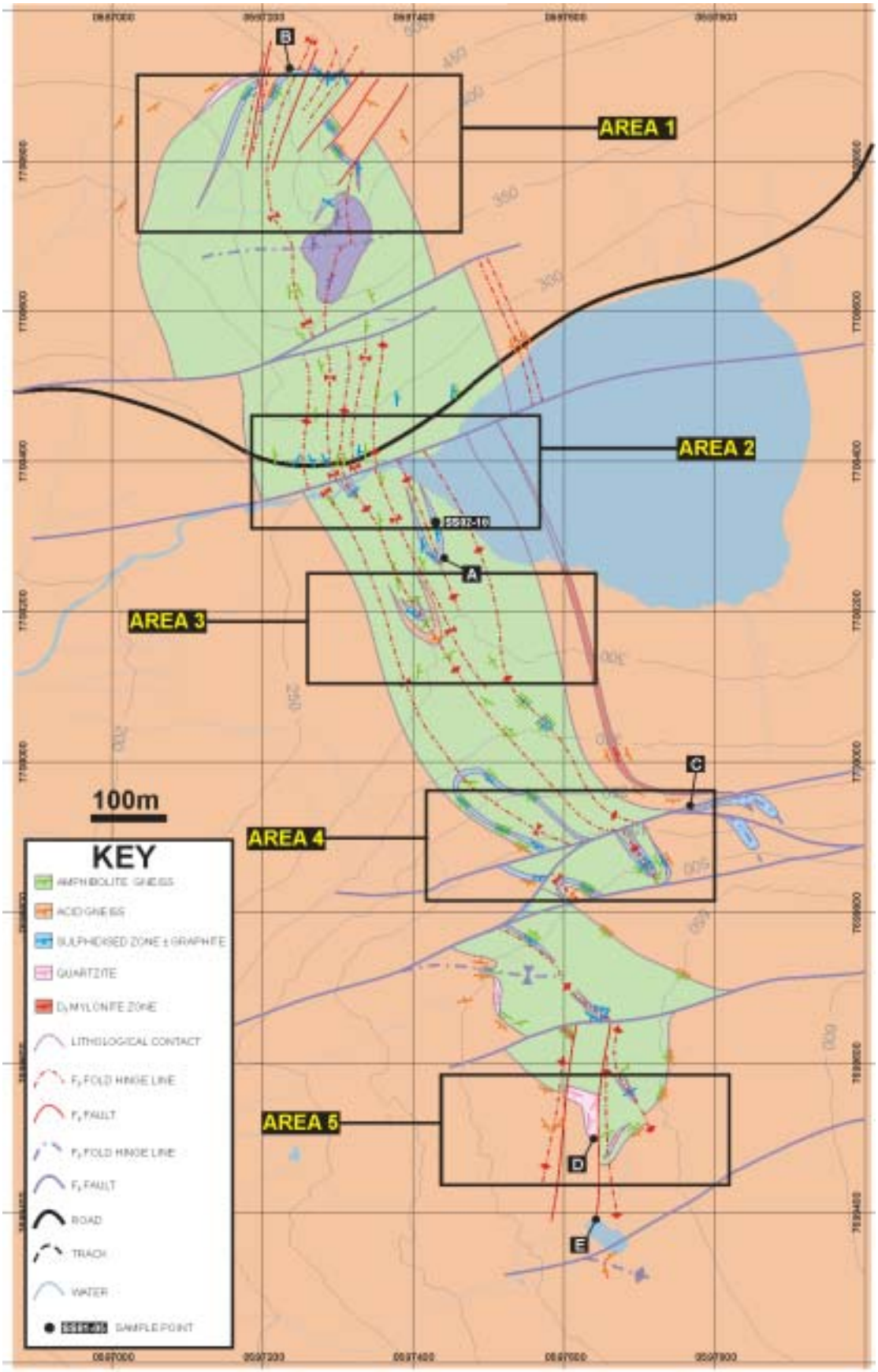
B
AREA 1
AREA 2
SS97-10
A
AREA 3
C
100m
AREA 4
KEY
AMPHIBOLITE GNEISS
ACID GNEISS
SULPHIDISED ZONE ± GRAPHITE
QUARTZITE
D1 MYLONITE ZONE
LITHOLOGICAL CONTACT
F2 FOLD HINGE LINE
F2 FAULT
F3 FOLD HINGE LINE
F3 FAULT
ROAD
TRACK
WATER
SAMPLE POINT
AREA 5
D
E

Figure 10: Detailed mapping from Krokelvdalen deposit. The full size mapping and cross-sections are *Enclosure 3* in the map pocket. The different areas refer to stereonet domains in Figure 12.

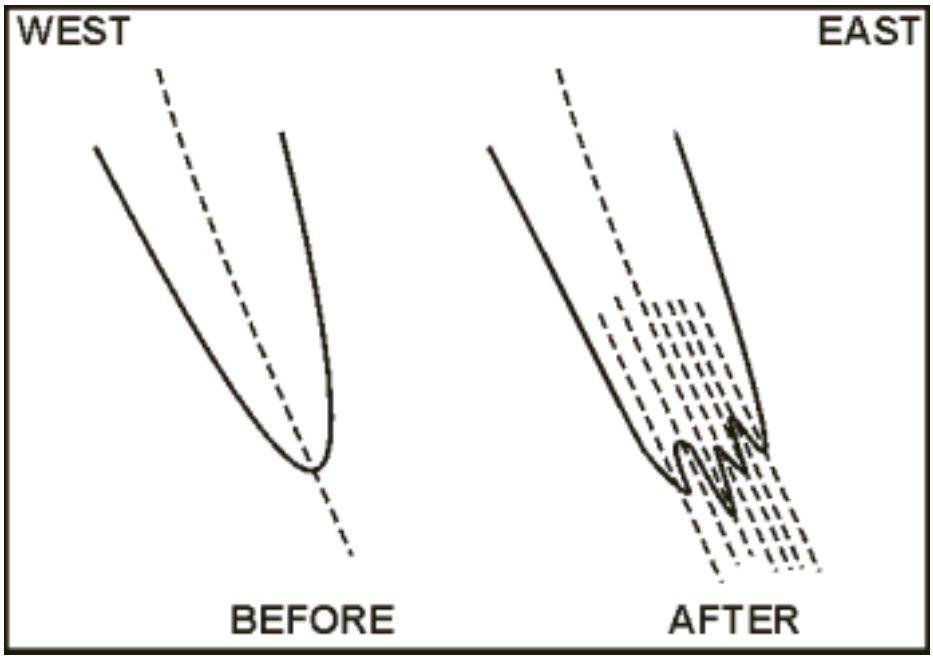

Figure 11: Simplified structural re-interpretation of the Krokelvdalen deposit The 'BEFORE' scenario shows a cross-section from the interpretation of Heldal & Lund (1985) whereas the 'AFTER' scenario from the present study demonstrates that the centre of the synform consists of a series of symmetric parasitic m-folds.

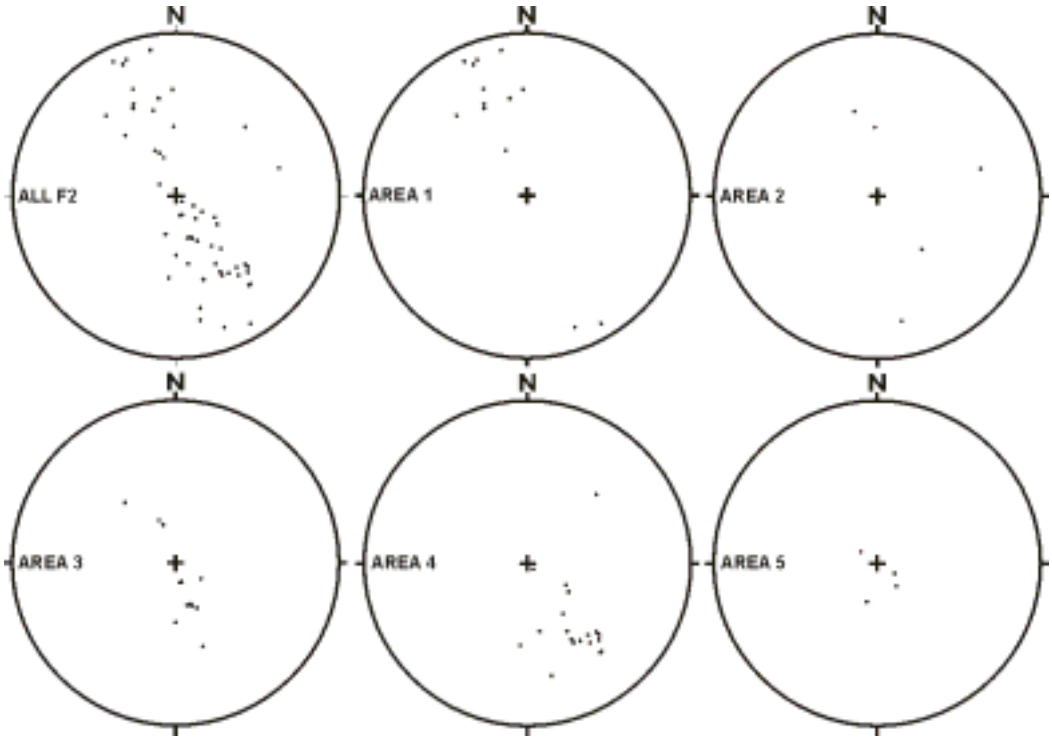

Figure 12: Variation in F_2 fold geometry (dots represent individual small-fold hinge-plunge) in different areas of the Krokelvdalen deposit. The distance from F_3 structures appears to play a role in the steepness of the F_2 fold hinges.

This may be a process which is also responsible for modification of the graphite. It is clear that on this northern fold closure that graphite is concentrated where there is a high concentration of F_2 axial planar fault structures and F_2 flexural slip. No graphite samples were collected from this deposit as the graphite was generally thin, of visibly poor quality and geographically not very extensive.

A quartz mylonite gneiss is observed in a minimum 10m wide band on the south east margin of the amphibolite syncline. This is possibly an early pre D_1 thrust structure as top to the east thrust kinematics are observed. (loc 176) The structure lies several metres into the acid gneiss to the east of the amphibolitic gneiss contact. The resulting rock-type appears more like a quartz mylonite than an acid gneiss.

A D_3 ductile shear zone marked as 'forkastning' on the Heldal & Lund (1985) map was studied in detail. This regional scale structure is in fact a 3m wide, very intense

retrograde ductile shear zone (marked *Point C* on **Figure 10**). The same structure has been observed several kilometres along strike to the east on the top of Krokelvtinden (**Figure 14**) confirming the regional nature of this structure. At this location on top of Krokelvtinden, the acid gneissic foliation is also bent into the fault in the same way, indicating strike-slip kinematics. These observations strengthen the hypothesis that these SSW-NNE structures that post-date the F_2 foliation are potentially mega S-plane secondary structures to the crustal scale bounding faults (Svanfjellet, Astridal and Torsnes).

Acid gneiss to the north of the shear zone is deformed into the shear zone suggesting a sinistral shear sense on the D_3 shear zone. Mineral lineation confirm an oblique strike slip component (see **Figure 15**). Small folds on the shear zone foliation zone suggest a later, ductile but dextral movement (see **Figure 13**). This suggests a complex ductile history of movement on this F_3 shear zone. A map scale dextral displacement of the amphibolitic gneiss contact of approximately 200m is suggested across the D_3 shear zone. This kinematic does not fit with the wall-rock displacement kinematics which are interpreted to be the main fault movement direction. Therefore, the amount of initial, sinistral displacement on this shear zone is interpreted to be an order of magnitude greater than the apparent dextral displacement observed today.

The presence of these F_3 structures has importance for the modification of the geometry of the graphite deposits. Shallowing of D_2 small-folds (see **Figure 16**) towards the south margin of the deposit is probably the result of F_3 upfolding (*Point D* on **Figure 10**).

Originally north-south graphite/rust zones are smeared parallel to the fault zone (east-west). Asymmetric folding of these sulphide zones occurs completely within the acid

gneiss south of the fault. These folds in the graphite suggest a sinistral movement on the shear zone (see **Figure 15**). Some indication of fault conjugacy is observed within this deposit. **Figure 10** shows that some minor D_3 faults connect strands of major D_3 fault segments. These connecting strands have a WNW-ESE trend. This may indicate a component of pure shear within the overall shear system. This observation is confirmed by the observation that the regional scale mega S-C fabric forms with two major directions of secondary S-structures (see **Section 6**). Several additional regional D_3 ductile shear zone are observed in the area and cut the Krokelvdalen deposit. One of these trends parallel with the Krokelven and has resulted in the bending of the acid gneiss foliation into an E-W orientation. This shear zone is inferred to intersect the Krokelvdalen deposit in the road section. This agrees with the observation of shallowed F_2 fold plunges in this locality.

Some evidence of axial planar sulphidised faults at the southern fault closure of the amphibolite gneiss (*Point E* on **Figure 10**). These north-south striking structures have not been previously mapped.

An amphibolitic anticline beyond the southern margin of the deposit on top of 647m summit, completely enclosed within acid gneiss, is found with an associated rust zone. Although this appears to be of poor quality, this structure has not been previously mapped. Some small, previously unmapped lenses of 'rust zone' are also present around the southern margin of the deposit on the D_3 fold closure.

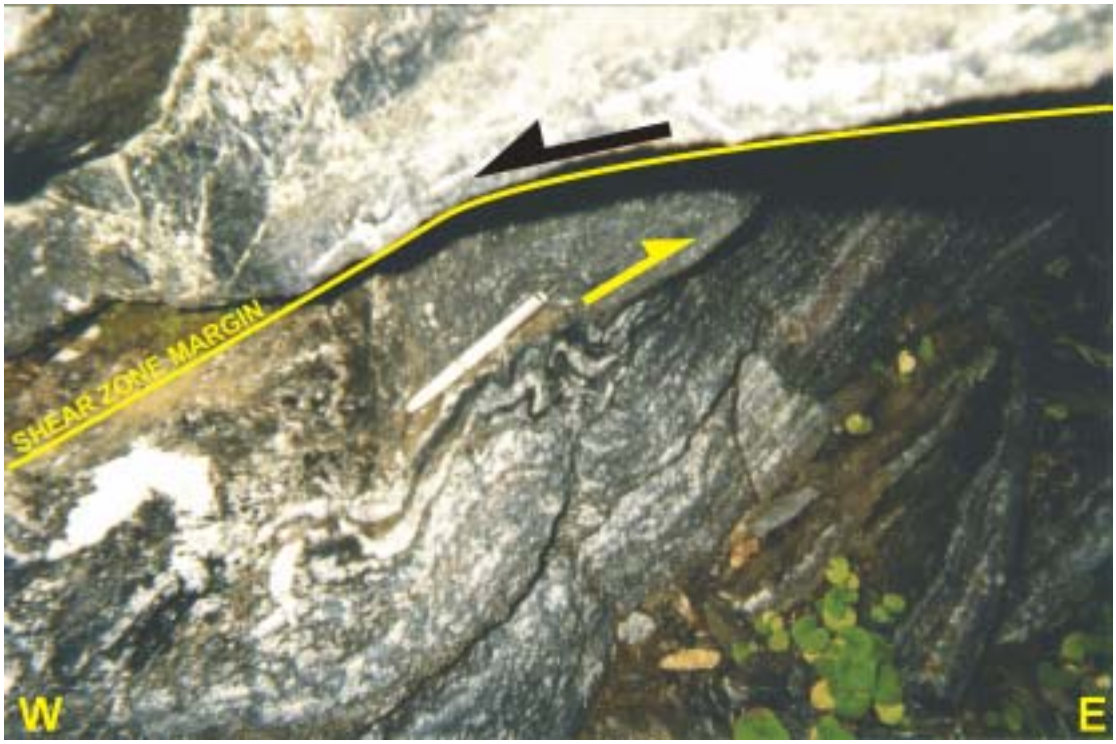

Figure 13: Detail of small-fold structures on the D_3 ductile structure intersecting the Krokelvdalen deposit at Point C on Figure 10.

Figure 14: Photo of the continuation of the ductile shear structure seen in Figure 10 on the summit of Krokelvtinden east of the Krokelvdalen deposit, showing that the structure is regional in magnitude. The dotted lines represent the D_3 shear zones. The one on the right is that shown in detail in Figure 13. Krokelvvatn is in the foreground.

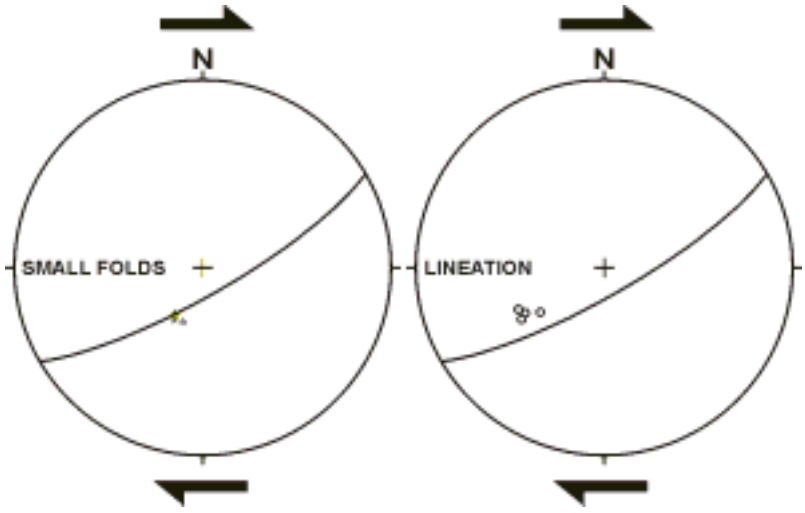

Figure 15: Fault kinematics for the ductile shear structure cutting the Krokelvdalen deposit. The small-folds and the lineation relative to the shear zone margin demonstrates a strike-slip dextral shear sense, whereas the large-scale deformation of the foliation into the shear zone suggests a sinistral displacement.

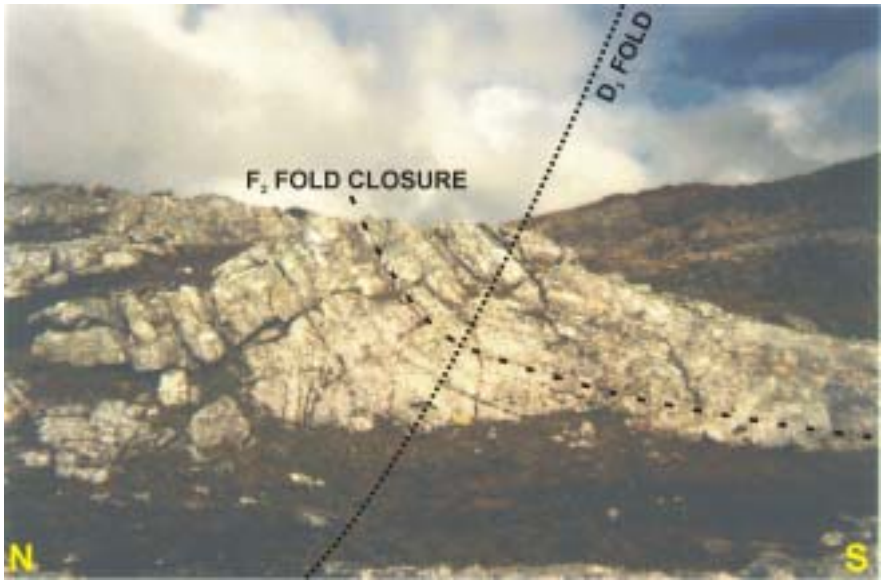

Figure 16: D_3 folding of the original D_2 foliation in acid gneiss at the southern tip of the Krokelvdalen deposit.

No graphite analyses were carried out from this deposit as the quality of the graphite appeared to be very poor and the geographically extend and downward extension of the graphite was observed to be rather limited.

5.3.4 Finnkona

Due to the nature of the poor weather on the day that this deposit was visited, the dangerous terrain and the extremely difficult vegetation conditions, time constraints limited the observations here to two outcrops and to a sketch interpretation of the structures observed looking onto the main (west-facing) wall of the mountain (**Figure 17**). The deformation of leucocratic lenses within the amphibolitic wall-rock allows the geometry and structures present in this mountain to be determined. An extremely overturned (to the south) F_2 fold is observed. This has been rotated, presumably by D_3 folding, and now has an axial plane striking approximately east-west. This D_3 axial plane has itself been deformed so that the axial plane forms an open synclinal structure with an upright, east-west axial plane. This may be the result of late D_3 (D_{3II}) deformation or to a later deformation episode (D_4). This is the only observation of D_4

deformation from all of the localities observed by this author on Senja. The age of this deformation is unknown and may indeed be Caledonian in age.

No graphite analyses were carried out from this deposit.

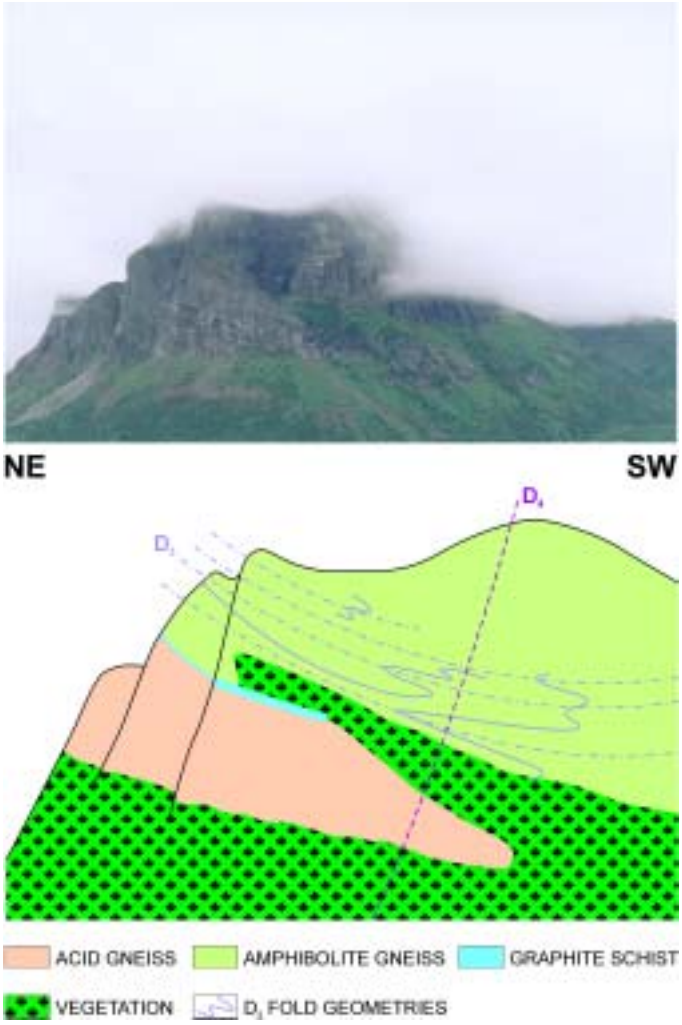

Figure 17: Photo interpretation of the Finnkona deposit. It was not possible to visit this locality so interpretations have been made from observations of these structures from a distance-

5.3.5 Bukkemoen

This deposit lies to the north-east of Lysvannet. The original mapping was carried out by Heldal & Lund (1987). This determined the presence of a very small deposit (maximum 50m long) at low altitude on the eastern slopes of the 'Bukke' mountain. The present fieldwork by this author has confirmed that this deposit is located wrongly on the Heldal & Lund map. The south-eastern tip of the deposit is actually

200m north of where it is shown on the Heldal & Lund map. In addition, the deposit is much bigger than is suggested by the existing mapping of Heldal & Lund (1987) and Lund and Opheim (1985) and extends westwards and northwards and extensively outcrops on the top of Bukken mountain. Detailed structural mapping of the whole deposit has now been carried out at a scale of 1:5000 (**Figure 18**). The following section summarises the main features of this deposit.

As a result of the structural complexity (**Figure 19**) in the area and subsequent deformation of the deposit after the formation of the graphite, the deposit has been dissected into two geographically and geometrically distinct deposit areas. The most south-easterly part of the deposit is located in an E-W striking stream. This series of outcrops forms the southern limb of a D_3 fold with an axis striking E-W. In these outcrops, acid gneiss is closely associated with a rust zone.

An F_2 syncline is interpreted in the stream section ((*Point A* on **Figure 18**) with acid gneiss in core and a minor, but continuous 'rust zone' on both sides of the acid gneiss. This F_2 structure is affected in a minor fashion by D_3 folding as the axial trace of the F_2 fold forms a sinuous pattern in the stream section. The F_2 fold becomes more overturned to the north further upstream (*Point B* on **Figure 18**). The rust zone is concordant with the acid gneiss all the way up river until loc 48 where only the rust zone is seen. The rust zone in the river strikes E-W, whereas the rust zone above the river is north-south striking. The contact between the two is clearly discordant (*Point C* on **Figure 18** and **Figure 20a**). Therefore the rust zone striking east-west in the river must be an (F_3 or late F_2) axial planar fault zone. Acid gneiss outcrops outside of the river section are deformed into this fault zone demonstrating a dextral shear sense on the fault. The rust zone stops outcropping at this locality as the foliation swings

around clockwise 90° to strike north-south. The next east-west locality of rust zone 'jumps' several hundred metres to the north. This north-south foliation therefore represents the north limb of an F_3 fold.

A flat-lying rust zone (*Point D* on **Figure 18**) represents an F_3 hinge line. The east-west striking foliation here continues westward uphill to the ridge on the southern side of Bukken.

On the top of the ridge south of Bukken top is a prominent syncline (*Point E* on **Figure 18**). Here the rust zone swings back into a north-south strike and runs northwards parallel to the Bukken ridge.

On the top of the Bukken ridge there are several F_2 anticline-syncline pairs and at least 4 separate rust zones which are probably repeated due to the F_2 folding. These F_2 folds are on the northern limb of an F_3 syncline. The F_2 folds are extremely asymmetrical and overturned to the west.

Several samples were analysed for total organic carbon from this deposit. These analyses are shown as yellow numbers on **Figure 18**. 5 samples were taken on the stream section in the southern part of the deposit and 6 samples were taken on the northern part of the deposit on the top of Bukken. This area was more affected by the D_3 folding. Although the graphite contents range from 0.5% up to 19%, there appears to be no distinct systematic picture of the relationship of graphite content variation relative to structure location (e.g. the graphite content is not more extensive on the fold hinges), or relative to the thickness of the graphite layer. However, it is very clear from the Bukken deposit that the presence of graphite is more extensive where there are D_3 structures.

Figure 18: Detailed mapping from the Bukkemoen deposit. The full size mapping and cross-sections are *Enclosure 4* in the map pocket.

The geometrical affect of theD_3 structures on the F_2 fold geometry cab be seen in the difference between two F_2 folds geometries in **Figure 21** and **Figure 22**.

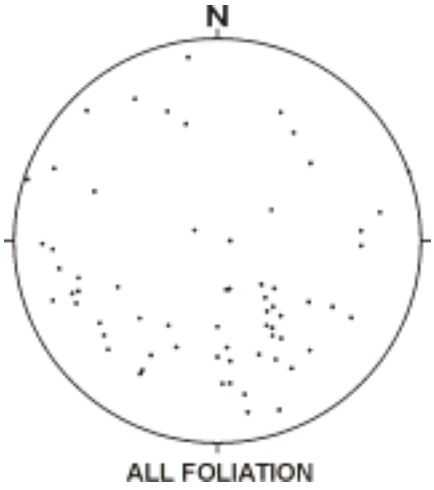

Figure 19: All foliation measurements from the Bukkemoen deposit showing a very large scatter. Part of the structural study carried out on this study was to attempt to systemise the structural complexity.

Figure 20: Examples of different structures present in the Bukkemoen deposit. (A) Axial planar fault observed at the top of the stream section (Point C marked on Figure 18). The graphite has acted as an activation surface to lubricate the fault. (B) F_2 parasite fold on the top of Bukken (Point F marked on Figure 18). (C) internal thrusting of a graphite layer a few metres NW of the Bukken summit (marked G on Figure 18). (D) Pegmatites injected into amphibolitic layering on a shallow limb of an asymmetrical D_3 fold south of Bukken summit (marked H on Figure 18).

However, the F_3 fold geometries are highly non-cylindrical as can be seen from **Figure 23** meaning that predictions of the plunge of graphite zones must be limited to individual small-fold hinges and do not necessarily reflect the large-scale folds geometry.

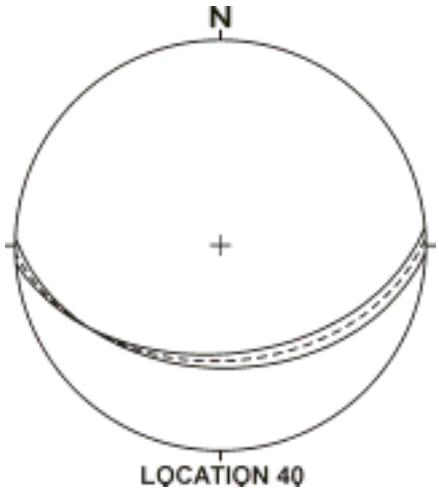

Figure 21: Stereonet data representative for the 'stream section area' of the Bukkemoen deposit. The structure measured is marked '40' on Figure 18. Closed lines represent the fold limbs while the dashed line represents the axial plane.

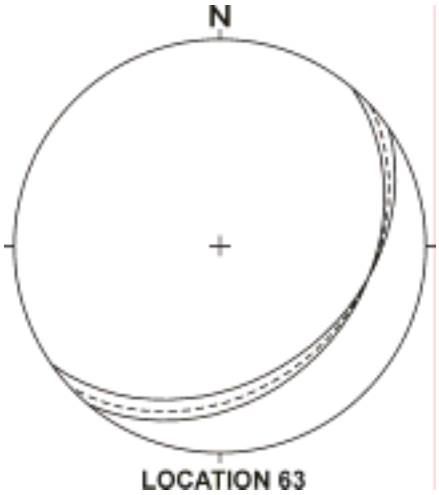

Figure 22: Stereonet data for F_2 fold on top of the Bukken (marked '63' on Figure 18). This should be compared with the structures observed in Figure 21. Closed lines represent the fold limbs while the dashed line represents the axial plane.

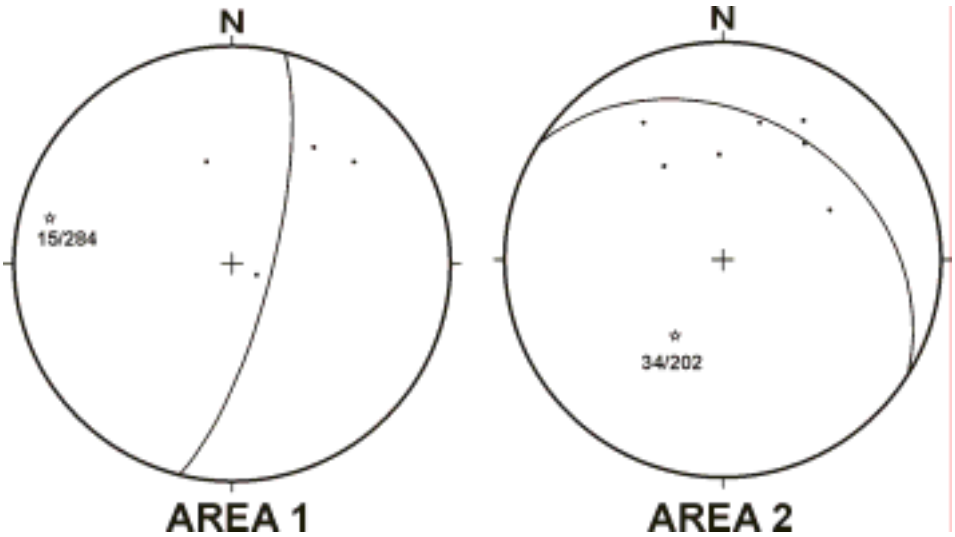

Figure 23: Representative geometries of D_3 fold structures which are modifying the initial F_2 fold geometry on Bukkemoen (locations are marked on Figure 18). The dots represent the poles to foliation. An average great circle is taken for these data and the normal to the great circle is the hinge plunge. These two stereonets clearly demonstrate that the D_3 fold modification is non-cylindrical and therefore highly unpredictable. This pattern is also seen at Vardfjellet.

5.3.6 Geitskaret

Geitskaret was not studied in great detail in the 2001 field season due to it's original low priority and also because of bad weather conditions combined with rough terrain. However, more extensive work was attempted in 2002. The observations made here are summarised below.

The Geitskaret deposit consists of an overall synform geometry with several anticline-syncline pairs were observed based on small-fold relationships in the acid gneiss in the immediate ground 400-500m west of the amphibolitic gneiss which hosts the rust zones. This suggests that the structures in the amphibolitic gneiss are therefore hosted in a more complex structural framework than that shown from the existing mapping. The most westerly of the two rust zones marked on the existing mapping of Heldal & Lund (1987) is no more than a mild orange discolouration of the host amphibolitic gneiss. The existing model of Heldal & Lund of a steeply south-plunging anticline fits well with the small-scale

fold observations made by this author. However, the northerly termination of both the major rust zones in this deposit appear to lie within minor synclines based on small-fold data. This accounts for their northerly termination.

Previously unmapped acid gneiss is found in the core of the major anticlinal structure a few metres south of Geitskarvatn.

The southward termination of rust zones in this deposit is clearly controlled by minor fold closures within the overall anticlinal structure. The small scale parasitic fold structures observed here are among the best seen in all of the graphite deposits and clearly control the outcrop pattern of the rust zones. For example, the thin rust zone which lies to the east of Geitskarvatn appears to terminate towards the south where it enters an F_2 parasitic fold hinge (see **Figure 24** at *Point A*).Several D_2 shear zones were observed in the Geitskaret deposit and have an importance for the outcrop pattern of the graphite. These are steeply-dipping and strike parallel to the F_2 axial planes. These appear to occur mostly on the margins between acid gneiss and amphibolitic gneiss and are testament to the development of ductile flexural slip between the layers of differing competence. These structures can also occur completely enclosed within the acid gneiss. The appear in the field to involve a concentration of the folded S_1 fabric and these S_2 fabrics appear to be mylonitic in places. However, they clearly truncate the syncline termination hosting the graphite to the south of Geitskarvatn. These structures are in places often associated with quartzite bands within the acid gneiss.

A rust zone which has been mapped near the northern closure of the deposit is in fact a red stained, hydrothermal altered layer within the amphibolitic gneiss (*Point*

B on **Figure 24**). Unfortunately, no thin section was made of this sample but the large, dark crystals present in outcrop are most likely hornblende whereas the white groundmass is made up of calcite and a feldspar. This lithology is interpreted as forming from the hydrothermal alteration of the amphibolitic schist. This layer, however, appears to have sharp contacts with the surrounding amphibolitic schists (**Figure 25**).

This 'hydrothermal unit is mappable as a separate unit but is not observed elsewhere in Senja. This has clearly been omitted from the previous mapping.

The Geitskaret deposit appears to be unaffected by F_3 folding but the outcrop pattern appears to be strongly dislocated by the presence of D_3 faults or shear zones. These were not observed in outcrop but there presence has been inferred from F_2 fold segmentation and the presence of stark gullies in the topography. The outcrop pattern of the F_2 fold in the south of the Geitskaret deposit on the col is clearly affected by F_3 folding. The southern termination of the Geitskaret deposit appears to be controlled by an extremely overtightened F_2 fold hinge.

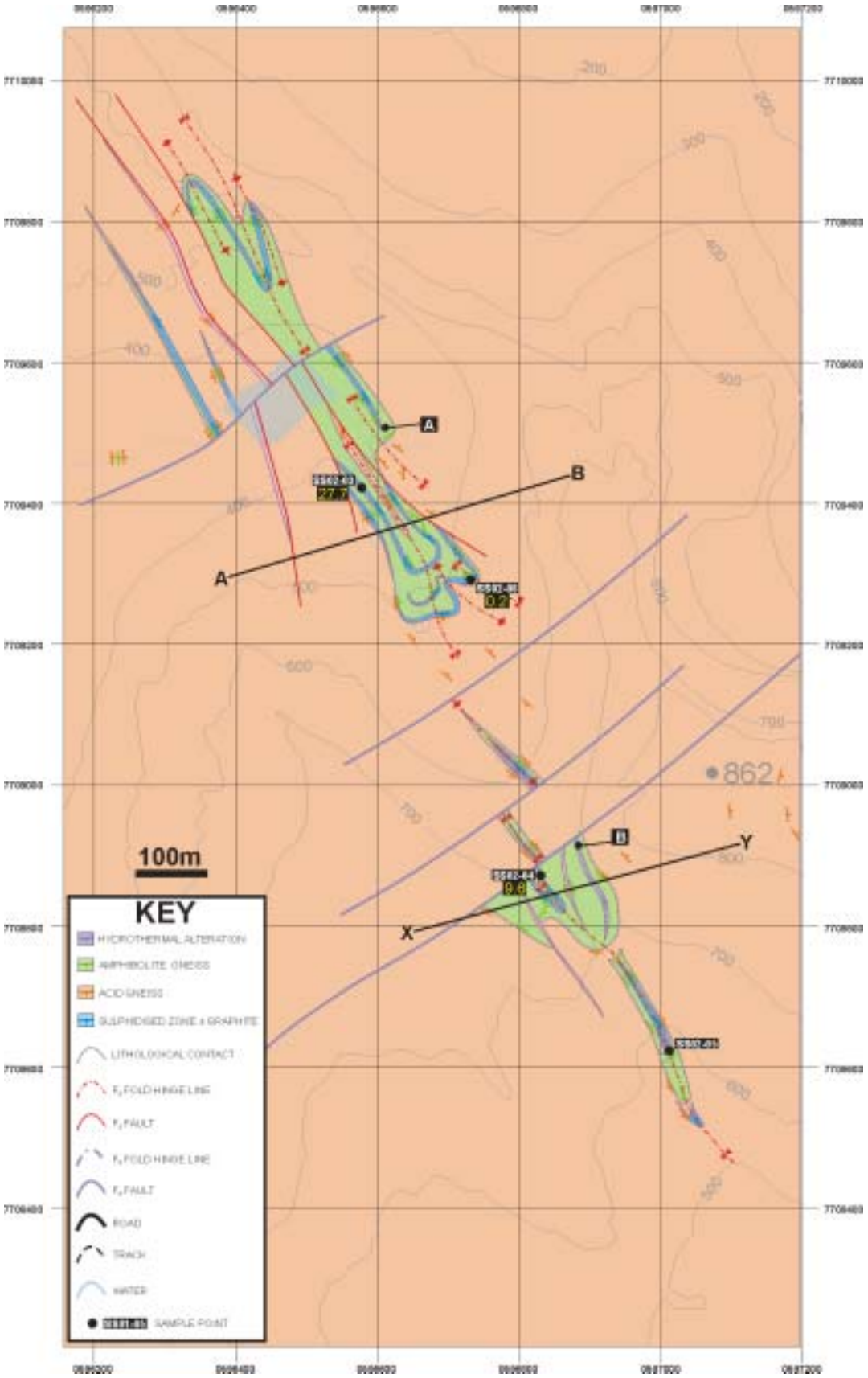

Figure 24: Detailed mapping from Geitskaret deposit. The full size mapping and cross-sections are *Enclosure 5* in the map pocket.

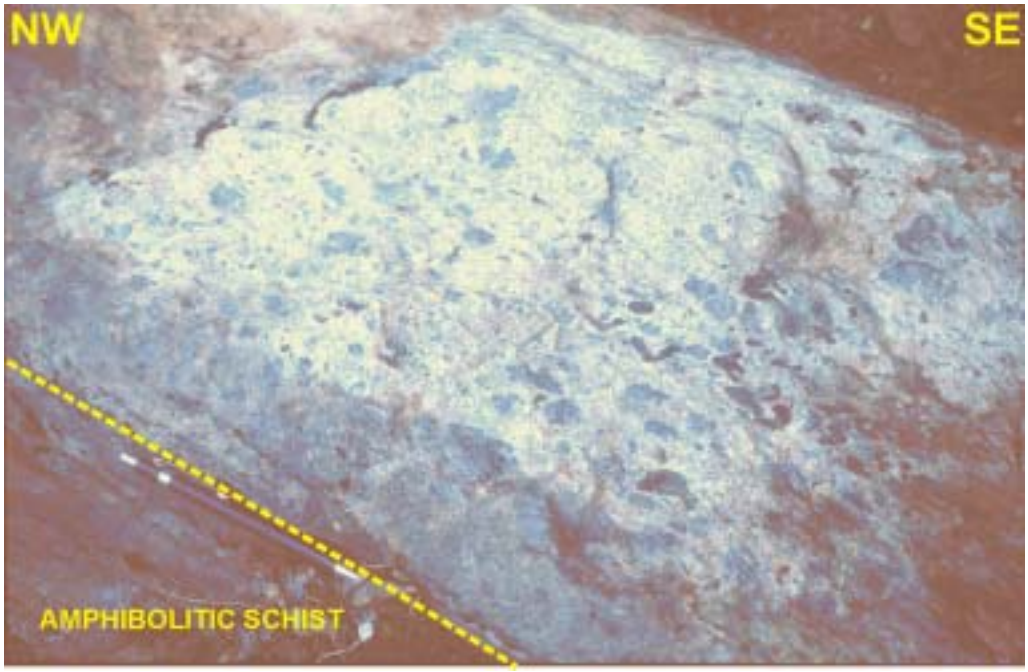

Figure 25: Hydrothermally altered layer occurring solely in the Geitskaret deposit.

Graphite analyses from this deposit give greater optimism for this deposit than had been previously expressed by Johannesen (1989). Three samples were analysed giving a range of 0.2-27.7% total organic carbon. There appears, like Bukken, to be no systematic relationship between structural location and graphite grade, or related to geographical location in the deposit. However, there are probably too few samples from this deposit to be certain about this hypothesis. However, this author is in agreement with Johannesen (op.cit.) regarding the extent of the deposit. This deposit is rather geographically limited with thin graphite lenses and it's geometry is clearly 'degraded' due to the segmentation of the deposit by D_3 fault structures.

5.3.7 Vardfjellet

The Vardfjellet deposit has been mapped over two field seasons from 2001 and 2002 and forms the most geographically extensive of the deposits studied here. Previous mapping by Heldal and Lund (1987) identified a 200m wide by approximately 500m long 'lense' of graphite to the west of Vardfjellet summit. This study has identified

additional graphite zones and mapped the area identified in previous mapping in more detail. In total, an area of approximately 8km^2 has been mapped at a scale of 1:6250 (see **Figure 26**).

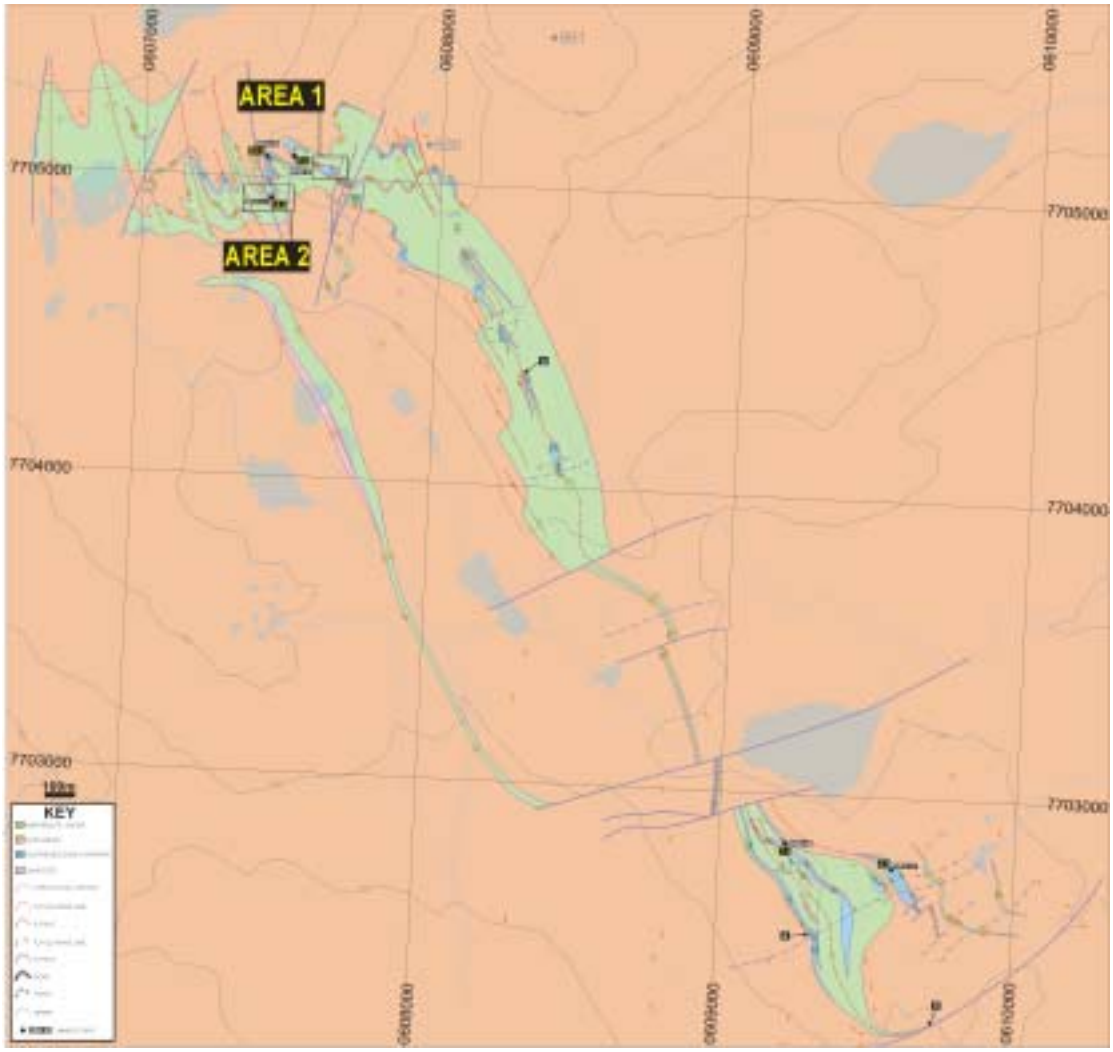

Figure 26: Detailed mapping from the Vardfjellet deposit. The full size mapping and cross-sections are *Enclosure 6* in the map pocket.

Two main graphite deposit areas have therefore been identified within the Vardfjellet deposit as a whole. The southern deposit, lying on the Hesten Summit, is referred to as 'Hesten'. This has not been previously recognised from existing mapping at a scale of 1:50 000. It consists of a SSE plunging F_2 syncline of amphibolitic schist within the acid gneiss. The amphibolitic schist is a thick lense across the Hesten summit but rapidly thins both north and south. Several thin and visibly poor quality graphite

lenses are present within the amphibolitic schist. The concentrated presence of D_3 folding in the area around this part of the deposit has tectonically widened the amphibolitic outcrop. One large scale WSW-ENE D_3 fold is interpreted intersecting the Hesten summit but several are seen as small folds in outcrop (*Point A* on **Figure 26**). The main D_3 fold here is an open anticline plunging steeply to WSW (**Figure 27**). An additional lense of graphite has been identified to the east of the Hesten summit in a thin amphibolitic package contained within a D_2 anticline. This graphite lense is not geographically extensive and is not interpreted to extend to any great depth. Its northern extent is terminated by the D_2 fold closure and its southern extent appears to be terminated by D_3 fault structures. However, these outcrop relationships demonstrate that D_3 modification has enhanced a 'rust' zone in this location and demonstrates the importance of D_3 structures in creating additional deposits of graphite.

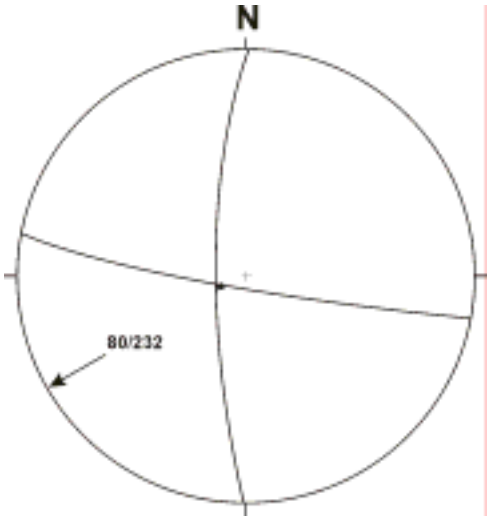

Figure 27: Stereonet of small fold observations made on the top of Hesten suggesting the presence of a D_3 fold which appears to have tectonically thickened the amphibolitic/graphite schist package. The closed lines represent the fold limbs and their intersection point is the fold direction and plunge.

Moving north from the 'Hesten' deposit towards the main (and previously mapped) part of the Vardfjellet deposit, the NS-striking amphibolitic syncline becomes very

thin. This appears to be the result of D_3 faulting which is extensive in the zone north of Hesten. This 'thinning' suggests a considerable displacement on the D_3 fault structures to expose a different part of the F_2 fold structure. Four inferred D_3 fault structures are passed before the amphibolitic schist again becomes several hundred metres thick. In this zone on the 1:50 000 Heldal & Lund (1987) mapping a discontinuous band of graphite is shown. It is clear from this new mapping that the terminations of individual graphite lenses is due solely to the presence of F_2 parasitic fold closures (e.g. *Point B* on **Figure 26**). Many fold closures occur associated with the presence of acid gneiss north of the individual rust zones on the way up hill towards Vardfjellet. This gives a side-stepping parasitic form and not a straight outcrop pattern as is shown on the Heldal & Lund map.

The main part of the deposit just to the west of the Vardfjellet summit has previously been interpreted on the 1:50 000 map of Heldal and Lund (1987) and also in the regional mapping of Zwaan (2003) as a 200m wide to several hundred metre long lense of graphite. This lense is elongated parallel to the F_2 foliation. However, the new mapping of this study reveals a more complicated picture. The deposit consists of not one graphite lense but at least 7 individual and isolated lenses within the amphibolitic schist country rock (**Figure 26**). None of these graphite lense is more than 5 metres wide. The main part of the deposit consists of a very complicated M-folding pattern related to the regional termination of a F_2 fold. This termination has previously not been interpreted from any 1:50000 scale mapping. At least 25 separate small-fold (m-fold) hinges have been identified within the F_2 fold termination.

The outcrop pattern of the graphite in relation to these m-folds strongly suggests that the graphite has been localised on the m-fold geometries. For example, where there is

no parasitic fold structure (i.e. straight NNW-SSE D_2 foliation) graphite is most likely not present.

Extensive acid gneiss lenses occur frequently as pods and lenses in the complex M-fold closures. This complexity had not previously mapped. An extremely interesting feature of the Vardfjellet deposit is the nature of the F_2 fold closures. These show a highly *non-cylindrical* behaviour. This means that the geometry of the small-fold closures does not mimic the geometry of the regional fold closure. For example, **Figure 28** shows that small folds from various places on the fold closure display completely different geometries. In reality, this creates significant problems in terms of predicting the location of fold structures at depth and of therefore providing a reliable structural model for potential mine workings.

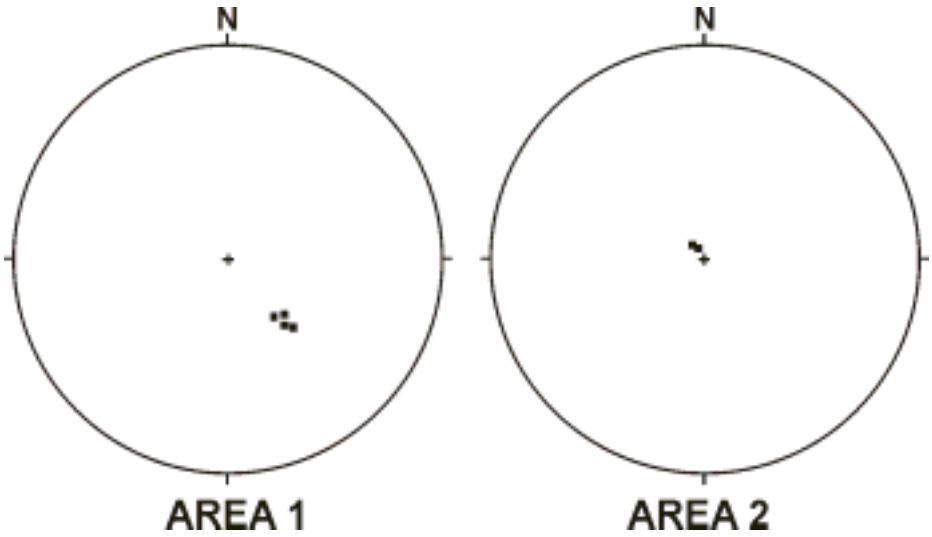

Figure 28: Stereonets comparing the orientation of F_2 small fold hinges within the m-fold regional scale fold termination. Areas are shown on Figure 26. This shows that the geometries are high variable, non-cylindrical and therefore unpredictable.

As a further complication to the F_2 m-folding, the regional F_2 fold termination in the northern fold closure is cut by late, sub-axial planar faults (see **Figure 26**). These structures are interpreted as D_3 shear zones as they do not follow the F_2 foliation but appear to cut straight across the F_2 structures. These structures appear to have large

displacements (up to 300-400m) and appear to increase in displacement towards the west. They displace and completely cut out the graphite/amphibolitic schist package which should exist on the western limb of the regional scale F_2 fold structure. The western limb of the F_2 amphibolitic schist package does not exist. This absence is testament to the control of the tectonic structures on the presence and geometry of the graphite deposits.

North of the northern fold closure of the amphibolitic schist, north-south trending acid gneiss appears to be juxtaposed against the E-W trending amphibolitic gneiss on a regional scale. Although there was no time available to observe these outcrops (which were at several kilometres distance to the north of the Vardfjellet deposit), this may suggest that an E-W regional fault (F_3) is responsible for the development of F_3 folds, which therefore terminate the amphibolitic gneiss outcrop.

However, it is without a doubt clear that the D_3 shear zone structure play an important part in terminating the southern part of the deposit south of 'Hesten'. The F_2 fold hinges are rotated into a major fault structure here and then disappear to the south of the shear zone (*Point C* on **Figure 26**). This is a sinistral shear zone. It is rather important to note at this stage, prior to a discussion on the regional significance of these D_3 structures, that a NE continuation of the strike of this shear zone structure towards Bukkemoen would essentially also terminate the north-westward continuation of the graphite deposits on Bukken. The outcrop pattern of folding on Bukken and the topographic relationships there suggest that a major fault zone lies in the valley to the north-west of Bukken and that the shape of the graphite deposits there show a D_3 deformation related to sinistral shearing on a major structure to the north-west. Such speculations are discussed in the next chapter (**Section 6**) on regional considerations.

5 samples were taken for graphite analysis from the Vardfjellet deposit. These show a range from 3%-34.3 total organic carbon. This deposit is the best deposit with regard to graphite content of all of those deposits studied, showing the highest graphite grades. Two samples taken from 'Hesten' show a slightly lower average grade than those samples from the northern part of the deposit at the fold closure. This may be related to enhanced concentration of the graphite related to the F_2 fold structures. However, it is clear that the presence of layers of graphite on the Hesten is coincident with D_3 deformation.

5.4 Summary of graphite analyses

Table 2 shows the graphite analyses which have been carried out on this study. This section briefly summarised the observations made for the individual deposits.

Sample No.	Deposit	%TOC	Comments
SS01.01	Bukkemoen	2.05	Lowest sample on stream section. F_2 limb.
SS01.02	Bukkemoen	5.07	Same structural position as SS01.01. Upstream.
SS01.04	Bukkemoen	5.56	In open F_3 fold hinge.
SS01.05	Bukkemoen	6.48	F_2 axial planar fault zone.
SS01.06	Bukkemoen	0.48	In thick F_2 fold termination.
SS01.07	Bukkemoen	3.74	In tight F_3 fold hinge at southern part of ridge.
SS01.08	Bukkemoen	3.67	In tight F_3 fold hinge at southern part of ridge.
SS01.09	Bukkemoen	10.00	In thin lense in F_2 fold structure on top of summit.
SS01.10	Bukkemoen	18.90	In thicker F_2 lense NW of summit.
SS01.11	Bukkemoen	2.00	In same lense as SS01.10. Further NE.
SS02.01	Vardfjellet	14.40	South plunging F_2 anticline hinge zone.
SS02.02	Vardfjellet	2.97	Limb of M-fold (F_2) at regional closure.
SS02.03	Geitskaret	27.70	Thin continuous lense on west limb of F_2 fold.
SS02.04	Geitskaret	9.59	Thin lense of F_2 folded graphite on col.
SS02.06	Hesten	7.84	Thickest lense on summit of Hesten.
SS02.07	Hesten	3.99	Subsidiary lense east of Hesten summit.
SS02.08	Geitskaret	0.16	F_2 fold termination.
SS02.09	Vardfjellet	34.3	North plunging F_2 anticline hinge zone.

Table 2: Summary of graphite analyses (%TOC) for the samples analysed in this study.

A total of 18 samples have been studied from three different deposits. These deposits appeared to have the best visible graphite in relation to the other deposits from which no samples were taken. The most striking feature of these graphite analyses is that they display a very wide range. However, there appears to be no distinct increase in graphite content related to a particular deposit, perhaps with the exception of the northern part of Vardfjellet at the regional F_2 fold termination. At present, it is extremely difficult to determine whether the large variation, on a regional scale but also very often on a deposit scale, is related to structural geometry or deformation or whether it relates to initial organic carbon content of the lithologies. However, further work could focus on analyzing more samples to determine this.

5.5 Gold analyses

Gold analyses were also carried out on the same set of samples which were analysed for total organic carbon. These analyses showed particularly disappointing results (**Table 3**). All samples were ubiquitously poor in gold, lying very near the lower detection limits.

Sample No.	Deposit	Au (ppm)	Comments
SS01.01	Bukkemoen	0.004	Lowest sample on stream section. F_2 limb.
SS01.02	Bukkemoen	0.0150	Same structural position as SS01.01. Upstream.
SS01.04	Bukkemoen	0.003	In open F_3 fold hinge.
SS01.05	Bukkemoen	0.009	F_2 axial planar fault zone.
SS01.06	Bukkemoen	0.003	In thick F_2 fold termination.
SS01.07	Bukkemoen	0.007	In tight F_3 fold hinge at southern part of ridge.
SS01.08	Bukkemoen	0.008	In tight F_3 fold hinge at southern part of ridge.
SS01.09	Bukkemoen	0.005	In thin lense in F_2 fold structure on top of summit.
SS01.10	Bukkemoen	0.008	In thicker F_2 lense NW of summit.
SS01.11	Bukkemoen	<0.002	In same lense as SS01.10. Further NE.
SS02.01	Vardfjellet	0.060	South plunging F_2 anticline hinge zone.
SS02.02	Vardfjellet	0.004	Limb of M-fold (F_2) at regional closure.
SS02.03	Geitskaret	0.002	Thin continuous lense on west limb of F_2 fold.
SS02.04	Geitskaret	0.012	Thin lense of F_2 folded graphite on col.
SS02.06	Hesten	0.011	Thickest lense on summit of Hesten.
SS02.07	Hesten	0.004	Subsidiary lense east of Hesten summit.
SS02.08	Geitskaret	0.011	F_2 fold termination.
SS02.09	Vardfjellet	0.009	North plunging F_2 anticline hinge zone.

Table 3: Gold analyses for the same samples studied for total organic carbon in Table 2

5.6 Summary of structural observations

This section summarise briefly the main points to be gleaned from the preceding chapter. The critical observations can be summarised as:

- 7 deposits have been studied (Trælen, Skaland, Vardfjellet, Geitskaret, Krokelvdalen, Bukkemoen, Finnkona), 4 of these have been mapped in detail at a scale of 1:5000 (Vardfjellet, Bukkemoen, Geitskaret and Krokelvdalen) and two detailed sections have been made at a scale of 1:400 of parts of the Trælen deposit (North of Lyktegangen and Lyktegangen)

- Previous mapping at a scale of 1:50 000 by Heldal & Lund (1987) and at 1:2500 on Trælen by Heldal & Flood (1985) are generally of a very high quality and describe accurately the critical geometries.

- Several deposit show mostly F_2 fold geometries (Skaland, Krokelvdalen and Geitskaret) where the graphite appears confined and localized in the F_2 fold hinges and parasites. However, the new 1:5000 and 1:400 mapping shows a very much greater complexity in the amount of parasitic F_2 folds present and shows that F_2 parasitic fold terminations are often responsible for the termination of graphite layers.

- Several deposits (Finnkona, Trælen, Bukkemoen and Vardfjellet) are greatly affected by F_3 fold deformation and have complex geometries due to the interference of F_2 and F_3 fold geometries. Where D_3 fold structures are concentrated extensive graphite lenses are present, suggesting that the D_3 deformation has been, in part, responsible for graphite remobilisation.

- D_3 shear zones are also important factors in deposit geometry as they often delimit the margin deposits by shearing out the graphite lenses or the amphibolitic schists that host them. Large-scale regional D_3 structures are interpreted to be responsible for creating the D_3 fold structures. These are interpreted as drag folds on the ductile shear zones.

- In two deposits (Finnkona and Trælen) which both lie near to the south-bounding Svanfjellet Shear Zone, D_3 folds are interpreted to be very developed. It is here that a further fold episode is identified locally (D_4) which folds the F_2 and F_3 folds and produces very complicated outcrop patterns of graphite outcrop. This observation is critically important in the proposed further development of the Trælen deposit.

- Graphite analyses show grades up to 37% total organic carbon. However, there is no systematic variation in graphite grade between different deposits and in specific structural geometries. However, a more rigorous and comprehensive sampling campaign needs to be carried out within the structural framework established from this study.

6. Regional observations

It was necessary to make some regional observations of structural relationships within the Senja Shear Belt (SSB) for a number of reasons. These were:

- To place the graphite deposits and their associated structures in a more regional context
- To provide more kinematic information on the regional scale structures and to place these structures within a kinematic and process-oriented framework.

A key aim of this part of the field work was to examine the crustal-scale Svanfjellet Shear Zone (**Figure 29**), which forms the southern tectonic margin to the Senja Shear Belt (**Figure 33**).

Figure 29: Very intense mylonitic foliation in the Svanfjellet Shear Zone. The light and dark layers represent alternately more feldspathic and more mafic segregations. The rock type was most likely acid gneiss before shearing.

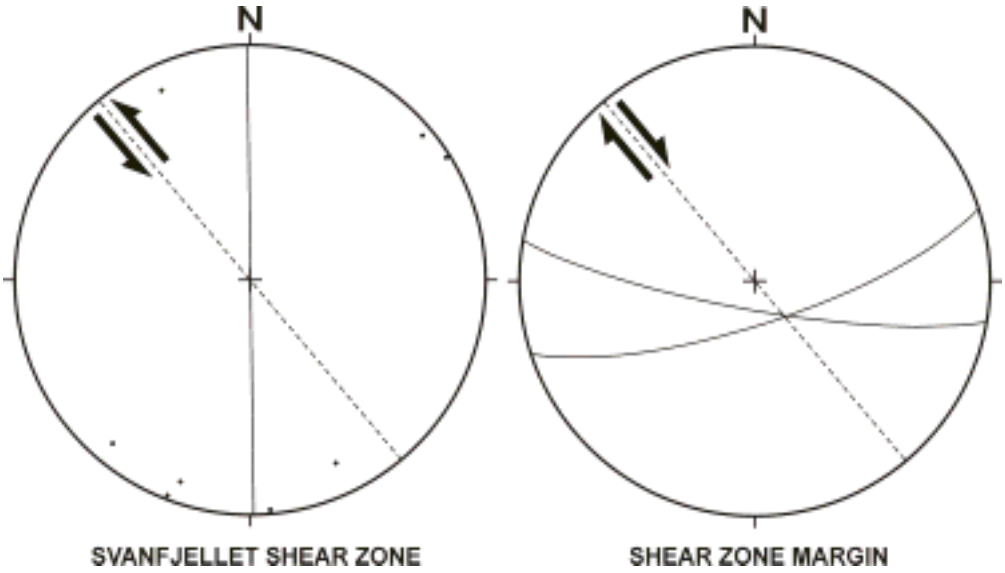

Figure 30: Stereonet of small-fold hinge plunges from within the Svanfjellet Shear Zone (Left) and on the northern margin of the shear zone (right). This shows that the shear zone itself displays a sinistral shear sense due to the fold asymmetry relative to the shear zone margins. However, the quartzite on the northern margin of the shear zone displays a dextral geometry from it's small-folds. This is interpreted as a reactivation of the Svanfjellet Shear Zone.

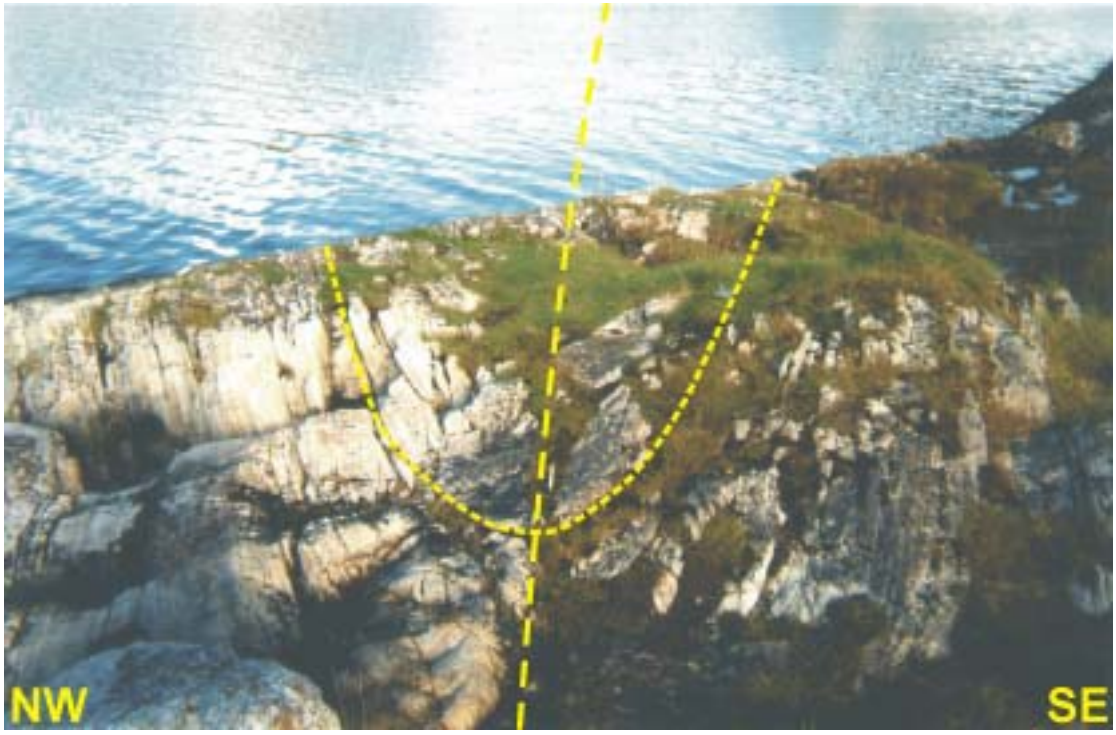

Figure 31: Small folds in a previously unmapped quartzite on the northern margin of the Svanfjellet Shear Zone. The orientation of the small folds suggests dextral shearing, contrary to the regional scale kinematics. This may suggests that some reactivation has occurred after initial sinistral shearing. This hypothesis has implications for the geochronology in Section 7.

The northern margin of the shear zone at the contact with the Senja Shear Belt was examined. This structure was examined for kinematics in a number of localities. However, the best locality was found at 0589691, 7700868 (*Point A* on **Figure 33**). Figure 30 shows several stereonets from this locality. The first stereonet is from within the Svanfjellet shear zone. This shows small-fold hinges which are rotated approximately 30° anti-clockwise from the orientation of the shear zone margin. This demonstrates that the shear sense for the main part of the Svanfjellet Shear Zone is sinistral, the small folds forming drag-folds in the shear zone fabric. However, on the northern contact zone of the shear zone the kinematic picture is more complicated This contact zone consist of a thin sliver of pure quartzite (**Figure 31**). Small-folds in this lithology provide much information on the kinematics of the shear zone. The shear zone small-folds have upright axial planes which are oriented approximately 20° anti-clockwise of the margins of the shear zone. This suggests a dextral shear sense on the shear zone (**Figure 30**; stereonet on right). Acid gneiss 20m into the Senja Shear Belt to the north are rotated into parallelism with the shear zone. This suggests a sinistral sense of shear on the shear zone, opposite to the evidence provided from the small-folds. This contradictory evidence clearly demonstrates that the shear zone has had a complex, multi-kinematic history.

This evidence, therefore, suggests that the Svanfjellet Shear Zone has had at least two episodes of movement, with different sense of shear. It is clear that the main sense of movement was sinistral, due to the bending in of the regional foliation into the shear zone, however, a late phase of dextral movement is suggested localised on the northern margin of the shear zone. The age of this dextral deformation episode is, as yet, unknown. It may be related to latest stage D_3 or to Caledonian movement, and may be responsible for the Caledonian ages of Dallmeyer (1992) amongst others.

SSW-NNE ductile shear zone structures in the Krokelvdalen (Section 5.3.3), Trælen (Section 5.3.2) and Lysvannet (Figure 32) deposits display similar kinematics to the Svanfjellet Fault Zone kinematics. These are preliminarily interpreted as being secondary shear structures related to movement on the Svanfjellet Shear Zone and are interpreted as mega-S-planes. Kinematic evidence from this shear zone (**Section 5.3.3**) also demonstrates that the main period of movement was sinistral and that this has been overprinted by a later, lower magnitude dextral movement.

Observations of amphibolitic-rich shear zones in several localities in the generally north-south striking acid gneiss shows that these shear zones are discordant with the regional foliation and are therefore tectonic discontinuities. These structures display reverse, thrust kinematics and are tentatively related to movement on the Svanfjellet shear zone.

Observations of the northern tectonic margin to the SSB, the Astridal Shear Zone, were limited to one outcrop. This structure displays an oblique-slip mineral lineation kinematic and an S-C fabric which suggests strike-slip kinematics. This provides additional data to strengthen existing models of tectonic activity in this zone.

Figure 33 provides a summary diagram of the possible relationship of the observed D_3 ductile shear zones in the Senja Shear Belt relative to the graphite deposits. This demonstrates that most of the graphite deposits are affected by SW-NE striking shear zones. Most of these shear zones display tens to several hundreds of metres of displacement of amphibolitic schists which host the graphite. These are considerable displacements relative to the complex F_2 and F_3 folding of the graphite. It is also noticeable that the deposits which have the greatest intensity of D_3 shear zones in their vicinity also have a large degree of D_3 fold modification. It is therefore clear that a

knowledge of the geometry and magnitude of the shear zone displacements and an understanding of the fold geometries is an important tool for further, predictive graphite prospecting.

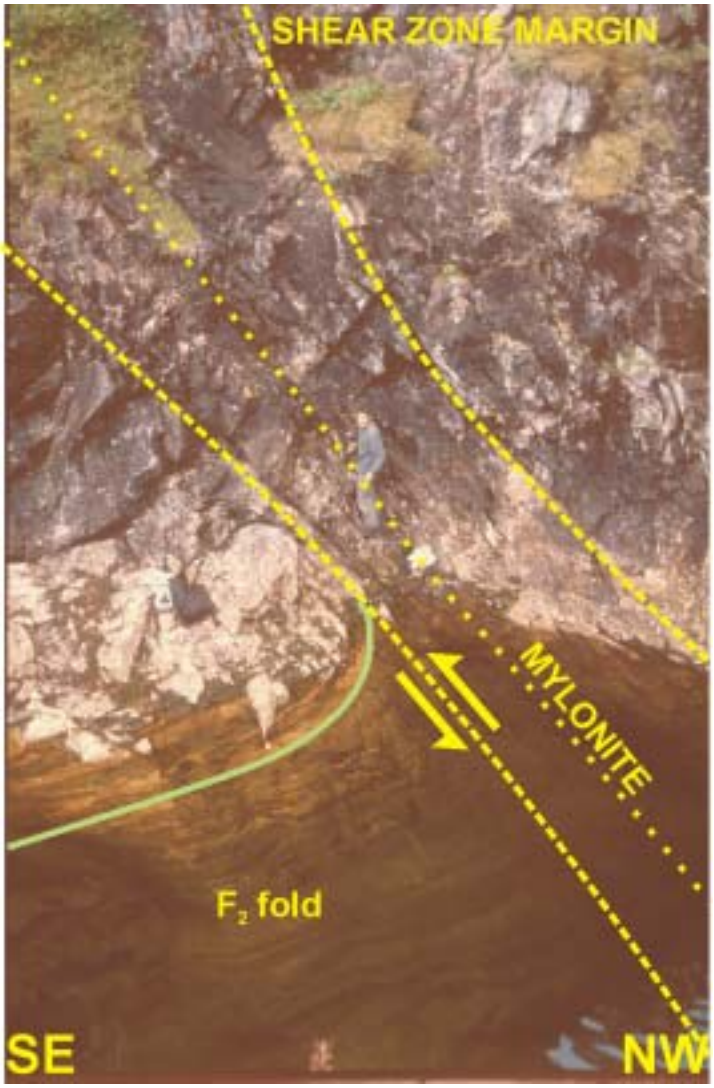

Figure 32: Mylonitic D_3 strike-slip shear zone south of the Vardfjellet deposit. The outcrop is located behind the hydro-electric power station west of Lysvannet. The shear zone is clearly D_3 as it deforms F_2 folds into its shear plane. The movement is sinistral. The shear zone is several metres wide, dips NW and has a mylonitic fabric over 10cm at its most intense core. This ductile shear zone is sinistral.

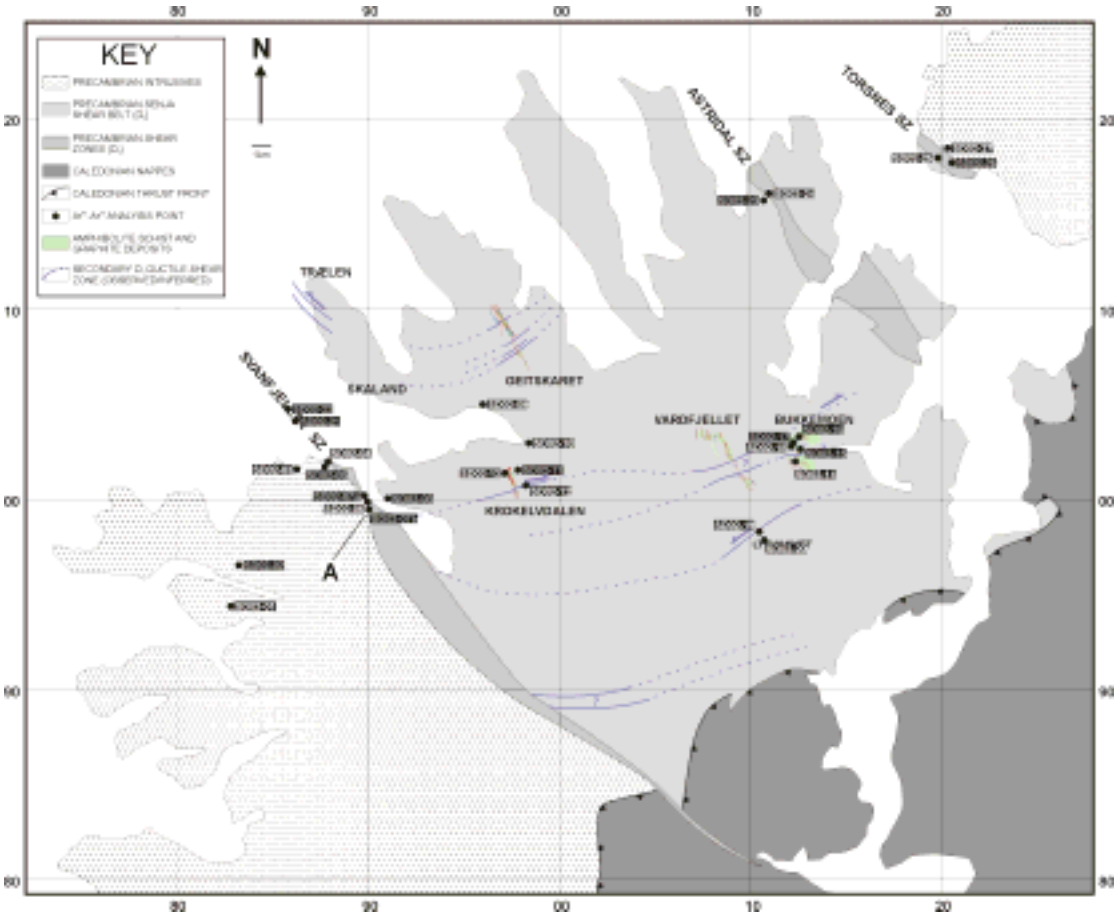

Figure 33:Structural interpretation from regional observations of the Senja Shear Belt and its surroundings.

7. ^{40}Ar-^{39}Ar Geochronology

7.1 Introduction

The geographic location of economic graphite mineralisation on the Island of Senja is controlled by the region's structural geology. In this part of the report we outline geochronological work within the Senja shear belt that has focused on D_3 structures related to the most recent phase of graphite remobilisation. This work was undertaken to further constrain the timing of deformation and to improve our understanding on the controls of graphite mineralisation. We begin by summarising key aspects of the structural geology and existing constraints on the timing of deformation.

7.2 Structural Framework

The Senja Shear Belt (SSB) exposed on the northern half of Senja to the west of the Caledonian nappes comprises an area bounded by two crustal-scale shear zones. The Svanfjellet Shear zone lies to the south and the Torsnes/Astridal Shear zones to the north (**Figure 33**; detailed in **Section 6**). The area bounded by these shear zones consists of isoclinally folded amphibolitic and K-feldspar-rich gneissic basement rocks. The SSB is a part of the western gneiss region in northern Norway, a province composed predominantly of variably deformed granites and gneisses with Rb-Sr intrusion ages of 1.7-1.8 Ga. (Andresen, 1980; Krill and Fareth, 1984; Williams et al., 1985).

Three phases of deformation have been identified within the SSB. D_1 corresponds to formation of the gneissose fabric (c. 1.7 Ga; Krill and Fareth, 1984) and has also been reported as internal folds of protolith lithology within the Krokelvdalen deposit (Lund and Opheim, 1985). D_2 isoclinal folds deform the gneissic fabric and occur regionally with north-south axial planes (**Figure 34**). The final phase of deformation D_3 (Zwaan

1995, Pederson, 1997) includes formation of the Svanfjellet, Astridal and Torsnes shear zones and is seen in the Bukkemoen deposit where D_2 folds are folded in D_3 axial planes. Mapped on a regional scale it can be seen D_2 axial planes verge into the shear zones indicating a sinistral sense of slip within the SSB (**Figure 34**).

A new finding of this study is that minor shear zones striking NE-SW and NW-SE exist within the SSB and are intimately related to D_3 folding; having a constant angular relationship of approximately 25° to the bounding crustal-scale D_3 structures (**Figure 34**). Furthermore evidence detailed in **Section 6** demonstrates minor dextral reactivation of the Svanfjellet shear zone suggesting D_3 deformation may have occurred as several distinct events and/or reactivations. As economic graphite mineralisation is found mainly within D_3 fold hinges and associated with the newly identified D_3 shear zones, understanding the timing and nature of D_3 deformation is of critical importance to the construction of exploration models for graphite mineralisation. Because graphite mineralisation has been remobilised by D_3 structures and is often intergrown with new D_3 micas, it may be possible to establish an age for graphite mineralisation/remobilisation.

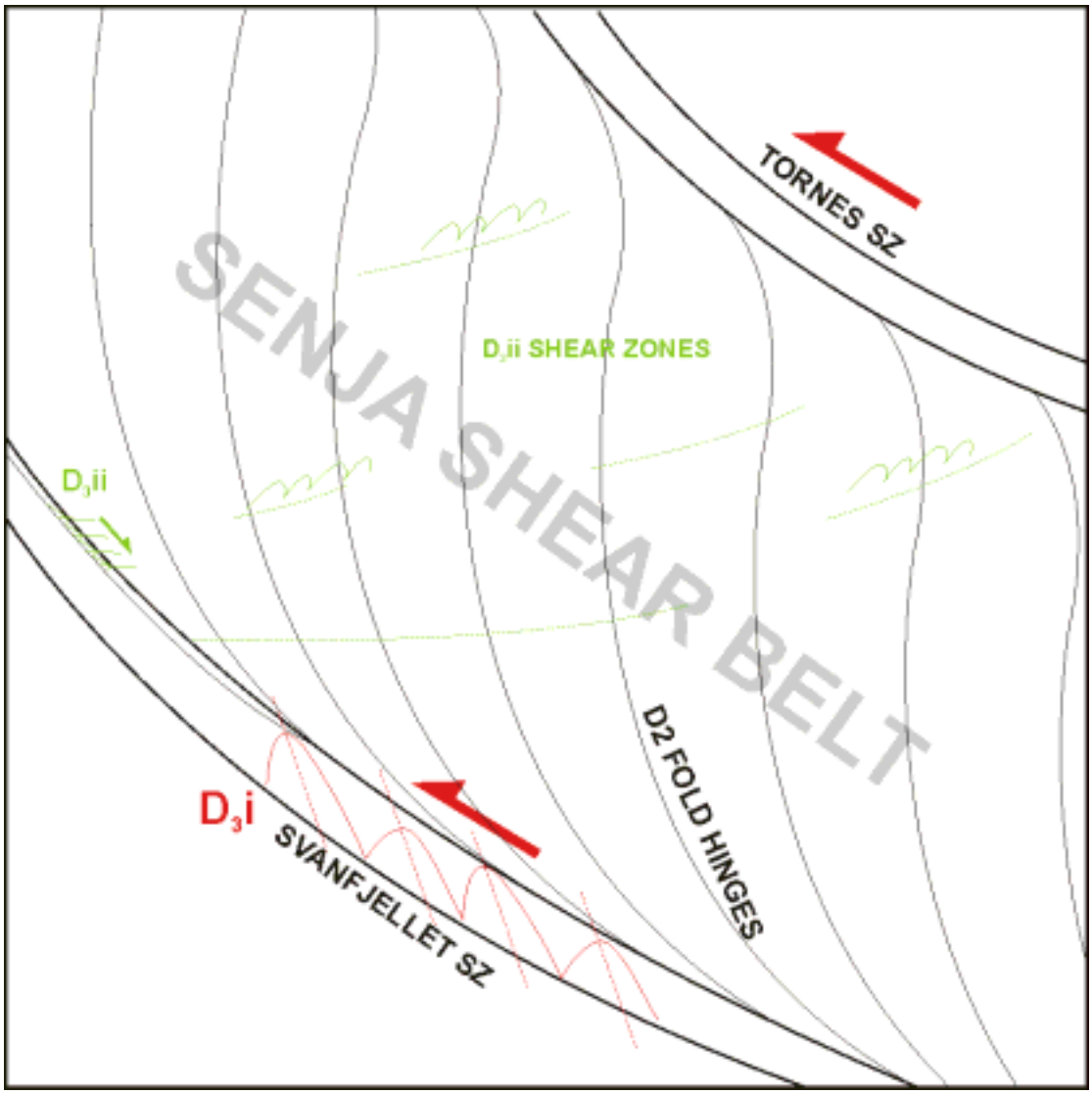

Figure 34: Schematic representation of the relationship between the bounding crustal-scale D_3 shear zones and the strike-slip shear zones and folds internal to the SSB.

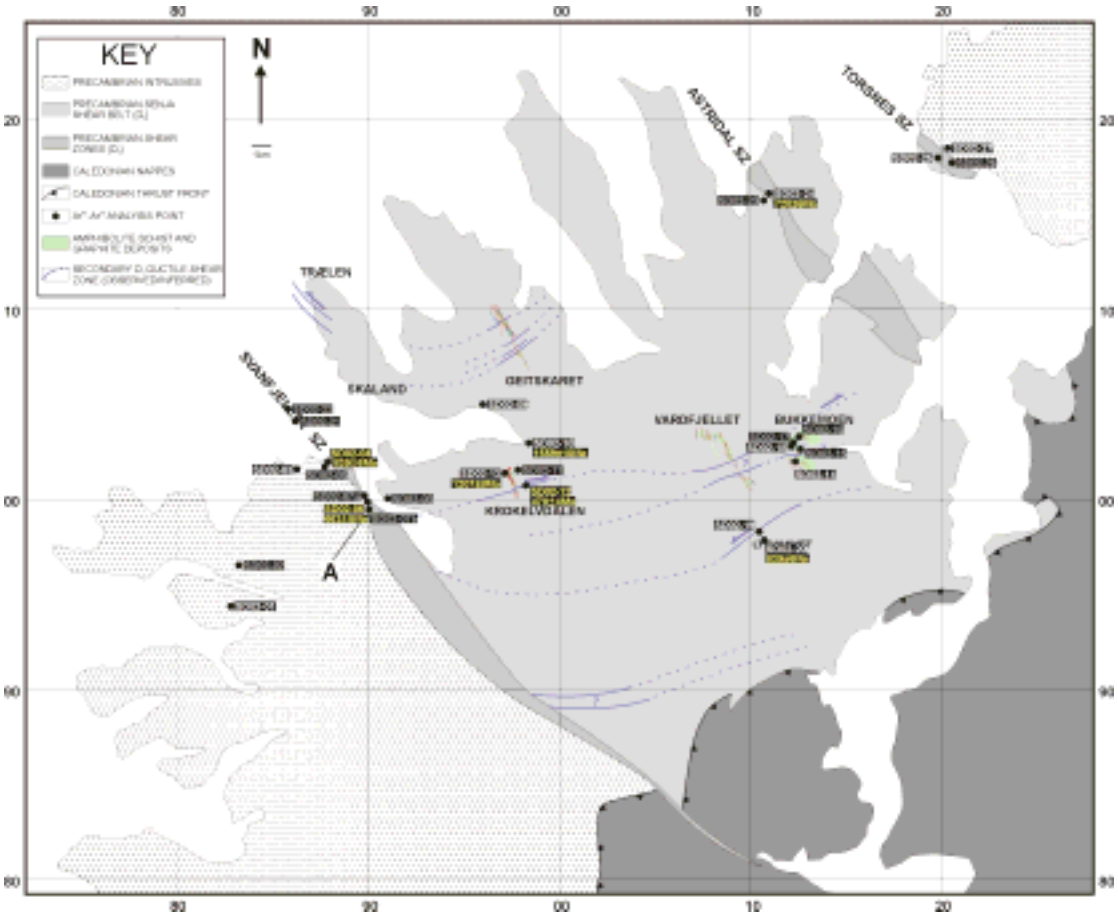

Figure 35: Sketch map over northern Senja and southern Kvaløya showing the main geological units, the critical structural features and ^{40}Ar-^{39}Ar age dates obtained so far. The age dates are shown in yellow.

7.3 Existing chronological constraints

Dallmeyer (1992) applied Ar-Ar dating to hornblendes from Senja and Kvaløya. The samples analysed exhibited Ar-loss giving poor spectra and ages ranging between that of the Rb-Sr protolith (D_1) ages, c. 1.7 Ga (Krill and Fareth, 1984; Williams et al., 1985), and well defined plateau at 941-916 Ma, interpreted to represent a second orogenic event (Dallmeyer 1992). Although these ages were in no way related to the structural fabric of the samples, the preservation of pre-Caledonian Ar-Ar ages in this part of the western gneiss region indicates that it may be possible to date the Precambrian deformation events including D_2 and D_3, by the Ar-Ar method.

The Svanfjellet shear zone cuts through the western gneiss region and bounds the southern limit of the study area (**Figure 35**). The shear zone offsets the western limit of the Caledonide deformation front by c. 4 km implying the shear zone was active during the closing stages of the Caledonian orogeny or at a later date.

The Caledonian orogeny and nappe assembly in this part of Norway has been constrained by several studies (see **Table 4**). Early Finnmarkian deformation ages of 481-432Ma are preserved in hornblendes from the Tromsø nappe complex, to the north of Senja (Dallmeyer and Andresen, 1992). In contrast Scandian rejuvenation ages of 430-410Ma dominate in the nearby Lyngen nappe complex, where hornblende and muscovite ages overlap each other characteristic of rapid cooling (Dallmeyer and Andresen, 1992). South of Senja in the Ofoten-Efjorden region the Narvik nappe complex is cut by dikes with U-Pb zircon ages of 437Ma providing a maximum age for tectonic assembly and metamorphism in this area (Northrup 1997). Furthermore, Ar-Ar studies in the Ofoten and Narvik nappe complexes yield typical hornblende ages of 425-394 Ma and muscovite ages of 400-360Ma, indicating a protracted cooling history (Coker et al., 1995, Northrup 1997).

Cumbest el al. (1994) undertook a detailed study of mylonitic hornblende from an amphibolite in the Svanfjellet Shear zone east of the Caledonian front and dated a phase of movement at 370Ma. This age is slightly younger than that of a nearby Rb-Sr age of 389±4 Ma (Hames and Sinha, 1985). These ages and the structural relationships therefore indicate that the Svanfjellet shear zone either formed during, or that a pre-existing shear zone was reactivated, by strike-slip deformation during the closing stages of the Caledonian orogeny after nappe emplacement (<400 Ma). Dallmeyer (1992) proposed that the Svanfjellet shear zone is a lineament of deep

significance separating two distinct crustal terranes. To the north on Senja Ar-Ar hornblende ages of 900-1700 Ma are distinct to those determined in the Lofoten area with predominantly Caledonian ages (Tull, 1977; Dallmeyer, 1992).

1.7-1.8 Ga	Western gneiss region protolith formation, D_1.
900 Ma	Orogenic event in western gneiss region inferred from Ar-Ar hornblende ages (Dallmeyer 1992). D_2 ?
c. 480 Ma	Finnmarkian deformation in Northern Norway, earliest Caledonian terrane accretion. Ar-Ar ages in the Tromsø nappe.
c. 430 Ma	Scandian deformation overprints earlier Ar-Ar ages in nappes surrounding Senja. Culminative stage of the Caledonian orogen, final continent-continent collision.
390-370 Ma	Strike slip movement on the Svanfjellet shear zone (D_3?), possibly related to orogenic collapse and extension as seen elsewhere in the Caledonides. The Caledonian nappes are offset.

Table 4: Timetable of geochronological events in Northern Norway.

7.4 Sampling rationale and objectives

In this study 25 samples have been collected in a profile through the Svanfjellet, Astridal and Torsnes shear zones and other potentially related structures within the Senja Shear Belt. The samples have been collected at varying distances from the Caledonian front to test for the possibility of Caledonian reactivation. Emphasis has been placed on the collection of well constrained D_3 shear fabrics with corresponding un-sheared, D_2 and D_1 background samples, sample locations are given on **Figure 35**.

Our understanding of the structural geology of Senja, and therefore of the factors controlling localisation of graphite mineralisation, will be improved in the following ways:

(1) Sampling of internal shear zones within the Senja shear belt in addition to the Svanfjellet, Astridal and Torsnes shear zones will test the contemporaneity of these D_3 structures.

(2) The extensive development of micas within the hinge zones of graphite-rich D_3 folds, especially on the summit of Bukkemoen, will enable the contemporaneity of the proposed D_3 folds and shear structures to be tested.

(3) Determination of a single age for all D_3 structures would confirm the structural model detailed in **Section 5**, and establish an age for graphite remobilisation on Senja.

(4) The profile through the Svanfjellet shear zone will test the proposal of Dallmeyer (1992) that the SSZ separates two distinct crustal terranes. Alternatively a terrane boundary may be unexposed in the 'sund' to the south of Senja.

(5) It may be possible to determine a preferred age for the D_2 fabric and test if this is the 900 Ma event alluded to by Dallmeyer 1992.

(6) If evidence is found for multiple episodes of deformation, collection of samples with varying distances from the Caledonian front will test the pervasivity of Caledonian reactivation.

(7) The work will improve our understanding of the Precambrian structure and deformation history in this part of northern Norway.

7.5 Preliminary results and discussion

Mineral separates have been obtained from the 25 samples collected in the field. From the different samples, one or more of; K-feldspar, biotite, muscovite or hornblende amphibole are available. In order to obtain these separates medium to fine grained

rocks must be crushed, milled, and sieved to obtain a mixture of loose mineral grains. Due to differing magnetic properties, habits and densities the individual mineral grains are then subjected to magnetic and gravity separation on a Wiffly table. Finally, a high purity mineral separate is achieved by hand picking under a binocular microscope. A complete sample set has now been prepared and is ready for irradiation. These results will be presented at a later date and are therefore outside of the scope of this report.

Preliminary results are however available from seven coarse grained rocks where it was possible to separate large biotite crystals using a knife prior to crushing. Data from these samples is presented graphically in **Figure 36** and summarised in **Table 3**. Good plateau have been obtained and are within error of isochron ages for 5/7 of the samples. The discrepancy in ages for sample SD02-04bio which has an isochron intercept of >2000, well above the atmospheric value of 295 indicates the presence of excess argon. Excess argon is argon not derived from atmospheric contamination or by radioactive decay of ^{40}K. It is often associated with ancient fluids trapped in fluid inclusions and has the effect of increasing a samples apparent age, as a result the lower isochron age is preferred. The discrepancy in ages for sample SD02-13bio which has a theoretically impossible isochron intercept of lower than the atmospheric value of 295, is attributed to the very poor fit of the isochron to the data; sums/(n-2) value of 258, and the older plateau age is therefore preferred. A comparison of ages, $^{40}Ar/^{36}Ar$ intercept values and the preferred sample ages are presented in **Table 5**.

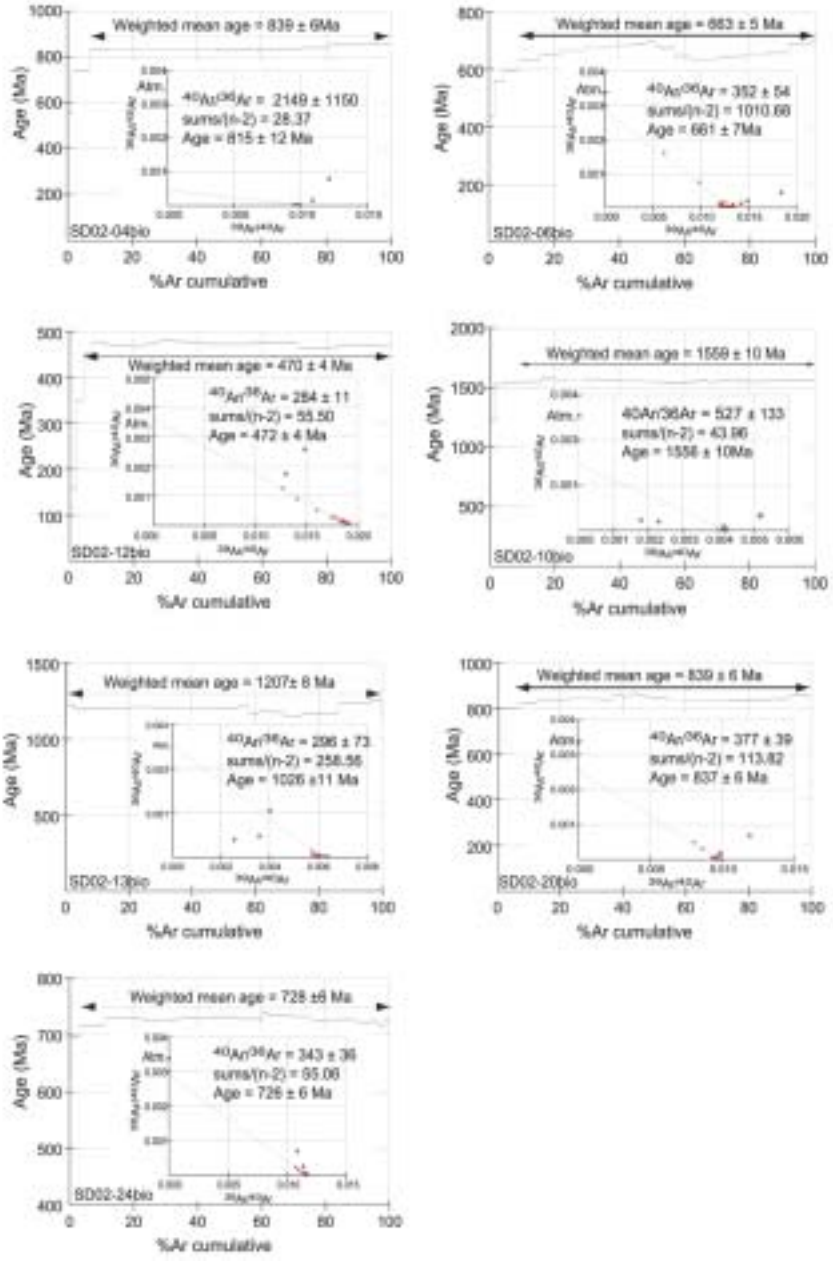

Figure 36: Graphical display of ^{40}Ar-^{39}Ar for samples analysed to date from Senja. An age spectrum plot with an inset inverse isochron diagram is shown for each sample. The age spectrum plot displays the apparent age of the sample on the vertical axis and the progress of the reaction on the horizontal axis as a percentage figure. The age of a sample is also calculated form the slope of the inset inverse isochron. Where the slope has a ^{40}Ar-^{39}Ar intercept of greater than 295 (plotted as the inverse) the presence of excess argon is implied an accounts for the discrepancy between the apparent ages calculated and the age calculated for the inverse isochron. The sums/(n-2) is a statistical measure of the goodness of fit. Values of greater than 50 indicate that the isochron regression is a poor fit and the age spectrum therefore gives a better measure of the samples age. Preferred ages are summarised in Table 4 and explained further in the text.

The samples analysed to date show a large spread of ages from the youngest early Caledonian age of 470 Ma, up to Proterozoic ages of 1560 Ma, approaching the D_1 protolith age of 1.7-1.8 Ga. The good plateaus determined (**Figure 36**) provide confidence that the ages determined are real and do not favour resetting of the Ar clock by partial Ar loss. The analysis of further samples, and especially the analysis of different minerals from some of the samples already analysed will provide a more complete picture of Senja's thermal history, and only then can proper attempts be made at answering the questions proposed above. However, the spread in ages which are oldest in the D_2 fabrics and younger in D_3 shear zones reflects the complex history of the western gneiss region in northern Norway and suggests that D_3 deformation may have been a multiphase event.

Sample			$^{40}Ar/^{39}Ar$ age		$^{40}Ar/^{36}Ar$	Sums /(n-2)	Preferred age (Ma)	Notes
			WMA	Iso. age				
Oldest ages obtained from D_2 rocks between the SSZ and ASZ								
SD02-20bio	Background to a relay zone	D2	839 ± 6	837 ± 6	377 ± 39	113.82	**839 ± 6**	
SD02-13bio	Amphibolite	D2	1207 ±8	1026 ± 11	296 ± 73	258.56	**1207 ± 8**	Poor fit to isochron
SD02-10bio	Regional shear zone	D3 or D2.5 ?	1559 ± 10	1556 ± 10	527 ± 133	43.96	**1559 ± 10**	Possible presence of fluids; excess Ar?
Younger ages obtained from the bounding D_3 shear zones								
SD02-04bio	Deformed gneiss part of SSZ	D3	839 ± 6	815 ± 12	2149 ± 1150	28.37	**815 ± 12**	excess argon
SD02-06bio	Deformed gneiss part of SSZ	D3	663 ± 5	661 ± 7	352 ± 54	1010.68	**663 ± 5**	Very poor fit to isochron
SD02-24bio	Highly deformed amphibolite part of ASZ	D3	728 ± 6	726 ± 6	343 ± 36	55.06	**728 ± 6**	
The youngest age obtained from a D_3 relay structure								
SD02-12bio	Shear zone relay structure D3	D3	470 ± 4	472 ± 4	284 ± 11	55.50	**470 ± 4**	

Table 5: Preliminary geochronology results obtained so far from the ^{40}Ar-^{39}Ar dating method. All samples are biotite.

8. Recommendations for further work

This section takes the key observations from the various types of data (structural analysis, sample analysis, regional observations and geochronology) and attempts to draw out the key areas in which more work is required. These additional areas of research can be summarised under their respect headings

8.1 Structural analysis

Several aspects suggest avenues for further research in the area on the deposits already studied. These are:

- The detailed sections constructed during this study from the 2 localities on Trælen demonstrate the very complex nature of the structural geology here and of the need for further study, particularly on the graphite lenses which had been planned for mine development.
- Detailed study on the Geitskaret was rather limited due to bad weather in the first filed season and due to the nature of the precipitous topography. Therefore, determination of the exact nature of the deposit terminations both north and south was imprecise. It would therefore be desirable to carry out more detailed study on this deposit.

8.2 Sampling

Only 18 samples were sampled and analysed for total organic carbon content. When the complexity of the structural geology is considered, it is not clear whether the large variation of the carbon grade is related to structural location or to primary lithological considerations. Therefore further work should be focussed in collecting a representative set of graphite samples, around a fold structure and on different types of fold structures (D_2 and D_3) with varying proximity to D_2 and D_3 fault systems.

8.3 Regional Geology

The regional geological observations which have been carried out during this study have been limited due to the need for concentration on a smaller scale, i.e. the detailed mapping of the graphite deposits. Further regional study should concentrate on:

- Identification of more examples of the D_3 ductile shear zones within the Senja Shear Belt
- More detailed work on the bounding shear zone to determine their complex kinematics and perhaps to determine their precise relationship to the D_3 shear zones internal to the Senja Shear Belt.

8.4 Geochronology

A remaining group of approximately 25 samples are in the process of being separated and hand-picked for amphiboles, and feldspars. These samples will be irradiated in the first half of 2003 and will be ready for analyses at some point in the second half of 2003. These samples should provide a better framework for interpreting the geochronological data already presented in this report and should go a long way to determining the precise timing relationships between the complex structural framework and the mineralisation.

9. Conclusions

- In, general, the quality of the structural mapping carried out by Heldal & Lund at a scale of 1:50 000 is excellent. The contribution of this new work is to add more detail to the basic structural framework already established.

- Four of the deposits, Bukkemoen, Krokelvdalen, Vardfjellet and Geitskaret have been newly mapped for structures in detail at a scale of 1: 5000.

- The Bukkemoen deposit is a much more extensive deposit than originally suggested on the Heldal & Lund mapping. It's geometry is wholly determined by D_3 folding suggesting that the presence of D_3 folding is a prerequisite for the remobilisation and enhancement of the graphite ore.

- Detailed work on Geitskaret, Krokelvdalen, and Vardfjellet have shown that the fold closures to the deposits are very complex and the deposit geometry is controlled by axial planar displacements on faults and by up-folding due to D_3 deformation.

- The outcrop pattern of rust zones is greatly controlled by the presence of secondary parasitic folds. Where these folds are present the mapped outcrop of the rust zones terminates on the Heldal & Lund 1: 5 0000 scale map.

- Detailed mapping on the Trælen deposit in two locations at a scale of 1:400 has revealed the complex nature of the interplay between different deformation episodes and fold geometries.

- Analyses on the graphite shows grades of up to 37% total organic carbon but no systematic variation between different deposits and no systematic

relationship to structural development. However, it appears that the aerial extent of graphite is more extensive where D_3 structures has modified the deposits.

- The crustal shear zones bounding the SSB have complex strike-slip kinematics suggesting more than one phase of movement. The SSW-NNE ductile shear zones cutting the SSB can be kinematically related to these structures and to the D_3 modification of the graphite deposits within the belt. These structures will be placed within a process-oriented model to provide a better understanding of the regional context of and controls on the geometry of the graphite deposits on Senja.

- Preliminary data from ^{40}Ar-^{39}Ar geochronology of biotite grains from different structural settings reveals a complex geochronology. New data from the Svanfjellet Shear reveals several different Precambrian ages, contrary to the data of previous authors, which show consistent, reactivated Caledonian ages.

In **Section 1**, several questions were posed to outstanding questions in the study of the graphite deposits and their structural environment. This report goes a long way in providing answers to these questions. These were:

- What is the sequence of structural events which are present in the deposits ?
  Original F1 layering has been refolded in F_2 isoclinal steeply-plunging regional folds. Some amount of remobilisation of graphite appears to have occurred at this stage. These folds were then modified by E-W trending open folds of D_3 age. In some areas on a local scale, D_4 folds have formed with a N-S trend.

- Do these events have a predictable geometry ?
  In some cases, yes, but not always. Where F_2 folds are unaffected by later fold interference fold axes are consistently steeply plunging but where F^3 fold are present the F_2 geometries are

unpredictable. Many fold show non-cylindrical geometries making predictions about 3D geometry problematic.

- Where does the genesis of the graphite deposits fit into this deformation sequence ?

  The graphite has clearly been present in the amphibolitic schists since at least prior to F_2 deformation as the graphite appears to have been enhanced by this deformation event. It is, as yet, unclear, if the graphite was present in the protolith or was introduced during the F_1 deformation phase.

- What are the structural geometries which have modified the ore deposits ?

  F_2 appears to have to some extend modified the geometry of the graphite as most graphite appears to be found in F_2 fold hinges. However, the most geographically extensive deposits of graphite are found where there has been extensive F_3 modification.

- Is there a relationship between graphite grade and structure ?

  There appears to be no systematic variation in graphite grades with respect to different structural settings and between deposits which are deformed after their genesis and those that are not. However, it appears that the aerial extent of graphite is more extensive where D_3 structures has modified the deposits.

- Is there a consistent regional structural framework ?

  D_3 folding and shear zones within the SSB appear to be related to crustal-scale movement on the bounding shear zones. The internal D_3 shear zone appear to be mega-scale S-C type structures to the bounding faults and the D_3 fold structures appear to be drag-folds on these structures. However, this simple picture is complicated by reactivation of the bounding structures and some of the internal shear zones.

- Where do the individual ore deposits fit into the regional geological interpretation ?

  The main geometry of the deposits was created during F_2 deformation. During F_3 deformation (which probably represents the docking of the SSB with the intrusive terrains to the north and south along the Svanfjellet and Torsnes Shear Zones) the deposit geometry was modified in those deposits which lay near to D_3 shear zones internal to the SSB.

- How can these relationships then be used to help predict the presence of further graphite deposits ?

  The structural analysis carried out here suggest that the best deposits will be found in one of two places: at complex F_2 fold terminations with m-folding geometries and where F_3 fold geometries are intense (This is most likely to be close to D_3 shear zone structures).

- What are the absolute ages of the various generations of faults, folds and mineralisation?

  Preliminary data so far show the bounding faults to preserve a Precambrian age, despite later reactivation in the Caledonian overthrusting, as has been documented by previous authors. Several dates from the SSB show a wide range of ages for F_2 deformation and therefore suggest a complex deformation history. Further study in this area is required.

10. Bibliography

This sections details the literature which has been used during this study and are divided up according to topic.

Local

Bang, N. (1985) Report Vestgangen, Geitskardalen, på Skaland.

Barkey, H. (1970) Strukturell geologisk flyfototolkning av fargepositiv flybilder over Trælen og Geitskarvannområdet, Berg i Troms. *NGU Rapport*, **976**.

Crossley. P. (2000) Graphite: High tech supply sharpens up. *Industrial Minerals*, November 2000, 31-47.

Dalsegg, E. (1994) CP-, SP- og ledningsevne-målinger ved grafittundersøkelser ved Hornvannet, Sortland, Nordland. *NGU Rapport*, **94.003**.

Dalsegg, E (1986) Elektriske målinger Skalands gruveområde, Senja, Troms *NGU Rapport*, **86.179**

Dalsegg, E. (1985) Geofysiske bakkemålinger Skalands grubeområde og Trælen, Senja, Troms. *NGU Rapport*, **85.187**

Elvevold, S. & Haug, T. (1985) Geologisk undersøkelse ved Geitskaret-Roaldsvann, Berg Kommune, Troms. NGU Rapport 85.188.

Fareth, E. (1983) Medfjordbotn, Berggrunnskart 1433 IV 1:50000, foreløpig utgave, *Norges Geologiske Undersøkelse*.

Fareth, E. (1983) Hekkingen, Berggrunnskart 1434 III 1:50000, foreløpig utgave, *Norges Geologiske Undersøkelse*

Flood, B. (1985) Trælen, Geologisk Kart (1:2500).

Flood, B & Heldal, T. (1985) Grafittprospektering: Trælen, Berg Kommune, Troms Fylke. *Rapport No. GT 85-20-01,*. 14p.

Flood, B. (1986) Skaland gruveområde prospekteringsprogram, Berg Kommune, Troms Fylke. *Rapport No. GT 86-20-03,* 16p.

Flood, B. (1990) Skaland grafittforekomst: Deformasjon og Remobilisering av malmer. Bergverkenes Landsammenslutnings industrigruppe, Teknisk rapport.

Flood, B & Johannessen, U. (2000) Oppfølgende diamantboring I Trælen grafittfelt, Berg kommune, Troms fylke. *Rapport No. GT 00-66-01*.12p.

Gautneb, H. & Tveten, E. (2003) The geology, exploration and characterisation of graphite deposits in the Jennestad area, Vesterålen, northern Norway. *NGU Bulletin (in press)*.

Gautneb, H. (1993) Grafittundersøkelser Hornvannet, Sortland Kommune, Nordland. *NGU Rapport*, **93.134**.

Gautneb, H. (1994) Grafittundersøkelser Hornvannet 1994, Sortland Kommune, Nordland. *NGU Rapport*, **95.076**.

Gautneb, H. & Tveten, E (1992) Grafittundersøkelser og geologisk kartlegging på Langøya, Sortland Kommune, Nordland. *NGU Rapport*, **92.155**.

Gautneb, H. & Wanvik, J.-E. (1997) Forprosjekt industrimineraler, Troms *NGU Rapport* **97.105**

Heldal, T. & Lund, E. (1987) Berggrunnsgeologisk kartlegging i Berg Kommune, Senja. Geologisk Kart (1:5000).

Hillestad, G. (1991) Seismiske grunnundersøkelser Skaland. *NGU Rapport No*. **1767**.

Haug, T. (1991) Mineralske Ressurser i Midt Troms,, Utviklingssenteret i Midt Troms, mineralutvikling A/S, Finnsnes, Tromsø, V, 56p.

Johannesen, G.A. (1987) Geologisk Berggrunnskartlegging på Senja, Berg Kommune.

G.A. Johannesen (1989) Mineralske ressurser på Senja- Status og framtidsmuligheter. 20p.

Lauritzen, T. (1988) CP-, SP- og VLF-målinger, Bukkemoen, Senja. *NGU Rapport*, 88.185.

Lund, E. (1988). Geologisk detaljkartlegging av tidligere påviste grafittmineraliseringer på Senja.

Lund, E & Opheim, J.A. (1985) Geologiske undersøkelser av grafittforekomster. Krokelvdal, Berg Kommune, Senja.

Opheim, J.A. (1988). Foreløpig rapport fra de geofysiske og geologiske undersøkelsene av grafittforekomster ved Bukkemoen, Lysvatn i Lenvik Kommune..

Rui, I.J. (1990) Deformasjon og Remobilisering av malmer. Bergv. Landsammenslutnings Ind. Gr. *Teknisk Rapport Nr*. **76**, 134-153.

Rønning, J.S. (1993) CP- og SP-målinger ved grafittundersøkelser på Vikeid, Sortland kommune, Nordland. *NGU Rapport*, **93.018**.

Torgersen, J. (1936) Grafittdraget, Skaland-Steinfjord. Tidsskr. Kjemi Bergv, 16, 61-62.

Flexural slip

Couples, G.D.; Lewis, H & Tanner, P.W.G (1998). Strain partitioning during flexural-slip folding. In: *Structural geology in reservoir characterization* (eds Coward, Daltaban & Johnson) *Geological Society Special Publication.* **127**; 149-165.

Dubey, A.K. (1982) Development of interlayer slip in non-cylindrical flexural slip folds. *Geoscience Journal*. **3**, 103-108.

Dubey, A.K. & Behzadi, H. (1981) Development of flexural slip folds, overlapping boudins and extension faults in multi-layered materials; field evidence and experimental model. *Journal of the Geological Society of India*. **22**; 274-284. 1981.

Dubey, A.K. & Cobbold, P.R. (1977) Non-cylindrical flexural slip folds in nature and experiment. *Tectonophysics*. **38**; 223-239.

Fowler, T.J. & Winsor, C.N. (1997) Characteristics and occurrence of bedding-parallel slip surfaces and laminated veins in chevron folds from the Bendigo-Castlemaine goldfields; implications for flexural-slip folding. *Journal of Structural Geology*. **19**; 799-815.

Fowler, T.J. (1996) Flexural-slip generated bedding-parallel veins from central Victoria, Australia. *Journal of Structural Geology*. **18**, 1399-1415.

Fitches, W.R., Cave, R., Craig, J. & Maltman, A.J. (1990) The flexural-slip mechanism; discussion. *Journal of Structural Geology*. **12**; 1081-1087.

Tanner, P.W.G (1989) The flexural-slip mechanism. *Journal of Structural Geology*. **11**; 635-655.

Tanner, P.W. G (1990) The flexural-slip mechanism; reply. *Journal of Structural Geology*. **12**; 8, 1085-1087.

Westjohn, D.B. (1996) Regional finite strain patterns in Proterozoic slates and quartzites; implications for heterogeneous strain related to flexural slip folding in the Marquette Synclinorium. In: *Institute on Lake Superior Geology; 42nd annual meeting; programs and abstracts*. (eds. Woodruff, L.G. & Nicholson-S.W., Part 1; Pages 64. 1996.

Yeats-R.S (1983) Faults related to flexural-slip folding. Eos, *Transactions, American Geophysical Union*. **64**; 45, Pages 854. 1983.

Fold-related graphite

Acharya, B.C. & Rao, D.S. (1998) Graphite in Eastern Ghat Complex of Orissa. In: Proceedings of workshop on the Eastern Ghats mobile belt. Ramakrishnan, M., Paul, D.K. & Mishra, R.N. (eds.) *Special Publication Series-Geological Survey of India*, **44**, 190-200.

Bonneau, J. & Raby, R. (1990) The Lac Knife graphite deposit. *Mining Magazine,* **63**, 12-14.

Chetty, T.R.K. & Murthy, D.S.N. (1994) Collision tectonics in the later Precambrian Eastern Ghats Mobile Belt: mesoscopic to satellite-scale structural observations. *Terra Nova*, **6**, 72-81.

Burton, W.C. & Southworth, C.S. (1993) Garnet-graphite paragneiss and other country rocks in granitic Grenvillian basement, Blue Ridge Anticlinorium, northern Virginia and Maryland. In: *Geological Society of America, Southeastern Section, 42nd annual meeting*. Abstracts with Programs - *Geological Society of America*. **25**; 6p.

Chamberlain, C.P. & Rumble, D. (1986) Fluid flow and graphite deposition during synmetamorphic thrusting, New Hampshire. *Eos, Transactions, American Geophysical Union*. **67**; 16, Pages 399. 1986.

Chetty, T.R.K. & Murthy, D.S.N. (1994) Collision tectonics in the late Precambrian Eastern Ghats Mobile Belt: mesoscopic to satellite scale structural observations. *Terra Nova*, **6**, 72-81.

Dissanayake, C.B. (1994) Origin of vein graphite in high-grade metamorphic terrains; role of organic matter and sediment subduction. *Mineralium Deposita*. **29**; 57-67.

Erdosh, G. (1970) Geology of Bogala Mine, Ceylon and the origin of vein-type graphite. *Mineralium Deposita*, **5**, 375-382.

Herber, L.J., Klasik, J.A. Van-Buskirk. M.C. (1986) Graphite deposits in the Transverse Ranges, Southern California. In: *The Geological Society of America, Cordilleran Section, 82nd annual meeting*. Abstracts with Programs - Geological Society of America. 18; 2, Pages 116. 1986.

Katz, M.B. (1987) Graphite deposits of Sri Lanka; a consequence of granulite facies metamorphism. *Mineralium Deposita*. ***22***; 18-25.

Kretz, R. (1996) Graphite deformation in marble and mylonitic marble, Grenville Province, Canadian Shield. *Journal of Metamorphic Geology*. **14**, 399-412.

Lumpkin, B.L., Stoddard, E.F. & Blake, D.E. (1994) Metamorphic and tectonic significance of the Raleigh graphite. In: *Geological Society of America, Southeastern Section, 43rd annual meeting.* Abstracts with Programs - *Geological Society of America*. 26, 25p.

Raith, J.G., Vali, H. (1998) Fibrous chlorite and muscovite from the Kaisersberg graphite mine, Styria, Austria. *The Canadian Mineralogist*. **36**, 741-754.

Simandl, G, Valiquette, G & Martignole, J. (1989) Genesis of graphite-wollastonite deposits, Grenville geological province, Quebec. In: *Geological Association of Canada, Mineralogical Association of Canada, annual meeting; program with abstracts*

Silva, K.K.M.W. (1974) Tectonic control of graphite mineralisation in Sri Lanka. *Geological Magazine*, **111**, 307-312.

Silva, K.K.M.W (1987) Mineralization and wall-rock alteration at the Bogala graphite deposit, Bulathkohupitiya, Sri Lanka. *Economic Geology and the Bulletin of the Society of Economic Geologists*. 82; 1710-1722.

Soman, K., Lobzova, R.V. & Sivadas, K.M. (1986) Geology, genetic types, and origin of graphite in South Kerala, India. *Economic Geology and the Bulletin of the Society of Economic Geologists*. 81; 997-1002.

Fold geometry

Kobberger, G. & Zulauf, G. Experimental folding and boudinage under pure constrictional conditions. *Journal of Structural Geology*. **17**; 1055-1063.

Mies, J.W. (1993) Structural analysis of sheath folds in the Sylacauga Marble Group, Talladega slate belt, southern Appalachians. *Journal of Structural Geology*, **15**; 983-993.

Narahara, D.K. & Wiltschko, D.V. (1986) Deformation in the hinge region of a chevron fold, Valley and Ridge Province, central Pennsylvania. *Journal of Structural Geology*. **8**; 157-168.

Andresen, A. (1980) The age of the Precambrian basement in western Troms, Norway, *Geol. För. Stockh. Förh*., **101**, 291-298.

Armitage, P.E.B. (1999) Kinematic analysis of a Precambrian meta-supracrustal deformation zone between Mjelde and Skorelvvatn, Kvaløya, Troms. *Cand. Scient., Universitet i Tromsø,* 172p.

Birkeland, T. (1975) Western Karmøy: An integral part of the Precambrian basement of south Norway. *NGT*, **55**, 213-241.

Coker, J.E., Steltenpohl, M.G., Andresen, A., Kunk, M.J. (1995) An $^{40}Ar/^{39}Ar$ thermochronology of the Ofoten-Troms region: Implications for terrane amalgamation and extensional collapse of the northern Scandinavian Caledonides, *Tectonics*, **14**, p435-447.

Cumbest, R.J., Johnson, E.L., Onstott, T.C. (1994) Argon composition of metamorphic fluids: Implications of $^{40}Ar/^{39}Ar$ geochronology, *Geol. Soc. Am. Bull*., **106**, p942-951.

Cumbest, R.J., Hames, W.E. McKinney, J.B. & Dallmeyer, R.D. (1984) Tectonothermal evolution of the northwestern basement terrain of the Norwegian Caledonides, Senja, Troms, Norway. In: *The Geological Society of America, Northeastern Section, 19th annual meeting*. Abstracts with Programs - *Geological Society of America*. **16**; 1, Pages 11.

Dallmeyer, R.D. (1992) $^{40}Ar/^{39}Ar$ mineral ages within the Western Gneiss Terrane, Troms, Norway: evidence for polyphase Proterozoic tectonothermal activity (Svecokarilian and Sveconorwegian), *Precambrian Research*, **57**, p.195-206.

Dallmeyer, R.D., and Andresen, A. (1992) Polyphase tectonothermal evolution of exotic Caledonian nappes in Troms, Norway: Evidence from $^{40}Ar/^{39}Ar$ mineral ages, Lithos, 29, p.19-42.

Hames, W.E. & Sinha, A.K. (1984) Rb-Sr geochronology of ductile strain zones within the Western Gneiss Terrane, Senja, Troms, Norway. : In: *The Geological Society of America, Northeastern Section, 19th annual meeting.* Abstracts with Programs - *Geological Society of America*. **16**; 1, Pages 11.

Henkel, H. (1991) Magnetic crustal structures in northern Fennoscandia. In: Wasilewski, P. & Hood, P. (eds.) *Magnetic Anomalies- Land and Sea Tectonophysics*, **192**, 57-79.

Huijsmans, J.P.P, Alexander, B.E.T.K. & Steenstra, S.E. (1981) On the structure of a high-grade metamorphic Precambrian terrain in Rogaland, south Norway. *NGT*, **61**, 183-192.

Krill, A.G & Fareth, E. (1984) Rb-Sr whole-rock dates from Senja, north Norway. *NGT*, **64**, 171-172.

Northrup, C.J. (1997) Timing Structural Assembly, Metamorphism, and Cooling of Caledonian Nappes in the Ofoten-Efjorden Area, North Norway: Tectonic Insights from U-Pb and 40Ar/39Ar Geochronology, *The Journal of Geology*, **105**, p565-582.

Olesen, O. & Solli, A. (1985) Geophysical and geological interpretation of regional structures within the Precambrian Kautokeino greenstone belt, Finnmark, north Norway.

Olesen, O., Torsvik, T.H., Tveten, E. & Zwaan, K.B. (1993) The Lofoten-Lopphavet Project. An integrated approach to the study of a passive continental margin. *NGU Rapport*, **93**.129, 54pp.

Olesen, O. & Sandstad, J.S. (1993) interpretation of the Proterozoic Kautokeino Greenstone Belt, Finnmark, Norway, from combined geophysical and geological data. *NGU Bulletin*, **425**, 43-64.

Pedersen, B.R.S. (1997) Strukturell analyse av en prekambrisk, duktilt deformert metasuprakrustalsone (Astridal-skjærsonen ?) på NØ-Senja, Troms. *Cand.Scient., Universitetet i Tromsø, 179p.*

Tull, J.F. (1977) Geology and Structure of Vestagøy, Lofoten, Northern Norway. *NGU Bulletin*, **42**.

Tveten, E. & Zwaan, K.B. (1993) Geology of the coast region from Lofoten to Loppa with special emphasis on faults, joints and related structures. *NGU Rapport*, **93.083**, 25pp.

Van Kranendonk, M.J. & Wardle, R.J. (1994) Promontory indentation, transpression and disharmonic folding in the formation of the Paleoproterozoic Torgnat Orogen, northeastern Canada. *Terra Nova*. **6**, Suppl. 2; Pages 23.

Williams, T.J., Clark, A.H. & Dallmeyer, R.D. (1984) Lithotectonic character of the Western Gneiss Terrane, Senja, Troms, Norway. In: *The Geological Society of America, Northeastern Section, 19th annual meeting*. Abstracts with Programs - *Geological Society of America*. **16**; 1, Pages 11.

Williams, T.J., Clark, A.H., Dallmeyer, R.D., and Andresen, A. (1985) Lithotectonic character of the western gneiss Terrane Senja, Troms, Norway. *Geol. Soc. Am. Abstr. Progs* **17**:11.

Zwaan, K. (1995) Geology of the West Troms basement complex, Northern Norway, with emphasis on the Senja shear belt; a preliminary account. *NGU Bull.*, **427**; 33-36.

Zwaan, K & Bergh, S.G. (1994) Geology of the Precambrian West Troms gneiss complex, Northern Norway, with special emphasis on the Senja shear belt; a preliminary account. In: Precambrian crustal evolution in the North Atlantic regions. *Terra Nova*. **6**, Suppl. 2; Pages 23.

Zwaan, K.B. (1992) Database for alle geologiske opplysninger om forkastninger og skjærsoner som opptrer på kartblad 1:250 000 Tromsø, *NGU Rapport*, **92.107**. 24pp.

Zwaan, B.K. (2003) Medfjordbotn, Berggrunnskart 1433 IV 1:50000, foreløpig utgave, *Norges Geologiske Undersøkelse*.

Zwaan, B.K. (2003) Hekkingen, Berggrunnskart 1434 III 1:50000, foreløpig utgave, *Norges Geologiske Undersøkelse.*

Enclosure 1: NORTH OF LYKTEGAN SECTION : DETAILED STRUCTURAL MAPPING

KEY

- AMPHIBOLITE GNEISS
- ACID GNEISS
- LITHOLOGICAL CONTACT
- F_2 FOLD HINGE (observed)
- F_2 FOLD HINGE (inferred)
- F_2 FAULT
- F_3 FOLD HINGE LINE
- F_3 FAULT

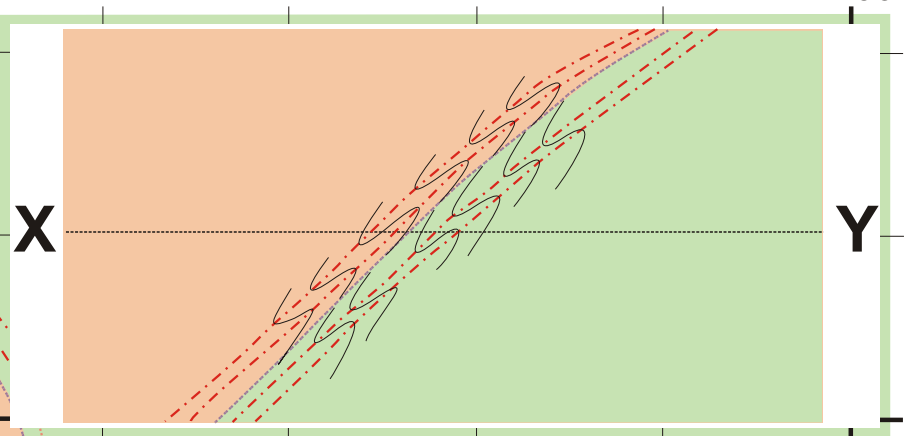

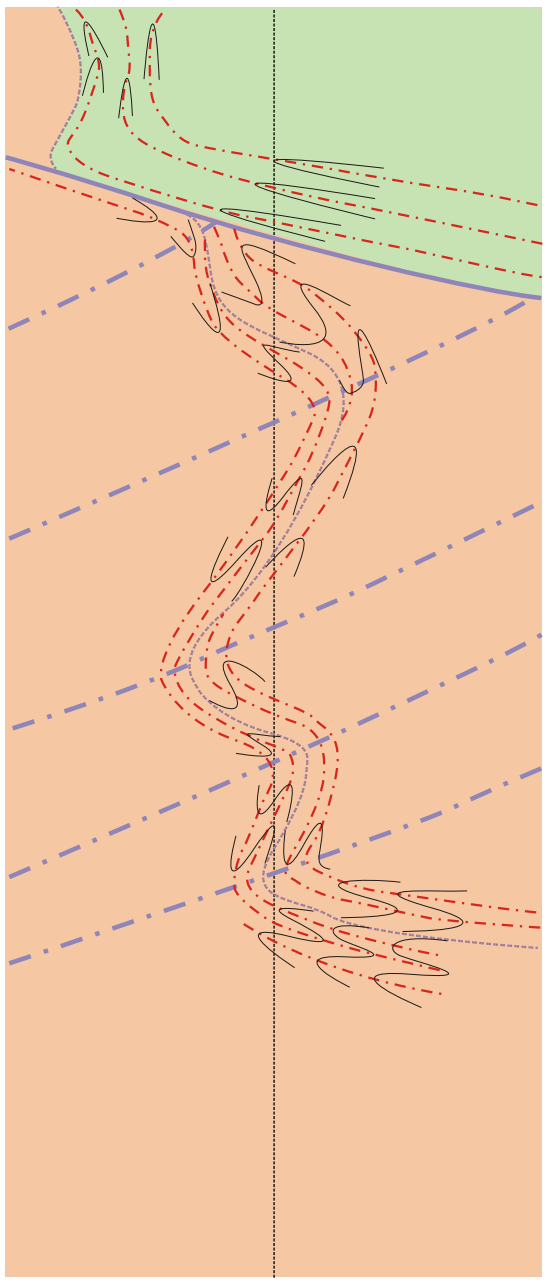

12300 12350 12400

1281600 1281550 1281500

B A X Y

N

SCALE 1: 400

Enclosure 3: KROKELVDALEN: DETAILED STRUCTURAL MAPPING

SCALE 1:5000

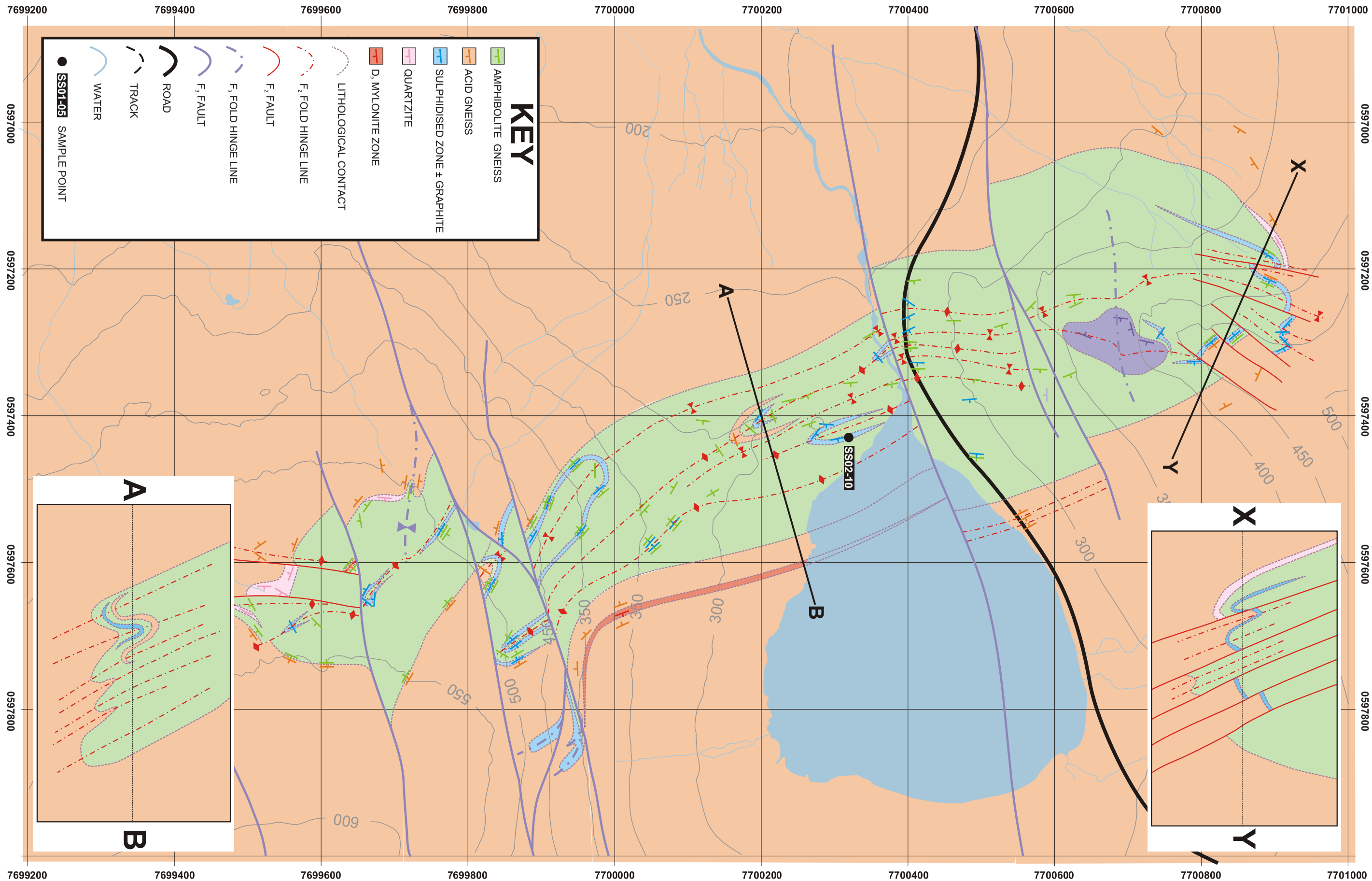

Enclosure 2: LYKTEGANGEN SECTION : DETAILED STRUCTURAL MAPPING

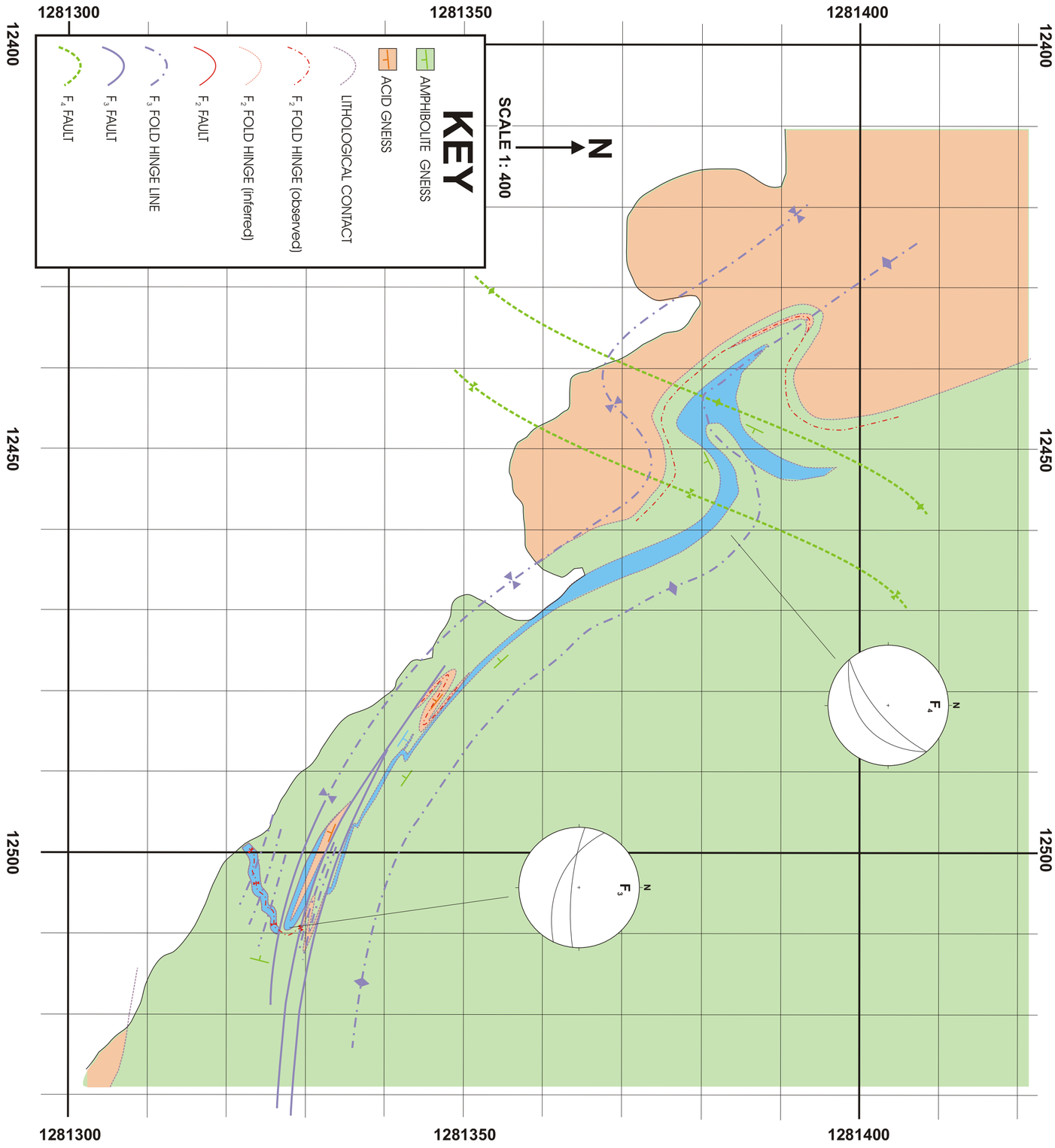

Enclosure 4: BUKKEMOEN: DETAILED STRUCTURAL MAPPING

SCALE 1:5000

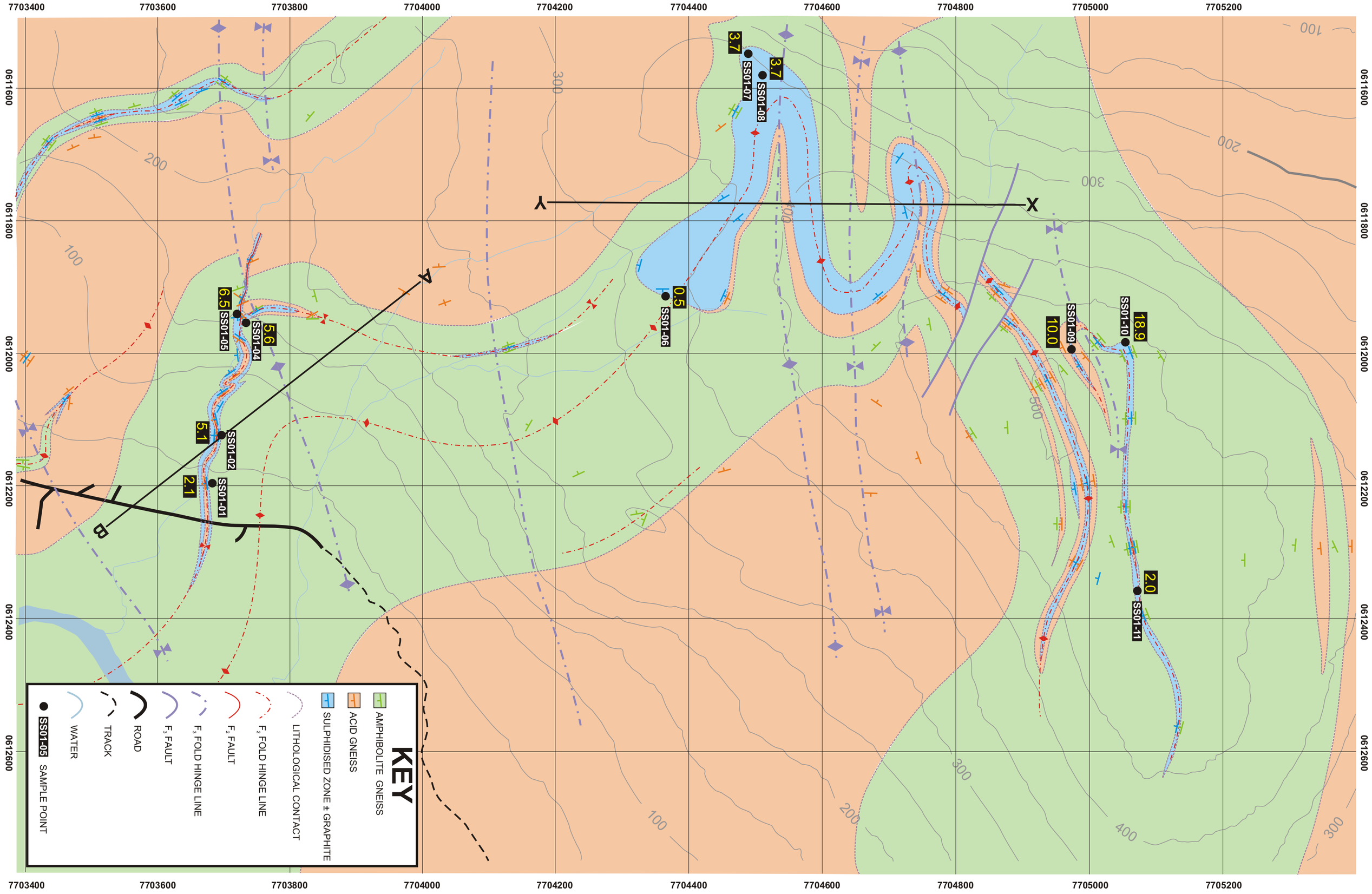

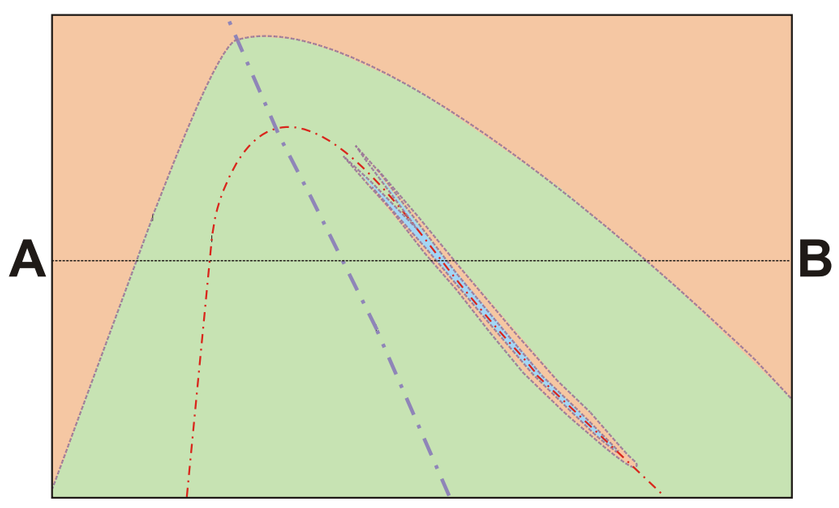

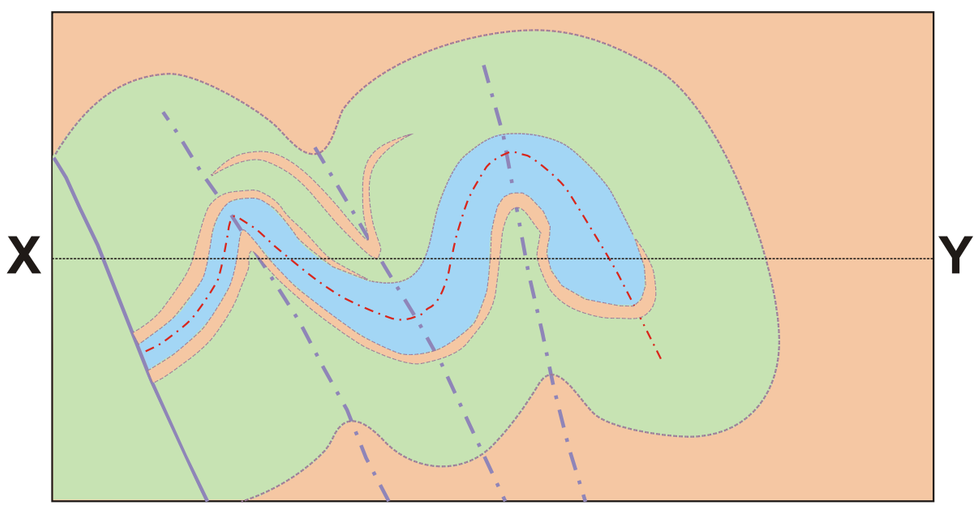

Enclosure 5: GEITSKARET DETAILED STRUCTURAL MAPPING

SCALE 1:5000

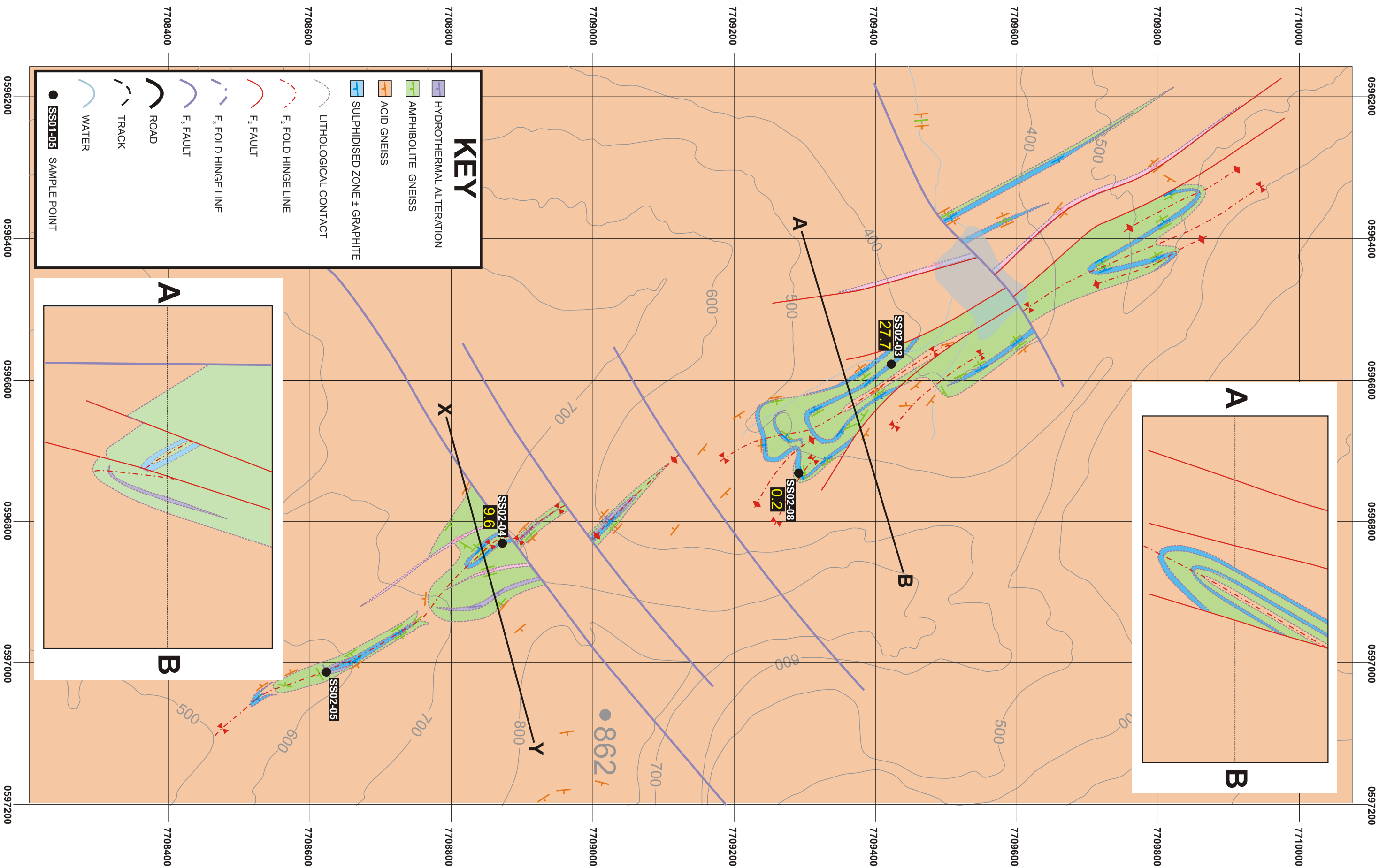

Enclosure 6: VARDFJELLET: DETAILED STRUCTURAL MAPPING

SCALE 1:6250

0607000 0608000 0609000 0610000

7705000

7704000

7703000

661 630 427

SS02-09 34.3 3.0 SS02-02

SS02-01 14.4

SS02-06 7.8 SS02-07 4.0

X Y

A B

KEY

- AMPHIBOLITE GNEISS
- ACID GNEISS
- SULPHIDISED ZONE ± GRAPHITE
- QUARTZITE
- LITHOLOGICAL CONTACT
- F_2 FOLD HINGE LINE
- F_2 FAULT
- F_3 FOLD HINGE LINE
- F_3 FAULT
- ROAD
- TRACK
- WATER
- SS01-05 SAMPLE POINT